



# **Natural variation in leguminous species and rice shows physiological and molecular adaptation to abiotic stress**

Inaugural-Dissertation

zur Erlangung des Doktorgrades  
der Mathematisch-Naturwissenschaftlichen Fakultät  
der Heinrich-Heine-Universität Düsseldorf

vorgelegt von

**Heithem Ben Abdallah**

aus Gafsa, Tunesien

Düsseldorf, März 2018

aus dem Institut für Botanik  
der Heinrich-Heine-Universität Düsseldorf

Gedruckt mit der Genehmigung der  
Mathematisch-Naturwissenschaftlichen Fakultät der  
Heinrich-Heine-Universität Düsseldorf

Berichtersteller:

1. Prof. Dr. Petra Bauer
2. Prof. Dr. Laura Rose

Tag der mündlichen Prüfung:

*Success in life comes when you simply refuse to give up, with goals so strong that obstacles, failure, and loss only act as motivation.*

*Unknown.*

## Acknowledgements

I would like to express my deepest thank to **Prof. Dr. Petra Bauer** first for giving me the opportunity to join her group at the botanical institute of the Heinrich Heine University in Dusseldorf. Second, for the financial support and for the experience of working in her lab during my PhD.

Especial thank to **Prof. Dr. Laura Rose** for accepting of my PhD supervision and also for the correction of my dissertation.

Especial thank to **Dc. Hans- Jörg Mai** for answering all my questions and helping me with all my problems and doubts during my PhD. Many thanks to all the members of the Institute of Botany for all nice time and unique moments. A special thank goes to my best colleague **Imran Khan** for the support, motivation through all these years. I would like to thank our Postdocs **Tzvetina** and **Rumen** for the personal support. Thanks to **Angelika** for technical support and the good moment in all situation. Thanks to **Elke** and **Ginte** for the technical support for the moral and technical help.

A very special thanks to my parents **Fatma El Bair** and **Younes Ben Abdallah** for supporting me and believing in me. Thanks to my brothers, **Nader Abdallah** and **Wael Ben Abdallah**. Special thanks to my beautiful sister **Abir Ben Abdallah**.

To all my friends, especially **Salah Bougroura**, **Assma El Hajjar**, **Abdo ben Fattah**, **Abdelhedi boulifia**, **Taoufik**, **Mohamed Ali Malha** and **Kamal** for being on my side all the time, thank you. Especial thanks to my second family **Lesjak**, **Barbara**, **Michael**, **Karin**, and my nice neighbours: **Liz**, **Helmod**, **Jotta**, **Klaus**, etc.

Last but not least, I want to thank **Khadija Raad** for the constant help and support during my hard times.

## Abbreviations

A. thaliana	<i>Arabidopsis thaliana</i>
BIC	Bicarbonate
Chl	Chlorophyll
Ct	Cycle threshold (quantitation cycle)
DW	Dry weight
F6'H1	Feruloyl CoA ortho-hydroxylase 1
FER	FERRITIN
GWAS	Genome Wide Association Study
GM	Genetically modified
GFP	GREEN FLUORESCENT PROTEIN
GO	Gene Ontology
H <sub>2</sub> O <sub>2</sub>	Hydrogen peroxide
IRT1	IRON REGULATED TRANSPORTER 1
IRT2	IRON REGULATED TRANSPORTER 2
MA	Mugineic acid
MRL	Main Root Length
M. truncatula	<i>Medicago truncatula</i>
NSR	Number of Secondary Root
NA	Nicotianamine
PCR	Polymerase Chain Reaction
PS	Phytosiderophores
QTL	Quantitative Trait Locus
Rbfl	Riboflavin
ROS	Reactive oxygen species
RT qPCR	Reverse transcription quantitative PCR
SOD	Superoxide dismutase
TOM1	PHYTOSIDEROPHORE EFFLUX TRANSPORTER
VIT1	VACUOLAR IRON TRANSPORTER 1
WT	Wild type
YS1	YELLOW STRIPE 1
YSL	YELLOW STRIPE 1-like

## Table of content

<b>Acknowledgements</b> .....	<b>1</b>
<b>Abbreviation</b> .....	<b>2</b>
<b>Table of content</b> .....	<b>3</b>
<b>Statement of declaration</b> .....	<b>6</b>
<b>Summary</b> .....	<b>7</b>
<b>I. Introduction</b> .....	<b>10</b>
1. Crop and its application in biotechnology.....	10
2. Abiotic stress in plants.....	12
3. Salinity and its importance.....	13
4. Effect of salt stress on plant growth and yield.....	14
5. Importance of Fe for plants.....	15
6. Iron excess in plants.....	15
7. Iron deficiency homeostasis in plants.....	17
8. Overview of Combined stresses in plants.....	19
9. Examples of plant responses to stress combination.....	22
10. Natural variation and diversity.....	23
11. Objectives and Aims.....	26
12. References.....	28
<b>Manuscript 1: Quantitative Reverse Transcription qPCR-Based Gene Expression Analysis in Plants (<i>Hedysarum carnosum</i>)</b> .....	<b>36</b>
1. Introduction.....	38
2. Materials.....	39
2.1. DNA sequence analysis tools.....	39
2.2. General analysis of DNA and RNA.....	41
2.3. Reverse transcription- qPCR.....	41
3. Methods.....	42
3.1. Design of qPCR strategy and oligonucleotide primers.....	44
3.2. Mass standard preparation for qPCR.....	44
3.3. Test of qPCR oligonucleotide primers by PCR.....	45
3.4. Generation of plant material.....	45
3.5. RNA preparation and reverse transcription.....	45
3.6. qPCR set up and run.....	47

3.7. qPCR data analysis and presentation of gene expression data.....	47
4. Notes.....	49
<b>Manuscript 2: Natural variation of physiological and molecular responses of Tunisian <i>Hedysarum carnosum</i> subjected to iron deficiency.....</b>	<b>59</b>
Abstract.....	61
1. Introduction.....	62
2. Materials and methods.....	63
3. Results.....	67
3.1 Plant growth response to iron deficiency.....	67
3.2 Physiological analysis of shoot responses to iron deficiency .....	68
4. Discussion.....	70
5. References.....	76
<b>Manuscript 3: Natural variation reveals contrasting abilities to cope with alkaline and saline soil among different <i>Medicago truncatula</i> genotypes.....</b>	<b>90</b>
Abstract.....	90
1. Introduction.....	90
2. Materials and Methods.....	93
3. Results.....	94
4. Establishment of growth conditions using the <i>M. truncatula</i> reference line Jemalong A17.....	94
5. Screening of 11 Tunisian <i>M. truncatula</i> lines of the SARDI collection under combined stress.....	95
6. Analysis of selected tolerant and sensitive <i>M. truncatula</i> lines to the combined stress in a hydroponic system.....	98
7. Discussion.....	101
8. References.....	104
<b>Manuscript 4: RNA-sequencing analysis of contrasting rice genotypes exposed to high iron.....</b>	<b>108</b>
1. Introduction and aims.....	110
2. Material and method.....	113
3.1. Morphological changes in contrasting rice lines in response to Fe stress and a subsequent revival phase...116	
3.2. Physiological changes in Lachit and Hacha plants exposed to high Fe stress .....	118
3.3. Global comparative transcriptome analysis between contrasting lines using RNA-seq .....	120
3.3.1. Detailed comparative transcriptome analysis to identify differentially regulated genes in roots....123	
3.3.2. Detailed comparative transcriptome analysis to identify differentially regulated genes in leaves...126	
4. Discussion .....	134

5. References .....	130
6. Final Discussion and conclusions.....	135
7. References .....	141

## **Statement of declaration:**

I, **Heithem Ben Abdallah**, hereby declare that I have fully and independently written the submitted dissertation without additional unauthorized support and consultation beyond that permitted and specified in the dissertation to include the necessary and appropriate cited literary resources. I confirm that this thesis presented for the degree has not been submitted for any other degree or professional qualification. I played a major role in the preparation of the experimental work, the data analysis and the interpretation. Any contributions from colleagues and the collaborators are mentioned in the sections.

The work was done under the guidance and the supervision of Professor **Dc. Petra Bauer** at the Institute of Botany, Düsseldorf, Germany.

Düsseldorf, March 09, 2017

## SUMMARY

Abiotic stress conditions cause extensive losses of agricultural production worldwide. Salinity and alkalinity affect plant growth and availability of nutrients including Fe. Its deficiency as well as toxicity is serious agricultural problems and lead to heavy losses in yield. In our work, two leguminous plants (*Hedysarum carnosum* and *Medicago truncatula*) were used that originate from Tunisia and use as a fodder for animals and rice from India that presents important staple food in Asia.

The first section, consists of a protocol for a reliable RT-qPCR assay, which can be easily adapted to any plant species of interest. In this paper, we describe in detail all the steps and the workflow. We think that this protocol is very informative and can be used as a template for RT-qPCR analyses.

In the second section, we exposed three isolates from *Hedysarum carnosum* named according to their habitats Karkar, Thelja and Douiret to iron-deficiency stress, and we found that there is a difference in the responses between the isolates by developing chlorosis in the young leaves and showing a reduced biomass production. In this work, we find that under iron deficiency, iron contents of Karkar and Douiret were significantly lower than in their respective controls compared to Thelja. We conclude that the results of our physiological and gene expression analyses suggest that the individual lines have distinct adaptation capacities to react to iron deficiency, presumably involving mechanisms of iron homeostasis and internal distribution.

In the second section, we screened 11 Tunisian *M. truncatula* lines from the SARDI collection, since in the field, crops and other plants are routinely subjected to a combination of different abiotic stresses. We subjected *Medicago* lines to salinity and alkalinity stress. Therefore, the combined stress affected germination rates, shoot and root dry weights, pigment contents and root morphology parameters. From the 11 tested lines we selected 2 tolerant and 2 sensitive lines. We find that these lines differ in their responses to double stress. The analyses provided evidence that root architecture, flavin root localization in epidermal cells and flavin secretion are relevant tolerance mechanisms for salt and alkaline stress in *M. truncatula*.

The last section investigates the specific responses of contrasting rice genotypes to overload of iron, Hacha and Lachit. The root and shoot growth parameters, the leaf bronzing score showed that plants from the susceptible cultivar Hacha exhibited more severe symptoms of Fe toxicity than Lachit. To shed light on the molecular tolerance mechanisms we conducted a comparative transcriptomics RNAseq experiment of roots and L2 leaves. In this work, it is shown that the differentially expressed genes can be arranged into clusters reflecting either genotype, Fe regime or genotype Fe regime effects and we compared the molecular signatures of the tolerant versus the susceptible cultivars with previously reported mechanisms. From the physiological and molecular data we conclude that Lachit responds differently to Fe toxicity than the sensitive cultivar Hacha and also different from other Indica rice cultivars reported to be tolerant to high Fe.

## ZUSAMMENFASSUNG

Abiotische Stressbedingungen verursachen weltweit erhebliche Verluste in der landwirtschaftlichen Produktion. Salzgehalt und Alkalität beeinflussen das Pflanzenwachstum, die Photosynthese und die Verfügbarkeit von Nährstoffen einschließlich Fe. Sowohl der Mangel als auch die Giftigkeit sind schwerwiegende landwirtschaftliche Probleme und führen zu hohen Ausbeuteverlusten. In unserer Arbeit wurden zwei Leguminosen (*Hedysarum carnosum* und *Medicago truncatula*) aus Tunesien verwendet, die aus Tunesien stammen und als Futter für Tiere und Reis aus Indien, die in Asien wichtiges Grundnahrungsmittel darstellt.

Der erste Abschnitt besteht aus einem Protokoll für einen zuverlässigen RT-qPCR-Assay, der leicht an jede interessierende Pflanzenart angepasst werden kann. In diesem Dokument beschreiben wir detailliert alle Schritte und Arbeitsabläufe. Wir denken, dass dieses Protokoll sehr informativ ist und als Vorlage für RT-qPCR-Analysen verwendet werden kann.

Wir isolierten drei Isolate von *Hedysarum carnosum*, die nach ihren Lebensräumen Karkar, Thelja und Douiret benannt wurden, auf Eisenmangel-Stress. Wir fanden heraus, dass die Isolate und die Chlorose in den jungen Blättern unterschiedlich sind. In dieser Arbeit finden wir, dass die Eisengehalte von Karkar und Douiret unter Eisenmangel signifikant niedriger waren als in ihren jeweiligen Kontrollen im Vergleich zu Thelja. Wir schließen daraus, dass die Ergebnisse unserer physiologischen und Genexpressionsanalysen darauf hindeuten, dass die einzelnen Linien unterschiedliche Adaptationskapazitäten haben, um auf Eisenmangel zu reagieren, vermutlich unter Beteiligung von Mechanismen der Eisenhomöostase und der internen Verteilung.

Die zweite getestete Leguminosenpflanze war *Medicago truncatula*, wir untersuchten 11 tunesische *M. truncatula*-Linien aus der SARDI-Sammlung, da Feldfrüchte und andere Pflanzen auf dem Feld routinemäßig einer Kombination verschiedener abiotischer Belastungen ausgesetzt sind. Wir unterzogen *Medicago* Linien Salinität und Alkalinität. Daher beeinflusste die kombinierte Belastung die Keimungsraten, die Trockengewichte von Spross und Wurzel, den Pigmentgehalt und die Parameter der Wurzelmorphologie. Von den 11 getesteten Linien wählten wir 2 tolerante und 2 sensitive Linien zu kombinierter Belastung aus. Wir finden, dass diese Linien sich in ihren Reaktionen auf Doppelbelastung unterscheiden. Die Analysen lieferten Hinweise darauf, dass die Wurzelarchitektur, die Lokalisierung der Flavinkonzentration in epidermalen Wurzelzellen und die Flavinkonzentration relevante Toleranzmechanismen für Salz- und alkalischen Stress in *M. truncatula* sind.

Der letzte Abschnitt untersucht die spezifischen Reaktionen gegensätzlicher Reisgenotypen auf Eisenüberschuss. Das kontrastierende Paar Hacha und Lachit wurde mit überschüssigem Eisenstress verwendet. Die Wurzel- und Triebwachstumsparameter, der Blattbräunungsindex, dass Pflanzen aus der anfälligen Sorte Hacha schwerere Symptome der Fe-Toxizität aufwiesen als Lachit. Um die molekularen Toleranzmechanismen aufzuklären, führten wir ein vergleichendes Transkriptom-RNAseq Experiment von Wurzeln und L2-Blättern durch. In dieser Arbeit wird gezeigt, dass die differentiell exprimierten Gene in Cluster, die entweder Genotyp-, Fe-Regime- oder Genotyp-Fe-Regimeeffekte widerspiegeln, verglichen und die molekularen Signaturen der toleranten gegenüber den suszeptiblen Kultivaren mit zuvor beschriebenen Mechanismen

verglichen wurden. Aus den physiologischen und molekularen Daten schließen wir, dass Lachit anders auf Fe-Toxizität anspricht als die empfindliche Sorte Hacha und auch anders als andere Indica-Reissorten, von denen berichtet wurde, dass sie gegenüber weils Fe tolerant sind.

### 1. Crops and applications in biotechnology:

Since the antiquity, many crops have been vital for human kind. Because of this, crops are produced and commercialized worldwide and are nowadays having a high economic value. The most important crops were bred for human consumption to ensure food security (e.g. wheat, maize, and rice). Other crop varieties are exploited as fodders (oats, alfalfa) or in the industry of papers, textile, and clothes (Colombo et al. 2014; Fageria 2016). Various investigations have demonstrated that cereal crops display much higher yields than legume crops whereas the latter contain elevated protein and lipid content in the seeds (Fageria et al. 2006). It is well known that crop production is highly influenced by environmental change. Since the last decade, a global climate change associated with a global temperature increase was observed, and this is a controversial issue. This increase in global temperature results in drought in some regions or flooding in others causing stress to the growing plants. These types of stress are combined as abiotic stresses and can cause a reduction in plant growth and yield. Reduction in the global food supply is leading to hunger and starvation of human populations all over the world. Thus, agriculture and human race are facing many challenges mainly providing enough food for all human beings and maintaining the stability of that amount. This reduction in crop production can be counteracted with the application of biotechnology in agriculture. However, there are a number of open questions with regard to the assessment of costs and benefits as well as the institutional conditions that are required if new technologies are implemented. Furthermore, the public debate focused mainly on the risk that crop biotechnology brings about to the health of human beings and to the environment (Bauer 2005).

Biotechnology uses molecular techniques to modify the genetic basis of plants and animals to improve the quality of life. Biotechnology may encompass different technological branches such as the utilization of genomic innovations, specific reproducing, transformation rearing, plant tissue culture, molecular markers, and genetic engineering. The importance of the different approaches differs from one country to another taking into consideration the degree to which the food is important for human health and safety. Crop biotechnology has been developed in many parts of the world. In fact, from a scientific point of view, the application of biotechnology in agriculture is the result of gene technology evolution. Genetically modified organisms contain modified DNA and are generated using genetic engineering tools and methods. For crop improvement, scientists introduced resistance genes into crop plants. In Africa, particularly in Kenya, Bt cotton (cotton strain which contains a gene encoding a *Bacillus thuringiensis* toxin as an insecticide) is

## Introduction

extensively produced and commercialized (Tefera et al. 2016). In America, pumpkin is one of the most important crops as it is considered as an excellent source of energy. Due to its great importance, this crop has been intensively investigated and the genome sequenced for further biotechnology studies (Leke et al. 2016). In Europe, many scientists have developed Late Blight Resistant Potatoes (Jo et al. 2014), as this known disease threatens potatoes and crops in general. Globally, approximately 60% of all soybeans and 30% of cotton are genetically modified (James 2004). But there are risks apart from using this technology. The European Commission paid great attention towards these risks taking them very seriously. The risks of GM are health-related risks like potential allergic reactions. Also, transferred genes could mutate and could cause antibiotic resistance in pathogenic bacteria. The risks of biotech crops are related to fodders, plants, ecosystems, farmers, and agriculture (Murphy 2007). GM crops make these risks more complex. GM crops make these risks more complex. Nevertheless, we need to understand the use of GM according to the available agricultural tools. In the year 1996 the US started the large-scale cultivation of agriculturally important GMs and since then it is expanding. According to the recent statistics GM crops are cultivated over the 11% worlds cultivated land. These include 79% soybean, 70% cotton, and 32% maize of all the world (James 2014). Focus are on those crops important for both: maintaining the fertility of the soil and having nutritional value. *Vicia faba* is one example of pulse crops that contain high levels of protein and are used to sustain agriculture as it plays an important role in soil fertility and nitrogen fixation (Oliveira et al. 2016). *V. faba* is a forage legume that grows under different cropping systems but hardly *in vitro*. Nevertheless, for a successful biotechnological approach efficient *in vitro* regeneration is required. Therefore, previous reports showed that a successful *in vitro* growth could be established by organogenesis. Several plant organs were used as explants such as the meristematic regions, auxiliary buds, and embryonic axes (Ismail et al. 2011). The combination of conventional practices and the recent genomic approaches paved the way for a new type of crop development. This is due to the developments in DNA sequencing and transcriptomic studies on many plant species that facilitated relating the genotypes to the phenotype of the plants including their biochemical changes. The production of abiotic stress tolerant plants requires a better understanding of the gene regulation mechanisms employed by plants as a reaction to adverse environmental conditions. This understanding includes the gene expression and post-transcriptional regulation by non-protein coding small RNAs and micro RNAs (miRNAs). Therefore, the transfer of these molecular traits

## Introduction

will accelerate the development of tolerant crops. Indeed, miRNAs and their implementation in the improvement of many major crops have been recently reported (Noman et al. 2017; Zhang 2015). For example, activation of the C-kinase 1 receptor gene enhanced the drought tolerance in transgenic rice plants (Li et al. 2009). Another approach are the crop wild relatives (CWRs) as they represent many traits that are a source of natural variation under a scale of biotic and abiotic stress. Recently the term 'introgressomics' has come forward which consists in the interspecific breeding of wild plant species with crop varieties by looking into the specific traits within many populations. This approach will lead to the development of newly selected cultivars that can improve yield and performance resulting in a more efficient and sustainable agriculture under environmental changes (Prohens et al. 2017). Crop improvement has shifted to a new level by using the next generation sequencing technique that represents a revolutionary method to identify new genes directly related to tolerance to various stresses in plants. The sequences of many crop species like soybean, maize, and wheat have already been studied (Berkman et al. 2012; Edwards et al. 2013; Franssen et al. 2011).

### **2. Abiotic stress in plants:**

Because of the ever-changing climate, plant growth and yield are severely affected by certain abiotic and biotic stresses that occurred at the same time (Prasch and Sonnewald 2013; Ramegowda and Senthil-Kumar 2015; Suzuki et al. 2014). Plants growing under natural conditions, which have difficulties to achieve their full genetic potential for reproduction, are considered as being "stressed". Therefore, to adapt to a changing environment, plants have developed complex mechanisms to respond to stress. It was demonstrated that only 22% of the genetic potential yield contributed to the production of field-grown crops in the United States because of the impacts of unfavorable adverse environments (Boyer 1982). The 2007 FAO statistics showed that only 3.5% of the world land area was not impacted by some adverse environmental conditions. This problem is still growing because of decreases in water resources, the continued reduction of crop growing land, and an augmentation global warming problem and climate change (Lobell et al. 2011). Thus, there is not only one single environmental factor affecting the plants. Usually, there is a complex of factors. For example, environmental factors greatly influence the deficiency or toxicity of nutrients (Juneja et al. 2013). Reactive oxygen species (ROS) can be good or bad for plants under abiotic stress. High levels of ROS lead to lipid peroxidation and the damage of DNA and proteins (Mittler 2002; Schieber and Chandel

## Introduction

2014). Although ROS were previously considered harming cells, recent research suggested that cells developed strategies to use ROS as signals in the regulation of various genetic processes involved in cellular stress mechanisms (Dat et al. 2000) or in the regulation procedure of plant growth and development, like cell elongation (Foreman et al. 2003) or root differentiation (Tsukagoshi et al. 2010).

### 3. Salinity and its importance

Salinity is a major problem that is characterized by many factors that influence the stress response in plants, such as texture and composition of the soil, availability of water, alongside with environmental changes and cultural factors (Maas and Grieve 1987). Soil salinity affects about 6% of the land surface and secondary salinization of irrigation affects about 20% of the irrigated land (Munns and Tester 2008). Salinity can have different effects on a plant depending on the developmental stage and the plant species (Krishnamurthy et al. 2016; Tripathy et al. 2017; Zhang et al. 2017). High salt accumulation in the soil decreases the water absorption in the roots and increases the water loss in the aerial parts. Once high salinity occurs, plants accumulate more  $\text{Na}^+$  and  $\text{Cl}^-$  ions in their tissues. High  $\text{Na}^+$  concentration causes a block of  $\text{K}^+$  uptake. This leads to an ion imbalance in the cells and results in a significant decrease in crop yield (James et al. 2011). Plant growth in saline soils is usually hampered due to osmotic and oxidative stress and also to the toxic effects resulting from the high ion concentrations (Rengasamy 2016). In sodic soils, clay dispersion and soil structural degradation result from high  $\text{Na}^+$  cation amounts and negatively affect plant growth (Rengasamy 2016). In sodic soils, clay dispersion and soil structural degradation result from high  $\text{Na}^+$  cation amounts and negatively affect plant growth because high  $\text{Na}^+$  enhances soil alkalinity (Rengasamy 2016). For example, salinity and alkalinity are widespread in Tunisian soils (Kovda 2013), first, due to an occurrence of salt-affected soils in depressions and in the main "sebkhass" (dry alkaline flats, normally situated near the sea) and "chotts" (the interior salt lake areas away from sea), secondly, the irrigation water which contains high amount of salt results in secondary salinity. The effects of salinity can hamper plant germination and delay the flowering time (Moriuchi et al. 2016), reduce plant growth, and their establishment which result in lower yields or a complete loss of the crop (Rhoades and Loveday 1990). Ion toxicity from high sodium ( $\text{Na}^+$ ) and chloride ( $\text{Cl}^-$ ) can also occur. As salinity levels in the root zone increase, water becomes less likely to enter the roots and present such a barrier around the roots (Berezniak et al. 2017; Provin and Pitt 2001; Rhoades and Loveday 1990). Some plants

and animals live in the salt water and are adapted to the salinity, so salinity can help to understand if a plant or animal species can be expected to be present. We can conclude that each species can tolerate a certain threshold of salinity but have to determine its level of tolerance to salt stress.

#### 4. Effect of salt stress on plant growth and yield

Salt stress in plants affects germination, photosynthetic ability, growth, and oxidative stress. Due to the importance of the process of germination, which is the fundamental phase of growth, salinity affects many crop plants such as *Medicago truncatula*, rice, and wheat. The impact of salinity can be observed at different levels, such as reducing the mobilization of seed reserves (Marques et al. 2013), inhibition of the imbibition process in seeds due to a lower osmotic potential during germination (KATEMBE et al. 1998), changes in enzymatic activities, and perturbances in protein metabolism (Amirjani 2011; Hu et al. 2012). Besides germination, photosynthesis is an indispensable and vital procedure that produces the energy for plant growth. Photosynthesis, together with cell development, is among the essential procedures to be influenced by saltiness (Munns et al. 2006). Some plant species developed a strategy to adapt to these conditions by producing energy under difficult circumstances. The evolution played a major role in the complexation of leaf forms that prevent the loss of water under saline conditions (Grewell et al. 2016; Nguyen et al. 2017). Reports have also shown that under high salinity an increase of non-photochemical quenching and a decrease of maximum quantum yield of photosystems II (PSII) take place in many species including rice (Porcel et al. 2015), barley (Kosová et al. 2015) and *Medicago* (Panta et al. 2016). For this, the light-harvesting complex II (LHC II) is redistributed, thus adjusting the absorption between PSI and PSII. The photosynthetic response to salinity stress is very complex in *Oryza sativa* (Sultana et al. 1999) and *Medicago sativa* (Li et al. 2010) as it involves the interplay of limitations at different sites of the cell/leaf and at different time scales during plant development. Other plant species have adapted to saline conditions in ways similar to plants that live in dry, desert conditions. These plants decrease their osmotic potential in the roots and at the same time enhance their amino acid supply. This potential allows water to be transferred to the aerial part of the plants when water reaches the plant leaves during transpiration. Due to stomatal closure under salt stress the availability of CO<sub>2</sub> becomes limited in the leaves. This leads to the inhibition of carbon fixation exposing the chloroplasts to massive excitation energy which in turn results in an increase of ROS production and accumulation e.g. superoxide anions and hydrogen peroxide (Munne-Bosch and Pinto-Marijuan 2016; Xiang et al. 2015). ROS can cause

## Introduction

oxidation of proteins, peroxidation of lipids, perturbation of enzyme activity, and DNA damage. The increased ROS production results in ROS-mediated membrane damage which is a major cause of cellular toxicity and induces programmed cell death (PCD) among different crop plants (Eraslan et al. 2007; Tavakkoli et al. 2010). All those affected parameters lead to a significant decrease in the crop yield caused by high salinity in many crops such as *Medicago sativa* (Altinok et al. 2015), rice (Khairi et al. 2015), and wheat (Daei et al. 2009).

### 5. Importance of Fe for plants:

In nature, iron occurs in abundance and ranks fourth among all elements on Earth's surface (Kobayashi and Nishizawa 2012). First of all, plants look green and healthy due to the fact that iron plays a role when the plant produces chlorophyll. Therefore, under iron deficiency, plants show a yellowish color in their leaves. 30% of all arable soils are calcareous with high pH (Chen and Barak 1982) due to which iron is not readily available for plant uptake (Yi et al. 1994). Iron is considered as one of the essential micronutrients for all living beings because it plays an important role in different metabolic processes like DNA synthesis and respiration (Puig et al. 2017). In addition to its importance, excess in iron is a detriment to the cell because of its tendency to react with oxygen and therefore to generate free radicals by the Fenton reaction. Thus, an inner maintenance of iron homeostasis is critical to avoid the shortage caused by iron deficiency and the excess caused by iron overload. The homeostasis is directly dependent on the iron-storing ferritin proteins which are present and largely conserved in plants and animals (Arosio et al. 2009; Arosio and Levi 2002). Moreover, many metabolic pathways are activated by iron and are regulated by different enzymatic activities. Iron chlorosis is caused mainly by the imbalance between the solubility, soil texture, and pH (Sahrawat 2016). The chlorosis is corrected by adding an iron fertilizer, or balancing the soil pH (Nathan 2017).

### 6. Iron excess in plants

*Oryza sativa* presents an important staple food for all over the world's population and it is grown in a wide range of environments (Birla et al. 2017). The majority (90%) of the global rice production is harvested in Asia where it is grown in irrigated or rainfed lowland rice fields. In the soil, many iron minerals are present. In submerged soils, where pH is low,  $Fe^{2+}$  is present in high levels which causes iron toxicity. In fact, whenever a large amount of iron is reduced to  $Fe^{2+}$  and the soil pH is low, iron toxicity occurs. One characteristic visual symptom is the modification in

## Introduction

the leaf color. The stress response depends on the severity and the duration of the stress and also on the environmental conditions. Therefore, suitable management of these crops by using tolerant cultivars to improve soil fertility, soil drainage at certain growth stages of the crop, use of manganese as antagonistic element in the uptake of  $\text{Fe}^{2+}$ , and planting  $\text{Fe}^{2+}$ -resistant rice cultivars can reduce the problem of iron toxicity (Matthus et al. 2015; Sikirou et al. 2016).

### Uptake and transport of iron in rice

Besides the uptake and absorbance of  $\text{Fe}^{3+}$  using the chelating phytosiderophores, rice plants are also able to absorb iron as  $\text{Fe}^{2+}$  (Ishimaru et al. 2006). Rice plants have the tendency of absorb more iron than most of the other plants, with  $\text{Fe}^{2+}$  being the iron species prevailing in paddy fields. The phytosiderophore 1 (TOM1) transporter of the mugineic acid (MA) family was identified by (Figure 1) (Nozoye et al. 2011). The complex of Fe(III)-MA is taken up into root cells via the YELLOW STRIPE 1-like (YSL) transporters (Inoue et al. 2009; Ishimaru et al. 2010; Kakei et al. 2012; Koike et al. 2004). Besides, rice is considered as a strategy I plant in contrast to most of the other grasses, since rice can take up  $\text{Fe}^{2+}$  via OsIRT1 (Iron-regulated transporter 1) and OsIRT2, (Nakanishi et al. 2006). Plants developed different strategies to tolerate high iron levels. The first scenario takes place at the level of root oxidation and by excluding  $\text{Fe}^{2+}$  from the rhizosphere: the root presents the first barrier by root ion selectivity and oxidation of the rhizosphere (Audebert and Sahrawat 2000; Becker and Asch 2005; Mongon et al. 2014). Another aspect of the root-based strategy is the formation of lateral roots and the retention of  $\text{Fe}^{2+}$  in inactive metabolically sites named 'dumping sites' (Becker and Asch 2005). The second scenario is done by taking up  $\text{Fe}^{2+}$  through lowering the pH in the rhizosphere. This results in a higher accumulation of  $\text{Fe}^{2+}$  in the roots. Therefore, the plants developed a strategy to avoid tissue damage by detoxification of iron. As a third strategy, plants are able to increase the pH in the apoplast under iron stress thus avoiding an uncontrolled accumulation or influx of  $\text{Fe}^{2+}$  into the leaf cells (Becker and Asch 2005).

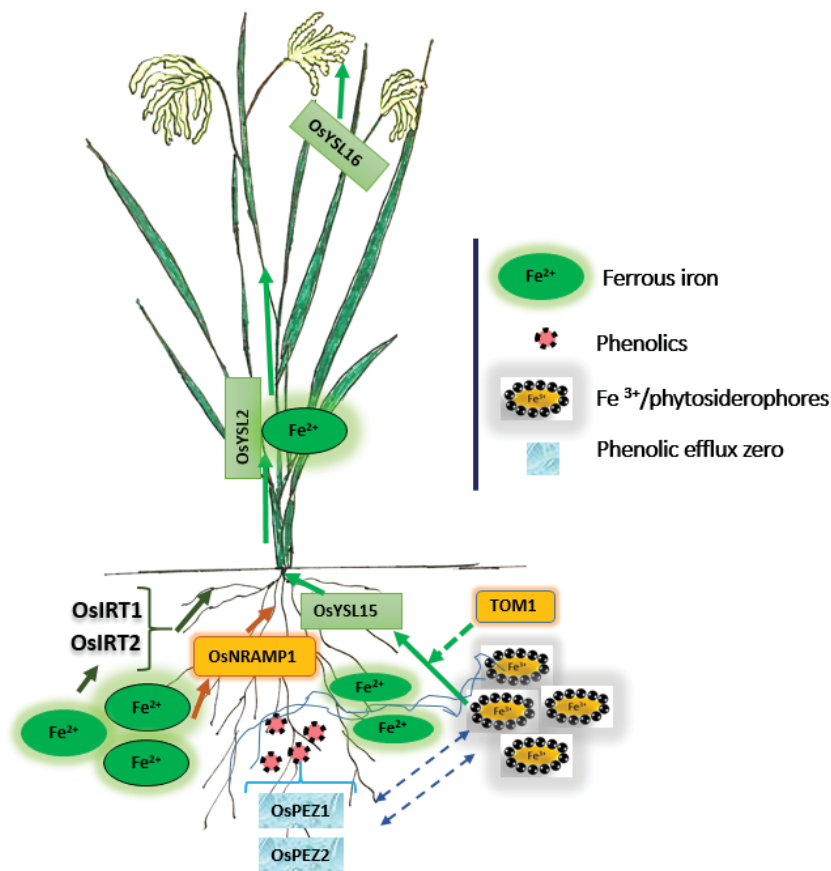


**Figure 1: Iron transport in rice:** Rice is a graminous plant which take up Fe (III)-PS complexes using strategy II, it can also take up  $\text{Fe}^{2+}$  via strategy I through OsIRT1 (Ishimaru et al. 2006). During strategy II, PS are exported via TOM1 to the rhizosphere to solubilize and chelate  $\text{Fe}^{3+}$  ions. After the chelation of Fe, these complexes are transported inside the root cell mediated by YELLOW STRIPE1-LIKE protein (Curie et al. 2008).

### 7. Iron deficiency homeostasis in plants

Iron is an essential chemical element for all living cells because it is involved in many processes in plants such as respiration, photosynthesis, and metabolism. However, under iron deficiency condition plants exhibit leaf chlorosis resulting in a reduction of growth and plant biomass (Rogovska et al. 2007). On the other hand, the excess of free Fe is harmful to living cells as iron ions react with oxygen and produce harmful free radicals (Ravet et al. 2009). Long distance iron transport requires different chelation and reduction processes since Fe binds to various chelators which facilitate its transport and remobilization between the organs and tissues (Kobayashi and Nishizawa 2012). The importance of a mitochondria-localized metal homeostasis protein, Frataxin, has been reported in Arabidopsis. In Arabidopsis cells, the presence of Frataxin is

## Introduction

indispensable for functional Fe-clusters, since it has an iron-binding property involved in heme synthesis (Chiang et al. 2016). Also, appropriate photosynthetic reactions require the presence of iron. This is considered as an evidence for the importance of iron metabolism in relation to the use of plant productivity. Therefore, the plant biomass is produced at a lower rate if the iron quantity is not sufficient. Plants absorb Fe from the soil mostly in the form of primary minerals like ferric iron ( $\text{Fe}^{3+}$ ) and the oxides:  $\text{Fe}(\text{OH})^{2+}$ ,  $\text{Fe}(\text{OH})_3$  and  $\text{Fe}(\text{OH})^{4-}$ . The pH plays a critical role in the availability of iron to plants, at high pH iron is predominately present in the insoluble ferric ( $\text{Fe}^{3+}$ ) form in the soil. Therefore to absorb iron plants have adopted different strategies for iron solubility and uptake from the rhizosphere (Guerinot and Yi 1994). Fe can be absorbed as  $\text{Fe}^{2+}$ ,  $\text{Fe}^{3+}$  and as complex Fe-chelate. Its absorption is metabolically controlled by plants. There are at least two strategies or processes involved (Kobayashi et al. 2014). Under iron deficiency, in strategy I, protons are pumped additional to the rhizosphere by activation of the proton ATPase, which acidifies the soil and enhances Fe solubility (Ramos et al. 2009).

### Reduction-based strategy (strategy I)

The reduction-based strategy, also called strategy I, is present in all plants, except Poaceae. The main feature of Strategy I plants, e.g. in Arabidopsis and leguminous plants, is that they acidify the soil via proton extrusion through an ATPase, reduce ferric to ferrous iron by a ferric chelate reductase (FCR), and take up the divalent iron (Figure 2) (Yi and Guerinot 1996). This lowers the soil pH, making Fe more soluble, Ferric reduction oxidase 2 (FRO2) then reduces  $\text{Fe}^{3+}$  to  $\text{Fe}^{2+}$ . The reduced iron is then transported by the iron-regulated transporter IRT1 (Eide et al. 1996). AtIRT1 also transports Zn, Mn, Cd, Co, and Ni (Eide et al. 1996; Korshunova et al. 1999; Schaaf et al. 2006). The divalent metal transporter IRT1 is an essential protein for Fe uptake and part of the ZRT/IRT-related protein family (Weber et al. 2004). The level of *IRT1* gene induction is used as a molecular marker for the iron-deficiency response regulation in Arabidopsis (Vert et al. 2002).

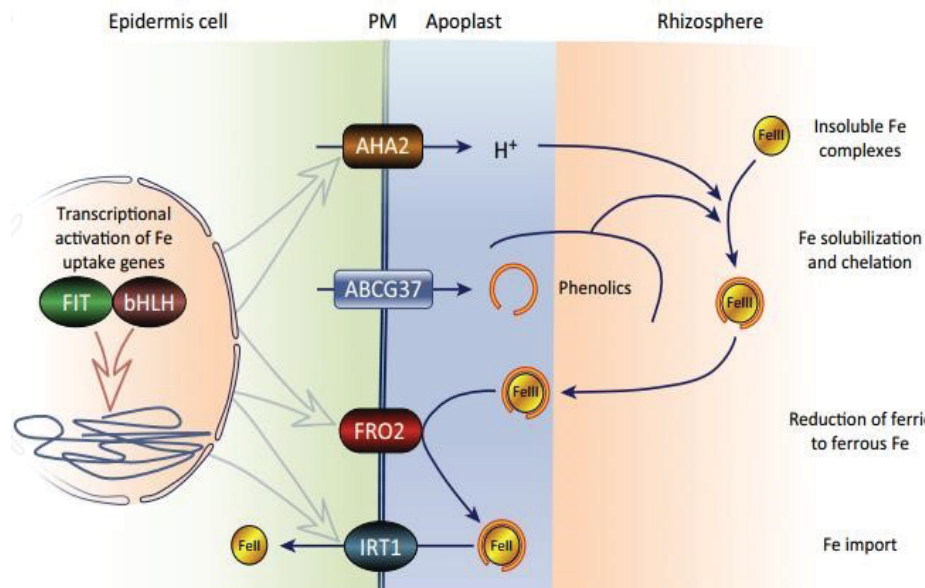


**Figure 2: Fe uptake of Strategy I plants:** The AHA2 pumps protons into the rhizosphere. The FRO2 reduces the ferric iron to the ferrous state. The reduced iron (ferrous) is then transported by the iron regulated transporter IRT1. The picture is taken from (Brumbarova et al. 2015).

## 8. Overview of combined stresses in plants

To study abiotic stress in plants, normally single stress conditions like salinity, alkalinity, or heat are applied under control laboratory conditions to analyze certain molecular aspects of the plant response. The aforementioned conditions are totally different from the naturally occurring ones where the plants are consistently subjected to the combined abiotic stresses simultaneously. To study yield loss by exposing to certain stresses simultaneously is well documented in different cultures (Mittler 2006). As many molecular studies took place in laboratories under specific conditions, their application happens in a different environment than the actual field conditions. As a result, there would be a fracture between the data acquired from either the laboratory or the field on how the plants develop. Looking into the analysis of stress combinations the results can be quite different. Depending on the intensity and the duration of the combined stress, the effect can be additive, synergistic, or antagonistic as shown in Figure 2.

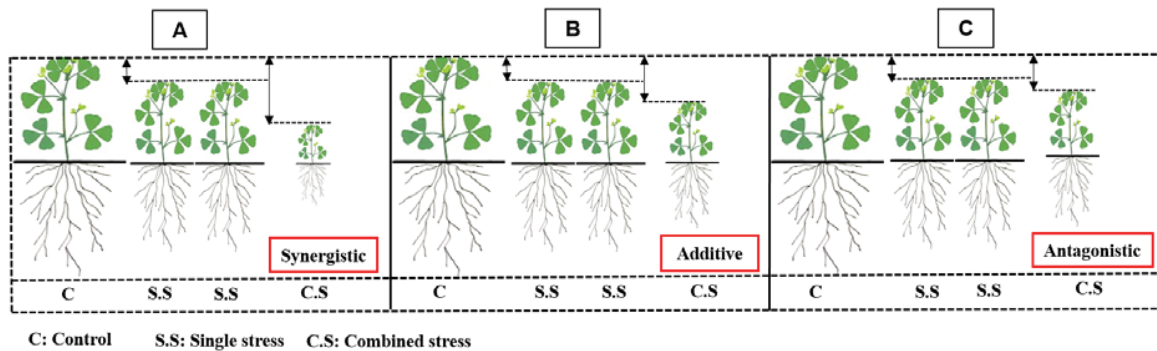


**Figure 2:** Overview of the effects of combined stress. A: Synergistic effect: It occurs when the effect of combined stresses is greater than the sum of their individual effects. B: Additive effect: the sum of combined stresses produced it is an effect that equals the sum of the individual stresses. C: Antagonist effect: the sum of combined stresses is less than the sum of the applied individual stresses.

In some cases, short or long recovery periods interfere with one or many stresses. Thus, stresses may not only be combined but also repetitive when it comes to plant breeding. For instance, repetitive stresses can be successive hot days, repetitive incidents of drought or high temperature (Pecinka et al. 2010). Agronomical accurate strategies are needed to be designed by the researchers to help them to generate a wide spectrum of stress-tolerant crops. This is because it is not always the case that the combination of stress factors on crops is additive as it rather depends on the output of the nature of the stress-response interactions (Atkinson et al. 2013; Pandey et al. 2015). Plants cope with combined stress factors by adopting certain unique and some common responses. To identify the impact of the combined effects of both biotic and abiotic stresses on plants it is important to investigate the nature of their interactions. Figure 3 shows an updated matrix collected from interactions between various environmental stresses and their effects on plant growth and development (Mittler 2006). The matrix demonstrates that the effect of stress combinations can be negative or positive. Observations demonstrated that crops showing high tolerance to combined abiotic and biotic stresses have many physio-morphological traits.

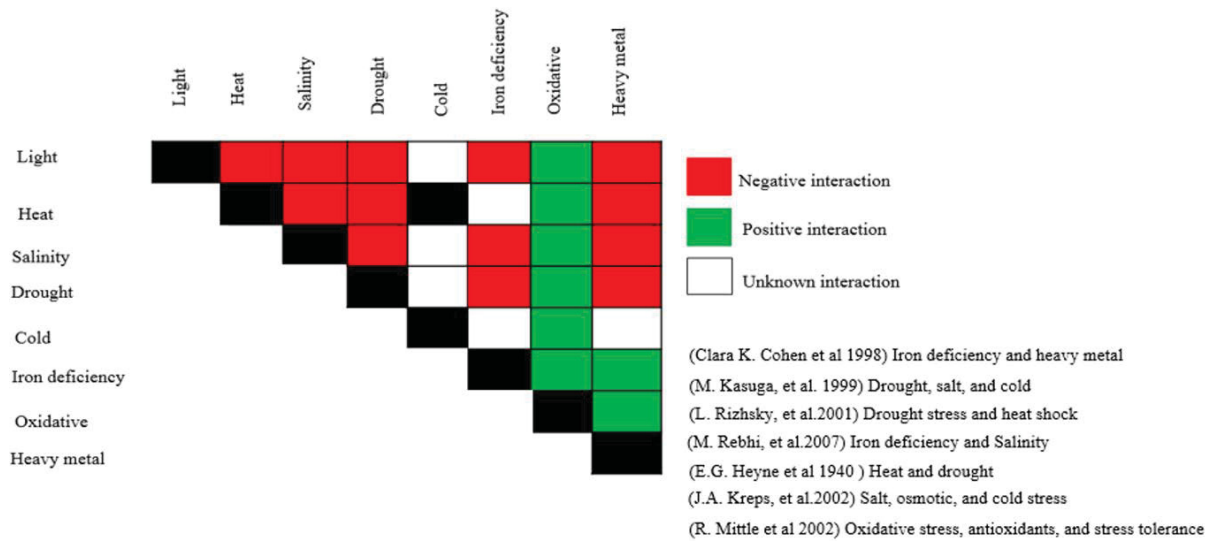


**Figure 3:** The stress matrix: A summary of agriculturally important stress combinations and their effects. The outcome of the different stress combinations is presented in different colors indicating the type of the interaction: red color (negative interaction), green (positive interaction), black (no interaction), and white (unknown interaction).

One of the first studies in stress combinations, especially alkalinity and salinity was performed by (Rabhi et al. 2007) using *Medicago ciliaris*. Plants adopt shared responses which are general physiological adjustments for guarding the plants against many stresses. Recently, certain adaptation strategies specific for multiple stress combinations have been reported (Mittler 2006; Prasch and Sonnewald 2013). Among different stress combinations that occur under field conditions, heat and drought stress and their interaction with pathogens are the most studied (Mittler 2006; Pandey et al. 2015; Ramegowda and Senthil-Kumar 2015). The adaptation strategy to a combination of two stresses consists of “shared” and “unique” responses. Molecular and physiological responses common to two different stresses are known as shared responses and those which are specific to an individual or combined stress are called unique responses (Rizhsky et al. 2002). The appearance of many abiotic stresses such as heat, salinity, alkalinity, and drought changes the reaction of plants to certain stresses. Depending on the plant species and stress intensity, the plants can either become resistant or susceptible in response to the output of the stress combination. Many transgenic plants subjected to single stress under standard laboratory conditions show enhanced tolerance but fail in the naturally occurring field conditions. Therefore, the combination of different stresses to study molecular, physiological, and metabolic aspects should be focused to obtain plants with enhanced tolerance to field stress conditions. Both

## Introduction

alkalinity and salinity can co-occur which leads to high concentration of sodium carbonates (Alkalinity). This soil has a poor texture, affecting its hydraulic conductivity, which ultimately leads to the low availability of water to the plants (Bernstein 1975; Rengasamy 2010). Therefore, plants tailored their osmotic adjustment in goal to cope with combined salinity and alkalinity. Because of these shared challenges, closely related lineages evolved in parallel with similar traits of mechanisms to tolerate both salt and alkaline stresses (Saslis-Lagoudakis et al. 2014). Saline and alkaline stress are well known in North African fields. *M. truncatula* accessions were tested under combined stress and it was demonstrated that contrasting lines have the ability to tolerate the combined stress (Abdallah et al. 2017).

### 9. Examples of plant responses to stress combination

A situation in which a plant is subjected to two or more abiotic and biotic stresses simultaneously is known as combined stress which leads to the major crop loss worldwide (Mittler 2006). However, it has been acknowledged as a major cause of crop loss worldwide (Mittler 2006). The response to a single stress is different to that observed in combined stress, which could be the main reason of the failure in obtaining tolerant transgenic plants. Recent studies clearly demonstrated the global effects of different kinds of combined stress. For instance, it has been reported that combined temperature and salinity stress impacts seed germination of various plant species (Gorai et al. 2014; Sanchez et al. 2014; Xu et al. 2016). However, while studying the effect of combined stress it was observed that it can affect the chlorophyll metabolism at both physiological and transcriptional levels resulting in a marked decrease in the photosynthetic rate and a clear reduction of the expression of the chlorophyll biosynthesis gene porphobilinogen deaminase (*PBGD*) (Hu et al. 2016). On the other hand, (Amirinejad et al. 2017) emphasized a noticeable loss in growth and yield in pepper (*Capsicum annuum L.*) exposed to the same combined stress. The plants recovered when adding salicylic acid which lead to an increase in the chlorophyll content, the relative water content, and inhibited proline accumulation. In the same way, (Rabhi et al. 2007) showed that *Medicago ciliaris* under combined alkalinity and salinity displayed a decline in chlorophyll content and consequently the biomass production which presents an additive response of the combined stress. Likewise, this combined stress caused a significant reduction in germination rate and radical elongation in the seedlings of *Medicago ciliaris*. Interestingly, similar studies also showed that there was a competitive interaction between  $\text{Na}^+$  and  $\text{K}^+$  ions under such stresses leading to an inversely proportional content of these two cations (Li et al. 2010). Furthermore, a recent

## Introduction

transcriptome analysis in alfalfa (*Medicago sativa*) subjected to the some stress combinations revealed an evident upregulation of the ROS scavenging pathway (An et al. 2016). The same author also demonstrated that flavonoids play a key role in the saline-alkaline stress tolerance mechanism (An et al. 2016). In other combined stress studies, the response to the combination of high temperature and drought stress in citrus was found to be genotype specific. In fact, compared to a sensible genotype, the tolerant genotype of citrus is characterized by a higher transpiration rate using a robust cooling system of the leaf surface modulated by a decrease in abscisic acid levels (Zandalinas et al. 2016). In wheat, the combination of drought and heat stress enhanced the expression of HSP (heat shock protein) greater than the expression observed in the single stresses. This result suggested that the type of interaction of the stress is not additive (Grigorova et al. 2011). Combined stress can lead to a loss or gain in plant yield. Therefore, scientists designed studies in different interactions between multiple stresses such as negative, positive, or neutral (Suzuki et al. 2014). Negative interactions of multiple stresses occur but plants are not able to recognize and respond correctly to them. It has been predicted by the climate change models that changes in drought and heat waves will occur in the future which will lead to a reduction in agricultural production. Therefore, it is important to study the individual stresses which could elicit a negative effect on plant growth and reproduction. Thus far many studies has been performed to show the resistance in barley to combined drought and salinity (Ahmed et al. 2013), salinity and nutrients (Mittler and Blumwald 2010), drought and heavy metal (de Silva et al. 2012). Positive interaction of combined stresses take place when compared to the individual stresses the stress combinations has positive effects on the plants. Unlike the combined negative effects of drought and heat stress on plant growth, the combined stress of salt and heat leads to the protection of tomato plants. While alone the effects of either the salt stress, salinity or heat causes damages (Rivero et al. 2014).

### 10. Natural variation and diversity

The natural variation of crops has been exploited for thousands of years of domestication by genetic manipulation of the characteristics in development and physiological adaptation related to agriculture (Brown et al. 2009). QTL analysis, which associates the phenotypic and allelic variation, is nowadays widely used in analyzing the genetic diversity in natural populations in many species (González-Martínez et al. 2006). QTL mapping used examples such as flowering time, plant height, and grain weight to map genomic regions associated with a particular phenotype. This approach used recombinant inbred lines (RIL) e.g. of wheat to get agronomic

## Introduction

traits of grain and yield loss. This resulted in using the trait marker in the selection of wheat variations (Cui et al. 2014; Velu et al. 2017). One good way to validate the QTL mapping is by using near-isogenic lines in many crop plants such as pea (Lavaud et al. 2015) and barley (Naz et al. 2014). Recently, various molecular tools and approaches have been developed for a deep genetic analysis and mapping of natural variation in cultivated and wild relative crops. For instance, many genetic resources are currently available for diverse crops such as rice (*Oryza sativa*) (Zhao et al. 2011), medic (*Medicago truncatula*) (Burghardt et al. 2017; Curtin et al. 2017), and barley (*Hordeum vulgare*) (Comadran et al. 2012). These genomic resources have been widely exploited for the identification of QTLs and genes involved in the tolerance to environmental constraints and yield quality (Zhang et al. 2009). In addition, the recent availability of genome sequences of many cultivated plant species and the use of the genome-wide association approach (GWAS) can be a powerful tool for the identification of new genes with important agronomic traits in many crop species, such as rice (Yano et al. 2016), wheat (*Triticum aestivum*) (Guo et al. 2017), and mais (*Zea mays*) (Saengwilai et al. 2016). Such investigations demonstrated the usefulness of the GWAS approach in decrypting the natural variation of desired agronomic traits that can be molecularly dissected. Rice is one of the most important crops which serve as an essential human nutrition all over the world. Therefore, there are many studies of natural variation to understand the genetic basis of these variations in rice plants in the morphology of flag leaf (Taguchi-Shiobara et al. 2015), root angle distribution (Tomita et al. 2017), and seed storage (Li et al. 2017). Another important crop are the legumes. Because of symbiotic bacteria, leguminous plants have the ability to fix nitrogen from the air to the nodules helping to increase soil fertility. Alfalfa presents the major legume crop, thereby many studies have been done in leaf development of *Medicago truncatula* (Liao et al. 2017), root growth (Patel et al. 2017) and nodulation (Curtin et al. 2017). Likewise, the analysis of natural variation in wild species has begun to elucidate the molecular basis of phenotypic differences related to plant adaptation to distinct natural environments and to determine the evolutionary and ecological processes that preserve these variations (Mitchell-Olds et al. 2007). A genome-wide association studies in the Tunisian *Medicago truncatula* lines showed around 10% of genetic variation between lines originated from saline and from non-saline areas (Friesen et al. 2010). Likewise, the analysis of fourteen *M. truncatula* lines in their resistance to pathogen infection identified a significant correlation between the tested traits and the geographical distribution of these lines. Moreover, the natural variation from these selected lines

## Introduction

of *M. truncatula* were more likely to be sensitive than tolerant to pathogens (Djébali et al. 2013). Similarly, analysis of natural variation in wildlife species elucidated some of the molecular basis of the plant-specific differences in the adaptation to distinct natural environments and to determine the evolutionary and ecological processes (Mitchell-Olds et al. 2007). The model plant *A. thaliana* is currently considered as the main resource to understand genes and nucleotide polymorphisms (Atwell et al. 2010; Cao et al. 2011; Gan et al. 2011). Its ubiquitousness as a weed plant as well as the small size of its completely sequenced genome has greatly added to its molecular characterization in the last decades. The genomic resource of this species cannot be extrapolated to in many other crops due to their genetic divergence. These scientists proposed other model species such as rice (Duan et al. 2017) and *Medicago truncatula* (Ronfort et al. 2006) by checking their genetic potential with their large collections to explore naturally occurring diversity in these species. Beside genomic analyzes, RNA-sequencing is widely used and useful in plant systems, aiming to improve the quality of bioinformatics tools and gene sequencing technology across many plant species (Comadran et al. 2012; Nam et al. 2017). In the last years, the development of RNA-Seq techniques and protocols increased whereas the cost decreased. RNA sequencing was also used for natural variation of maize genotypes under heat and cold stress to document regulatory features of genes related to combined stress (Waters et al. 2017). During germination, the natural variation in rice genotypes in genes controlling coleoptile growth were reported, which facilitates the direct breeding of rice seedlings (Hsu and Tung 2017).

## 11. Objectives and Aims

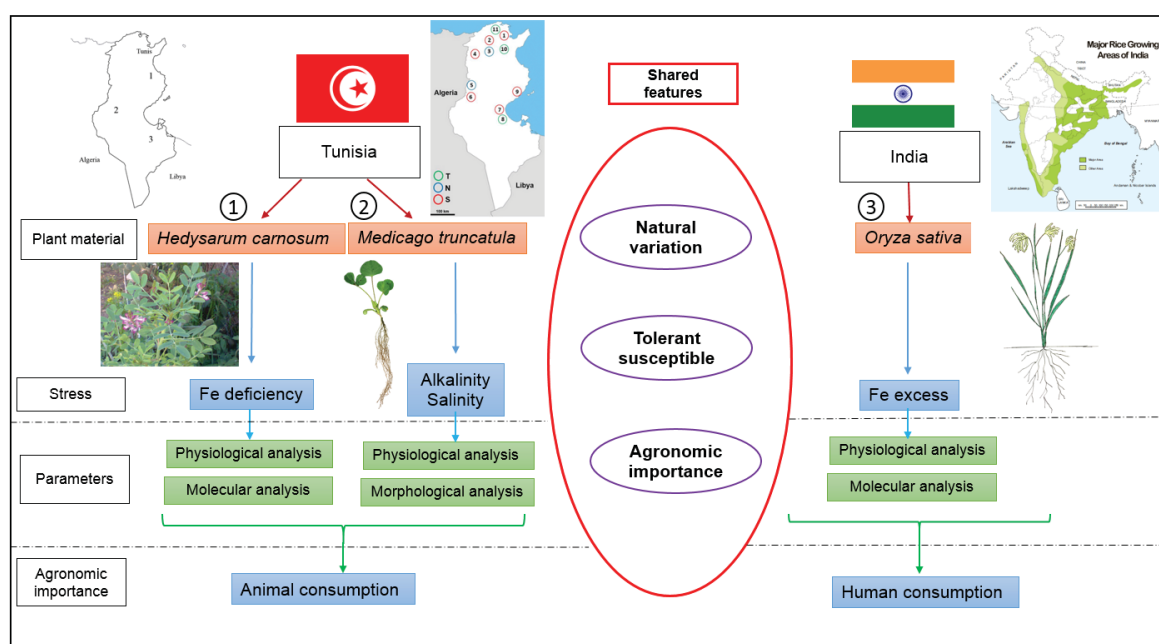


**Figure 4:** Summary and connection of the different chapters of my cumulative dissertation. It shows the plant material, applied stress, tested parameters, and commonly shared features.

Concerning the plant material, two leguminous plants were used that originate from Tunisia and are used as a fodder for animals and rice from India that presents important staple food in Asia. Stresses applied are iron-deficiency in *Hedysarum carnosum* and iron-overload in rice genotypes. Combined stress of alkalinity and salinity was used in the *Medicago* lines. The shared features in this work were natural variation, selection of contrasting lines to their responses to combined stress, and the economic, agronomic value of these lines. Figure 4 summarizes the different chapters of this dissertations, the plant species used, and the stresses analyzed in their physiological, morphological, or molecular plant responses. The first publication a protocol for a reliable RT-qPCR assay, which can be easily adapted to any plant species of interest. We describe in detail all the steps and setup, the protocol is very informative and can be used as design of the qPCR strategy. The main objective of the first section of the dissertation was to investigate the effects of iron deficiency at the physiological and molecular level of the non-model extremophile species *Hedysarum carnosum* and to compare the responses in three different isolates collected from different natural sites.

## Introduction

In the field, crops and other plants are routinely exposed to a combination of different abiotic stresses. Salinity and alkalinity are widespread in Tunisia where *Medicago truncatula* occurs as a native species. The main aim of the third chapter was to investigate the collective effects of both, the salinity and alkaline soil conditions, for different parameters like germination, plant growth, leaf pigment content, and root morphology in *M. truncatula* varieties. The specific objectives of this study were 1. To establish of growth conditions using the reference line Jemalong A17 and to check the effects of individual and combined stress in a hydroponic growth system, 2, to screen 11 Tunisian *M. truncatula* lines of the SARDI collection under combined stress, to analyze the selected tolerant and sensitive lines under the combined stress in the hydroponic system, and 3. To check the effect of combined bicarbonate and salt stress (BIC/NaCl) on the flavin concentration and cellular distribution in root tips of sensitive and tolerant *M. truncatula* lines. The last section investigates the specific responses of contrasting rice genotypes to excess iron. For this, RNA sequencing technique was used to identify transcriptional changes in the response to short exposure to Fe excess. This will allow a better understanding of the responses of rice plants and suggests the involvement of novel genes in Fe metabolism under Fe toxicity.

### 12. References:

- Abdallah HB, Mai H-J, Álvarez-Fernández A, Abadía J, Bauer P (2017) Natural variation reveals contrasting abilities to cope with alkaline and saline soil among different *Medicago truncatula* genotypes. *Plant and Soil* 418: 45-60.
- Ahmed IM, Dai H, Zheng W, Cao F, Zhang G, Sun D, Wu F (2013) Genotypic differences in physiological characteristics in the tolerance to drought and salinity combined stress between Tibetan wild and cultivated barley. *Plant Physiology and Biochemistry* 63: 49-60.
- Altinok S, Yurtseven E, Avci S, Öztürk HS, Selenay MF (2015) The effects of different irrigation water salinities and leaching ratios on green and dry forage yields of alfalfa (*Medicago sativa* L.). *Poljoprivreda i Sumarstvo* 61: 85.
- Amirinejad A, Sayyari M, Ghanbari F, Kordi S (2017) Salicylic acid improves salinity-alkalinity tolerance in pepper (*Capsicum annuum* L.). *Advances in Horticultural Science* 31: 157.
- Amirjani MR (2011) Effect of salinity stress on growth, sugar content, pigments and enzyme activity of rice. *International Journal of Botany* 7: 73-81.
- An Y-M, Song L-L, Liu Y-R, Shu Y-J, Guo C-H (2016) De novo transcriptional analysis of alfalfa in response to saline-alkaline stress. *Frontiers in plant science* 7.
- Arosio P, Ingrassia R, Cavadini P (2009) Ferritins: a family of molecules for iron storage, antioxidation and more. *Biochimica et Biophysica Acta (BBA)-General Subjects* 1790: 589-599.
- Arosio P, Levi S (2002) Ferritin, iron homeostasis, and oxidative damage 1, 2. *Free Radical Biology and Medicine* 33: 457-463.
- Atkinson NJ, Lilley CJ, Urwin PE (2013) Identification of genes involved in the response of *Arabidopsis* to simultaneous biotic and abiotic stresses. *Plant Physiology* 162: 2028-2041.
- Atwell S, Huang YS, Vilhjálmsson BJ, Willems G, Horton M, Li Y, Meng D, Platt A, Tarone AM, Hu TT (2010) Genome-wide association study of 107 phenotypes in *Arabidopsis thaliana* inbred lines. *Nature* 465: 627-631.
- Audebert A, Sahrawat KL (2000) Mechanisms for iron toxicity tolerance in lowland rice. *Journal of Plant Nutrition* 23: 1877-1885.
- Bauer MW (2005) Distinguishing red and green biotechnology: cultivation effects of the elite press. *International journal of public opinion research* 17: 63-89.
- Becker M, Asch F (2005) Iron toxicity in rice—conditions and management concepts. *Journal of Plant Nutrition and Soil Science* 168: 558-573.
- Berezniak A, Ben-Gal A, Mishael Y, Nachshon U (2017) Manipulation of Soil Texture to Remove Salts from a Drip-Irrigated Root Zone. *Vadose Zone Journal*.
- Berkman PJ, Lai K, Lorenc MT, Edwards D (2012) Next-generation sequencing applications for wheat crop improvement. *American journal of botany* 99: 365-371.
- Bernstein L (1975) Effects of salinity and sodicity on plant growth. *Annual review of phytopathology* 13: 295-312.
- Birla DS, Malik K, Sainger M, Chaudhary D, Jaiwal R, Jaiwal PK (2017) Progress and challenges in improving the nutritional quality of rice (*Oryza sativa* L.). *Critical reviews in food science and nutrition* 57: 2455-2481.
- Boyer JS (1982) Plant productivity and environment. *Science* 218: 443-448.
- Brown TA, Jones MK, Powell W, Allaby RG (2009) The complex origins of domesticated crops in the Fertile Crescent. *Trends in Ecology & Evolution* 24: 103-109.
- Brumbarova T, Bauer P, Ivanov R (2015) Molecular mechanisms governing *Arabidopsis* iron uptake. *Trends in plant science* 20: 124-133.
- Burghardt LT, Guhlin J, Chun CL, Liu J, Sadowsky MJ, Stupar RM, Young ND, Tiffin P (2017) Transcriptomic basis of genome by genome variation in a legume-rhizobia mutualism. *Molecular Ecology*.

## References

- Cao J, Schneeberger K, Ossowski S, Günther T, Bender S, Fitz J, Koenig D, Lanz C, Stegle O, Lippert C (2011) Whole-genome sequencing of multiple *Arabidopsis thaliana* populations. *Nature genetics* 43: 956-963.
- Chen Y, Barak P (1982) Iron nutrition of plants in calcareous soils. *Advances in agronomy* 35: 217-240.
- Chiang S, Kovacevic Z, Sahni S, Lane DJ, Merlot AM, Kalinowski DS, Huang ML-H, Richardson DR (2016) Frataxin and the molecular mechanism of mitochondrial iron-loading in Friedreich's ataxia. *Clinical Science* 130: 853-870.
- Cohen CK, Fox TC, Garvin DF, Kochian LV (1998) The role of iron-deficiency stress responses in stimulating heavy-metal transport in plants. *Plant Physiology* 116: 1063-1072.
- Colombo C, Palumbo G, He J-Z, Pinton R, Cesco S (2014) Review on iron availability in soil: interaction of Fe minerals, plants, and microbes. *Journal of Soils and Sediments* 14: 538-548.
- Comadran J, Kilian B, Russell J, Ramsay L, Stein N, Ganai M, Shaw P, Bayer M, Thomas W, Marshall D (2012) Natural variation in a homolog of *Antirrhinum CENTRORADIALIS* contributed to spring growth habit and environmental adaptation in cultivated barley. *Nature genetics* 44: 1388-1392.
- Cui F, Zhao C, Ding A, Li J, Wang L, Li X, Bao Y, Li J, Wang H (2014) Construction of an integrative linkage map and QTL mapping of grain yield-related traits using three related wheat RIL populations. *Theoretical and applied genetics* 127: 659-675.
- Curie C, Cassin G, Couch D, Divol F, Higuchi K, Le Jean M, Misson J, Schikora A, Czernic P, Mari S (2008) Metal movement within the plant: contribution of nicotianamine and yellow stripe 1-like transporters. *Annals of botany* 103: 1-11.
- Curtin SJ, Tiffin P, Guhlin J, Trujillo DI, Burghardt LT, Atkins P, Baltes NJ, Denny R, Voytas DF, Stupar RM (2017) Validating genome-wide association candidates controlling quantitative variation in nodulation. *Plant physiology* 173: 921-931.
- Daei G, Ardekani M, Rejali F, Teimuri S, Miransari M (2009) Alleviation of salinity stress on wheat yield, yield components, and nutrient uptake using arbuscular mycorrhizal fungi under field conditions. *Journal of plant physiology* 166: 617-625.
- Dat J, Vandenabeele S, Vranová E, Van Montagu M, Inzé D, Van Breusegem F (2000) Dual action of the active oxygen species during plant stress responses. *Cellular and Molecular Life Sciences CMLS* 57: 779-795.
- de Silva NDG, Cholewa E, Ryser P (2012) Effects of combined drought and heavy metal stresses on xylem structure and hydraulic conductivity in red maple (*Acer rubrum* L.). *Journal of experimental botany* 63: 5957-5966.
- Djébali N, Aribi S, Taamalli W, Arraouadi S, Aouani ME, Badri M (2013) Natural variation of *Medicago truncatula* resistance to *Aphanomyces euteiches*. *European journal of plant pathology* 135: 831-843.
- Duan P, Xu J, Zeng D, Zhang B, Geng M, Zhang G, Huang K, Huang L, Xu R, Ge S (2017) Natural variation in the promoter of *GSE5* contributes to grain size diversity in rice. *Molecular Plant* 10: 685-694.
- Edwards D, Batley J, Snowdon RJ (2013) Accessing complex crop genomes with next-generation sequencing. *Theoretical and Applied Genetics* 126: 1-11.
- Eide D, Broderius M, Fett J, Guerinot ML (1996) A novel iron-regulated metal transporter from plants identified by functional expression in yeast. *Proceedings of the National Academy of Sciences* 93: 5624-5628.
- Eraslan F, Inal A, Savasturk O, Gunes A (2007) Changes in antioxidative system and membrane damage of lettuce in response to salinity and boron toxicity. *Scientia Horticulturae* 114: 5-10.
- Fageria NK (2016) The use of nutrients in crop plants. CRC press.
- Fageria NK, Baligar VC, Clark R (2006) Physiology of crop production. CRC Press.
- Foreman J, Demidchik V, Bothwell JH, Mylona P (2003) Reactive oxygen species produced by NADPH oxidase regulate plant cell growth. *Nature* 422: 442.

## References

- Franssen SU, Shrestha RP, Bräutigam A, Bornberg-Bauer E, Weber AP (2011) Comprehensive transcriptome analysis of the highly complex *Pisum sativum* genome using next generation sequencing. *BMC genomics* 12: 227.
- Friesen ML, Cordeiro MA, Penmetsa RV, Badri M, Huguet T, Aouani ME, Cook DR, Nuzhdin SV (2010) Population genomic analysis of Tunisian *Medicago truncatula* reveals candidates for local adaptation. *The Plant Journal* 63: 623-635.
- Gan X, Stegle O, Behr J, Steffen JG, Drewe P, Hildebrand KL, Lyngsoe R, Schultheiss SJ, Osborne EJ, Sreedharan VT (2011) Multiple reference genomes and transcriptomes for *Arabidopsis thaliana*. *Nature* 477: 419-423.
- González-Martínez SC, Krutovsky KV, Neale DB (2006) Forest-tree population genomics and adaptive evolution. *New Phytologist* 170: 227-238.
- Gorai M, El Aloui W, Yang X, Neffati M (2014) Toward understanding the ecological role of mucilage in seed germination of a desert shrub *Henophyton deserti*: interactive effects of temperature, salinity and osmotic stress. *Plant and Soil* 374: 727-738.
- Grewell BJ, Castillo JM, Thomason MJS, Drenovsky RE (2016) Phenotypic plasticity and population differentiation in response to salinity in the invasive cordgrass *Spartina densiflora*. *Biological Invasions* 18: 2175-2187.
- Grigorova B, Vaseva II, Demirevska K, Feller U (2011) Expression of selected heat shock proteins after individually applied and combined drought and heat stress. *Acta physiologiae plantarum* 33: 2041-2049.
- Guerinot ML, Yi Y (1994) Iron: Nutritious, Noxious, and Not Readily Available. *Plant Physiology* 104: 815-820. doi: 10.1104/pp.104.3.815.
- Guo Z, Chen D, Alqudah AM, Röder MS, Ganai MW, Schnurbusch T (2017) Genome-wide association analyses of 54 traits identified multiple loci for the determination of floret fertility in wheat. *New Phytologist* 214: 257-270.
- Heyne E, Brunson AM (1940) Genetic studies of heat and drought tolerance in maize. *Journal of the American Society of Agronomy* 32: 803-814.
- Hsu S-K, Tung C-W (2017) RNA-seq analysis of diverse rice genotypes to identify the genes controlling coleoptile growth during submerged germination. *Frontiers in plant science* 8.
- Hu L, Li H, Pang H, Fu J (2012) Responses of antioxidant gene, protein and enzymes to salinity stress in two genotypes of perennial ryegrass (*Lolium perenne*) differing in salt tolerance. *Journal of plant physiology* 169: 146-156.
- Hu L, Xiang L, Li S, Zou Z, Hu XH (2016) Beneficial role of spermidine in chlorophyll metabolism and D1 protein content in tomato seedlings under salinity-alkalinity stress. *Physiologia plantarum* 156: 468-477.
- Inoue H, Kobayashi T, Nozoye T, Takahashi M, Kakei Y, Suzuki K, Nakazono M, Nakanishi H, Mori S, Nishizawa NK (2009) Rice OsYSL15 is an iron-regulated iron (III)-deoxymugineic acid transporter expressed in the roots and is essential for iron uptake in early growth of the seedlings. *Journal of Biological Chemistry* 284: 3470-3479.
- Ishimaru Y, Masuda H, Bashir K, Inoue H, Tsukamoto T, Takahashi M, Nakanishi H, Aoki N, Hirose T, Ohsugi R (2010) Rice metal-nicotianamine transporter, OsYSL2, is required for the long-distance transport of iron and manganese. *The Plant Journal* 62: 379-390.
- Ishimaru Y, Suzuki M, Tsukamoto T, Suzuki K, Nakazono M, Kobayashi T, Wada Y, Watanabe S, Matsuhashi S, Takahashi M (2006) Rice plants take up iron as an Fe<sup>3+</sup>-phytosiderophore and as Fe<sup>2+</sup>. *The Plant Journal* 45: 335-346.
- Ismail RM, Elazab HE, Hussein GM, Metry EA (2011) In vitro root induction of faba bean (*Vicia faba* L.). *GM crops* 2: 176-181.

## References

- James C (2004) Double-digit growth continues for biotech crops worldwide. Ithaca, NY: International Service for the Acquisition of Agri-biotech Applications.
- James C (2014) Global status of commercialised biotech/GM crops: 2013, ISAAA Brief No. 46. International Service for the Acquisition of Agri-Biotech Applications, Ithaca, NY. ISBN 978-1-892456-55-9. [www.isaaa.org/resources/publications/briefs/46](http://www.isaaa.org/resources/publications/briefs/46).
- James RA, Blake C, Byrt CS, Munns R (2011) Major genes for Na<sup>+</sup> exclusion, Nax1 and Nax2 (wheat HKT1; 4 and HKT1; 5), decrease Na<sup>+</sup> accumulation in bread wheat leaves under saline and waterlogged conditions. *Journal of experimental botany* 62: 2939-2947.
- Jo K-R, Kim C-J, Kim S-J, Kim T-Y, Bergervoet M, Jongsma MA, Visser RG, Jacobsen E, Vossen JH (2014) Development of late blight resistant potatoes by cisgene stacking. *BMC biotechnology* 14: 50.
- Juneja A, Ceballos RM, Murthy GS (2013) Effects of environmental factors and nutrient availability on the biochemical composition of algae for biofuels production: a review. *Energies* 6: 4607-4638.
- Takei Y, Ishimaru Y, Kobayashi T, Yamakawa T, Nakanishi H, Nishizawa NK (2012) OsYSL16 plays a role in the allocation of iron. *Plant molecular biology* 79: 583-594.
- KATEMBE WJ, UNGAR IA, MITCHELL JP (1998) Effect of salinity on germination and seedling growth of two *Atriplex* species (Chenopodiaceae). *Annals of Botany* 82: 167-175.
- Khairi M, Nozulaidi M, Jahan MS (2015) Effects of different water levels on physiology and yield of salinity rice variety. *Australian Journal of Basic and Applied Sciences* 9: 339-345.
- Kobayashi T, Itai RN, Nishizawa NK (2014) Iron deficiency responses in rice roots. *Rice* 7: 27.
- Kobayashi T, Nishizawa NK (2012) Iron uptake, translocation, and regulation in higher plants. *Annual review of plant biology* 63: 131-152.
- Koike S, Inoue H, Mizuno D, Takahashi M, Nakanishi H, Mori S, Nishizawa NK (2004) OsYSL2 is a rice metal-nicotianamine transporter that is regulated by iron and expressed in the phloem. *The Plant Journal* 39: 415-424.
- Korshunova YO, Eide D, Clark WG, Guerinot ML, Pakrasi HB (1999) The IRT1 protein from *Arabidopsis thaliana* is a metal transporter with a broad substrate range. *Plant molecular biology* 40: 37-44.
- Kosová K, Vítámvás P, Hlaváčková I, Urban M, Vlasáková E, Prášil I (2015) Responses of two barley cultivars differing in their salt tolerance to moderate and high salinities and subsequent recovery. *Biologia plantarum* 59: 106-114.
- Kovda V (2013) FERTILITY: PROBLEMS OF SALINITY, ALKALINITY, COMPACTION. *Arid Land Irrigation in Developing Countries: Environmental Problems and Effects*: 211.
- Krishnamurthy S, Sharma P, Sharma S, Batra V, Kumar V, Rao L (2016) Effect of salinity and use of stress indices of morphological and physiological traits at the seedling stage in rice.
- Lavaud C, Lesne A, Piriou C, Le Roy G, Boutet G, Moussart A, Poncet C, Delourme R, Baranger A, Pilet-Nayel M-L (2015) Validation of QTL for resistance to *Aphanomyces euteiches* in different pea genetic backgrounds using near-isogenic lines. *Theoretical and applied genetics* 128: 2273-2288.
- Lawlor DW, Cornic G (2002) Photosynthetic carbon assimilation and associated metabolism in relation to water deficits in higher plants. *Plant, cell & environment* 25: 275-294.
- Leke WN, Khatabi B, Fondong VN, Brown JK (2016) Complete genome sequence of a new bipartite begomovirus infecting fluted pumpkin (*Telfairia occidentalis*). *Archives of virology* 161: 2347-2350.
- Li C, Shao G, Wang L, Wang Z, Mao Y, Wang X, Zhang X, Liu S, Zhang H (2017) QTL Identification and Fine Mapping for Seed Storability in Rice (*Oryza sativa* L.). *Euphytica* 213: 127.
- Li D-H, Hui L, Yang Y-L, Zhen P-P, Liang J-S (2009) Down-regulated expression of RACK1 gene by RNA interference enhances drought tolerance in rice. *Rice Science* 16: 14-20.
- Li R, Shi F, Fukuda K, Yang Y (2010) Effects of salt and alkali stresses on germination, growth, photosynthesis and ion accumulation in alfalfa (*Medicago sativa* L.). *Soil Science & Plant Nutrition* 56: 725-733.

## References

- Liao F, Peng J, Chen R (2017) LeafletAnalyzer, an automated software for quantifying, comparing and classifying blade and serration features of compound leaves during development, and among induced mutants and natural variants in the legume *Medicago truncatula*. *Frontiers in Plant Science* 8.
- Lobell DB, Schlenker W, Costa-Roberts J (2011) Climate trends and global crop production since 1980. *Science* 333: 616-620.
- Maas E, Grieve C (1987) Sodium-induced calcium deficiency in salt-stressed corn. *Plant, Cell & Environment* 10: 559-564.
- Marques EC, de Freitas PAF, Alencar NLM, Prisco JT, Gomes-Filho E (2013) Increased Na<sup>+</sup> and Cl<sup>-</sup> accumulation induced by NaCl salinity inhibits cotyledonary reserve mobilization and alters the source-sink relationship in establishing dwarf cashew seedlings. *Acta physiologiae plantarum* 35: 2171-2182.
- Matthus E, Wu L-B, Ueda Y, Höller S, Becker M, Frei M (2015) Loci, genes, and mechanisms associated with tolerance to ferrous iron toxicity in rice (*Oryza sativa* L.). *Theoretical and applied genetics* 128: 2085-2098.
- Mitchell-Olds T, Willis JH, Goldstein DB (2007) Which evolutionary processes influence natural genetic variation for phenotypic traits? *Nature reviews Genetics* 8: 845.
- Mittler R (2002) Oxidative stress, antioxidants and stress tolerance. *Trends in plant science* 7: 405-410.
- Mittler R (2006) Abiotic stress, the field environment and stress combination. *Trends in plant science* 11: 15-19.
- Mittler R (2017) ROS are good. *Trends in plant science* 22: 11-19.
- Mittler R, Blumwald E (2010) Genetic engineering for modern agriculture: challenges and perspectives. *Annual review of plant biology* 61: 443-462.
- Mongon J, Konnerup D, Colmer TD, Rerkasem B (2014) Responses of rice to Fe<sup>2+</sup> in aerated and stagnant conditions: growth, root porosity and radial oxygen loss barrier. *Functional Plant Biology* 41: 922-929.
- Moriuchi KS, Friesen ML, Cordeiro MA, Badri M, Vu WT, Main BJ, Aouani ME, Nuzhdin SV, Strauss SY, von Wettberg EJ (2016) Salinity adaptation and the contribution of parental environmental effects in *Medicago truncatula*. *PloS one* 11: e0150350.
- Munne-Bosch S, Pinto-Marijuan M (2016) Free radicals, oxidative stress and antioxidants. *Encycl Appl Plant Sci* 2: 16-19.
- Munns R, James RA, Läuchli A (2006) Approaches to increasing the salt tolerance of wheat and other cereals. *Journal of experimental botany* 57: 1025-1043.
- Munns R, Tester M (2008) Mechanisms of salinity tolerance. *Annu Rev Plant Biol* 59: 651-681.
- Murphy DJ (2007) Future prospects for oil palm in the 21st century: Biological and related challenges. *European Journal of Lipid Science and Technology* 109: 296-306.
- Nakanishi H, Ogawa I, Ishimaru Y, Mori S, Nishizawa NK (2006) Iron deficiency enhances cadmium uptake and translocation mediated by the Fe<sup>2+</sup> transporters OsIRT1 and OsIRT2 in rice. *Soil Science & Plant Nutrition* 52: 464-469.
- Nam Y-J, Herman D, Blomme J, Chae E, Kojima M, Coppens F, Storme V, Van Daele T, Dhondt S, Sakakibara H (2017) Natural Variation of Molecular and Morphological Gibberellin Responses. *Plant physiology* 173: 703-714.
- Nathan MV (2017) Soils, plant nutrition and nutrient management.
- Naz AA, Arifuzzaman M, Muzammil S, Pillen K, Léon J (2014) Wild barley introgression lines revealed novel QTL alleles for root and related shoot traits in the cultivated barley (*Hordeum vulgare* L.). *BMC genetics* 15: 107.

## References

- Nguyen HT, Meir P, Sack L, Evans JR, Oliveira RS, Ball MC (2017) Leaf water storage increases with salinity and aridity in the mangrove *Avicennia marina*: integration of leaf structure, osmotic adjustment, and access to multiple water sources. *Plant, Cell & Environment*.
- Noman A, Fahad S, Aqeel M, Ali U, Anwar S, Baloch SK, Zainab M (2017) miRNAs: major modulators for crop growth and development under abiotic stresses. *Biotechnology letters*: 1-16.
- Nozoye T, Nagasaka S, Kobayashi T, Takahashi M, Sato Y, Sato Y, Uozumi N, Nakanishi H, Nishizawa NK (2011) Phytosiderophore efflux transporters are crucial for iron acquisition in graminaceous plants. *Journal of Biological Chemistry* 286: 5446-5454.
- Oliveira HR, Tomás D, Silva M, Lopes S, Viegas W, Veloso MM (2016) Genetic diversity and population structure in *Vicia faba* L. landraces and wild related species assessed by nuclear SSRs. *PLoS one* 11: e0154801.
- Pandey P, Ramegowda V, Senthil-Kumar M (2015) Shared and unique responses of plants to multiple individual stresses and stress combinations: physiological and molecular mechanisms. *Frontiers in plant science* 6.
- Panta S, Flowers T, Doyle R, Lane P, Haros G, Shabala S (2016) Growth responses of *Atriplex lentiformis* and *Medicago arborea* in three soil types treated with saline water irrigation. *Environmental and Experimental Botany* 128: 39-50.
- Patel N, Mohd-Radzman NA, Corcilus L, Crossett B, Connolly A, Cordwell SJ, Ivanovici A, Taylor K, Williams J, Binos S (2017) Diverse peptide hormones affecting root growth identified in the *Medicago truncatula* secreted peptidome. *Molecular & Cellular Proteomics*: mcp. RA117. 000168.
- Pecinka A, Dinh HQ, Baubec T, Rosa M, Lettner N, Scheid OM (2010) Epigenetic regulation of repetitive elements is attenuated by prolonged heat stress in *Arabidopsis*. *The Plant Cell* 22: 3118-3129.
- Porcel R, Redondo-Gómez S, Mateos-Naranjo E, Aroca R, Garcia R, Ruiz-Lozano JM (2015) Arbuscular mycorrhizal symbiosis ameliorates the optimum quantum yield of photosystem II and reduces non-photochemical quenching in rice plants subjected to salt stress. *Journal of plant physiology* 185: 75-83.
- Prasch CM, Sonnewald U (2013) Simultaneous application of heat, drought, and virus to *Arabidopsis* plants reveals significant shifts in signaling networks. *Plant Physiology* 162: 1849-1866.
- Prohens J, Gramazio P, Plazas M, Dempewolf H, Kilian B, Díez MJ, Fita A, Herraiz FJ, Rodríguez-Burruezo A, Soler S (2017) Introgressomics: a new approach for using crop wild relatives in breeding for adaptation to climate change. *Euphytica* 213: 158.
- Provin T, Pitt JL (2001) Managing soil salinity. Texas FARMER Collection.
- Puig S, Ramos-Alonso L, Romero AM, Martínez-Pastor MT (2017) The elemental role of iron in DNA synthesis and repair. *Metallomics* 9: 1483-1500.
- Rabhi M, Barhoumi Z, Ksouri R, Abdelly C, Gharsalli M (2007) Interactive effects of salinity and iron deficiency in *Medicago ciliaris*. *Comptes rendus biologies* 330: 779-788.
- Ramegowda V, Senthil-Kumar M (2015) The interactive effects of simultaneous biotic and abiotic stresses on plants: mechanistic understanding from drought and pathogen combination. *Journal of plant physiology* 176: 47-54.
- Ramos AC, Martins MA, Okorokova-Façanha AL, Olivares FL, Okorokov LA, Sepúlveda N, Feijó JA, Façanha AR (2009) Arbuscular mycorrhizal fungi induce differential activation of the plasma membrane and vacuolar H<sup>+</sup> pumps in maize roots. *Mycorrhiza* 19: 69-80.
- Rangani J, Parida AK, Panda A, Kumari A (2016) Coordinated changes in antioxidative enzymes protect the photosynthetic machinery from salinity induced oxidative damage and confer salt tolerance in an extreme halophyte *Salvadora persica* L. *Frontiers in plant science* 7.
- Ravet K, Touraine B, Boucherez J, Briat JF, Gaymard F, Cellier F (2009) Ferritins control interaction between iron homeostasis and oxidative stress in *Arabidopsis*. *The Plant Journal* 57: 400-412.

## References

- Rengasamy P (2010) Soil processes affecting crop production in salt-affected soils. *Functional Plant Biology* 37: 613-620.
- Rengasamy P (2016) Soil salinization.
- Rhoades J, Loveday J (1990) Salinity in irrigated agriculture. *Agronomy*: 1089-1142.
- Rivero RM, Mestre TC, Mittler R, Rubio F, GARCIA-SANCHEZ F, Martinez V (2014) The combined effect of salinity and heat reveals a specific physiological, biochemical and molecular response in tomato plants. *Plant, cell & environment* 37: 1059-1073.
- Rizhsky L, Liang H, Mittler R (2002) The combined effect of drought stress and heat shock on gene expression in tobacco. *Plant physiology* 130: 1143-1151.
- Rogovska NP, Blackmer AM, Mallarino AP (2007) Relationships between soybean yield, soil pH, and soil carbonate concentration. *Soil Science Society of America Journal* 71: 1251-1256.
- Ronfort J, Bataillon T, Santoni S, Delalande M, David JL, Prosperi J-M (2006) Microsatellite diversity and broad scale geographic structure in a model legume: building a set of nested core collection for studying naturally occurring variation in *Medicago truncatula*. *BMC Plant Biology* 6: 28.
- Saengwilai P, Schneider H, Nord EA, Johnson JM, Foerster J, Kaeppler SM, Brown KM, Lynch JP (2016) Phenotypic variation and Genome-wide association study of root anatomical traits in maize (*Zea mays* L.). ProQuest Number: 10005940: 116.
- Sahrawat KL (2016) Soil and Plant Testing for Iron: An Appraisal. *Communications in Soil Science and Plant Analysis* 47: 280-283.
- Sanchez PL, Chen M-k, Pessaraki M, Hill HJ, Gore MA, Jenks MA (2014) Effects of temperature and salinity on germination of non-pelleted and pelleted guayule (*Parthenium argentatum* A. Gray) seeds. *Industrial Crops and Products* 55: 90-96.
- Saslis-Lagoudakis CH, Hua X, Bui E, Moray C, Bromham L (2014) Predicting species' tolerance to salinity and alkalinity using distribution data and geochemical modelling: a case study using Australian grasses. *Annals of botany* 115: 343-351.
- Schaaf G, Honsbein A, Meda AR, Kirchner S, Wipf D, von Wirén N (2006) AtIREG2 encodes a tonoplast transport protein involved in iron-dependent nickel detoxification in *Arabidopsis thaliana* roots. *Journal of Biological Chemistry* 281: 25532-25540.
- Schieber M, Chandel NS (2014) ROS function in redox signaling and oxidative stress. *Current biology* 24: R453-R462.
- Sikirou M, Saito K, Dramé KN, Saidou A, Dieng I, Ahanchédé A, Venuprasad R (2016) Soil-based screening for iron toxicity tolerance in rice using pots. *Plant Production Science* 19: 489-496.
- Sultana N, Ikeda T, Itoh R (1999) Effect of NaCl salinity on photosynthesis and dry matter accumulation in developing rice grains. *Environmental and Experimental Botany* 42: 211-220.
- Suzuki N, Rivero RM, Shulaev V, Blumwald E, Mittler R (2014) Abiotic and biotic stress combinations. *New Phytologist* 203: 32-43.
- Sytar O, Kumar A, Latowski D, Kuczynska P, Strzałka K, Prasad M (2013) Heavy metal-induced oxidative damage, defense reactions, and detoxification mechanisms in plants. *Acta physiologiae plantarum* 35: 985-999.
- Taguchi-Shiobara F, Ota T, Ebana K, Ookawa T, Yamasaki M, Tanabata T, Yamanouchi U, Wu J, Ono N, Nonoue Y (2015) Natural Variation in the Flag Leaf Morphology of Rice Due to a Mutation of the NARROW LEAF 1 Gene in *Oryza sativa* L. *Genetics* 201: 795-808.
- Tavakkoli E, Rengasamy P, McDonald GK (2010) High concentrations of Na<sup>+</sup> and Cl<sup>-</sup> ions in soil solution have simultaneous detrimental effects on growth of faba bean under salinity stress. *Journal of Experimental Botany* 61: 4449-4459.
- Tefera T, Mugo S, Mwimali M, Anani B, Tende R, Beyene Y, Gichuki S, Oikeh SO, Nang'ayo F, Okeno J (2016) Resistance of Bt-maize (MON810) against the stem borers *Busseola fusca* (Fuller) and *Chilo partellus* (Swinhoe) and its yield performance in Kenya. *Crop protection* 89: 202-208.

## References

- Tomita A, Sato T, Uga Y, Obara M, Fukuta Y (2017) Genetic variation of root angle distribution in rice (*Oryza sativa* L.) seedlings. *Breeding science* 67: 181-190.
- Tripathy MK, Tiwari BS, Reddy MK, Deswal R, Sopory SK (2017) Ectopic expression of PgRab7 in rice plants (*Oryza sativa* L.) results in differential tolerance at the vegetative and seed setting stage during salinity and drought stress. *Protoplasma* 254: 109-124.
- Tsukagoshi H, Busch W, Benfey PN (2010) Transcriptional regulation of ROS controls transition from proliferation to differentiation in the root. *Cell* 143: 606-616.
- Velu G, Tutus Y, Gomez-Becerra HF, Hao Y, Demir L, Kara R, Crespo-Herrera LA, Orhan S, Yazici A, Singh RP (2017) QTL mapping for grain zinc and iron concentrations and zinc efficiency in a tetraploid and hexaploid wheat mapping populations. *Plant and Soil* 411: 81-99.
- Vert G, Grotz N, Dédaldéchamp F, Gaymard F, Guerinot ML, Briat J-F, Curie C (2002) IRT1, an Arabidopsis transporter essential for iron uptake from the soil and for plant growth. *The Plant Cell* 14: 1223-1233.
- Waters AJ, Makarevitch I, Noshay J, Burghardt LT, Hirsch CN, Hirsch CD, Springer NM (2017) Natural variation for gene expression responses to abiotic stress in maize. *The Plant Journal* 89: 706-717.
- Weber M, Harada E, Vess C, Roepenack-Lahaye Ev, Clemens S (2004) Comparative microarray analysis of Arabidopsis thaliana and Arabidopsis halleri roots identifies nicotianamine synthase, a ZIP transporter and other genes as potential metal hyperaccumulation factors. *The Plant Journal* 37: 269-281.
- Xiang L, Hu L, Hu X, Pan X, Ren W (2015) Response of reactive oxygen metabolism in melon chloroplasts to short-term salinity-alkalinity stress regulated by exogenous  $\gamma$ -aminobutyric acid. *Ying yong sheng tai xue bao= The journal of applied ecology* 26: 3746-3752.
- Xu S, Zhou Y, Wang P, Wang F, Zhang X, Gu R (2016) Salinity and temperature significantly influence seed germination, seedling establishment, and seedling growth of eelgrass *Zostera marina* L. *PeerJ* 4: e2697.
- Yano K, Yamamoto E, Aya K, Takeuchi H, Lo P-c, Hu L, Yamasaki M, Yoshida S, Kitano H, Hirano K (2016) Genome-wide association study using whole-genome sequencing rapidly identifies new genes influencing agronomic traits in rice. *Nature Genetics* 48: 927-934.
- Yi Y, Guerinot ML (1996) Genetic evidence that induction of root Fe (III) chelate reductase activity is necessary for iron uptake under iron deficiency. *The Plant Journal* 10: 835-844.
- Yi Y, Saleeba JA, Guerinot ML (1994) Iron uptake in Arabidopsis thaliana. *Biochemistry of Metal Micronutrients in the Rhizosphere*: 295-307.
- Zandalinas SI, Rivero RM, Martínez V, Gómez-Cadenas A, Arbona V (2016) Tolerance of citrus plants to the combination of high temperatures and drought is associated to the increase in transpiration modulated by a reduction in abscisic acid levels. *BMC plant biology* 16: 105.
- Zhang B (2015) MicroRNA: a new target for improving plant tolerance to abiotic stress. *Journal of experimental botany* 66: 1749-1761.
- Zhang H, Li X, Nan X, Sun G, Sun M, Cai D, Gu S (2017) Alkalinity and salinity tolerance during seed germination and early seedling stages of three alfalfa (*Medicago sativa* L.) cultivars. *Legume Research: An International Journal* 40.
- Zhang LB, Zhu Q, Wu ZQ, Ross-Ibarra J, Gaut BS, Ge S, Sang T (2009) Selection on grain shattering genes and rates of rice domestication. *New Phytologist* 184: 708-720.
- Zhao K, Tung C-W, Eizenga GC, Wright MH, Ali ML, Price AH, Norton GJ, Islam MR, Reynolds A, Mezey J (2011) Genome-wide association mapping reveals a rich genetic architecture of complex traits in *Oryza sativa*. *Nature communications* 2: 467.

# Manuscript 1

## Quantitative reverse transcription-qPCR-based gene expression analysis in plants (*Hedysarum carnosum*)

**Quantitative reverse transcription-qPCR-based gene expression analysis in  
plants (*Hedysarum carnosum*)**

Heithem Ben Abdallah<sup>1</sup> and Petra Bauer<sup>1,2</sup>

<sup>1</sup>Institute of Botany, Heinrich-Heine University, Universitätsstrasse 1, D-40225 Düsseldorf,  
Germany

<sup>2</sup>Center of Excellence in Plant Sciences (CEPLAS)

Corresponding author:

Petra Bauer

Institute of Botany

Heinrich-Heine University

Universitätsstrasse 1

D-40225 Düsseldorf

Germany

Tel.: +49 211 81-13479

Fax.: +49 211 81-12881

E-mail: [petra.bauer@uni-duesseldorf.de](mailto:petra.bauer@uni-duesseldorf.de)

**Running head:** Reverse transcription-qPCR

## Summary

The investigation of gene expression is an initial and essential step to understand the function of a gene in a physiological context. Reverse transcription-quantitative real time PCR (RT-qPCR) assays are reproducible, quantitative and fast. They can be adapted to study model and non-model plant species without the need to have whole genome or transcriptome sequence data available. Here, we provide a protocol for a reliable RT-qPCR assay, which can be easily adapted to any plant species of interest. We describe the design of the qPCR strategy and primer design, considerations for plant material generation, RNA preparation and cDNA synthesis, qPCR set up and run and qPCR data analysis, interpretation and final presentation.

**Key words:** gene expression, primer design, reverse transcription, cDNA, qPCR, reference gene, Cq value

## 1. Introduction

Gene expression analysis is used to identify the physiological context in which a gene is transcribed and the encoded protein produced in the cell. Precise quantification of expression levels can provide important clues to identify and verify the functions of key genes in cellular pathways and it helps to discriminate functional diversification within gene families. Molecular diagnostic tools based on gene expression are commonly developed to determine the physiological status of cells. Gene expression analysis is popular because of its versatility and applicability to model and non-model systems. Suitable transcript cDNA sequence information necessary for the gene expression assays is relatively easy and fast to obtain even for non-model systems.

Gene expression assays need to fulfill a number of pre-requisites to ensure reliability. Importantly, the assay needs to be sensitive, quantitative, specific for the gene of interest and reproducible across biological replicates and laboratories. When only a few genes are being investigated, fluorescence-based reverse transcription-quantitative PCR (RT-qPCR) has become the method of choice for most scientists as it meets all the above mentioned requirements. Semi-quantitative reverse transcription-PCR with analysis of PCR fragments by

agarose gel electrophoresis or Northern blot hybridization are not considered appropriate today to reach firm conclusions.

Our protocol for a SYBR Green-based fluorescence RT-qPCR assay is easy to establish even in non-specialist laboratories. SYBR Green fluorescence is measured after each cycle (real-time) and increasing levels of fluorescence during the qPCR are indicative of the amplification of double-stranded PCR fragments. The ‘quantification cycle’ (Ronfort et al.) value of a qPCR run is used for quantification and it reflects the time point and cycle during the exponential PCR phase at which a set threshold level of SYBR Green fluorescence is reached (Fig. 1A). The mass standard curve method can be used to correlate the C<sub>q</sub> value with the initial amount of template present in the qPCR reaction (Fig. 1A, B). The expression data for the genes of interest are normalized to reference gene expression data to account for possible variations in input in different biological samples (termed normalized absolute gene expression). In this chapter we summarize important criteria to consider, present a strategy for establishing and performing a reliable and robust assay and provide a framework for how to analyze and display the data. Detailed explanations and further guidelines for the usage of qPCR can be obtained from the MIQE (= Minimum Information for Publication of quantitative real-time PCR experiments) website at <http://miqe.gene-quantification.info> (Bustin et al. 2009). We use this RT-qPCR method as a diagnostic tool to determine the iron nutritional status of plant mutants and as a bioassay to study regulatory responses to iron deficiency, e.g. (Lingam et al. 2011; Schuler et al. 2012).

## 2. Materials

Prepare all solutions using ultrapure water and analytical grade chemicals. Store solutions at room temperature or as indicated by the manufacturer. Handle kits and enzymes following the manufacturers' instructions. Use filter tips during RNA preparation, cDNA and qPCR set up to avoid contamination of reagents in the reaction tubes. Use RNase and DNase-free reaction tubes.

### 2.1. DNA sequence analysis tools:

- DNA analysis: <http://www.ebi.ac.uk>

- Primer design: <http://primer3.ut.ee>

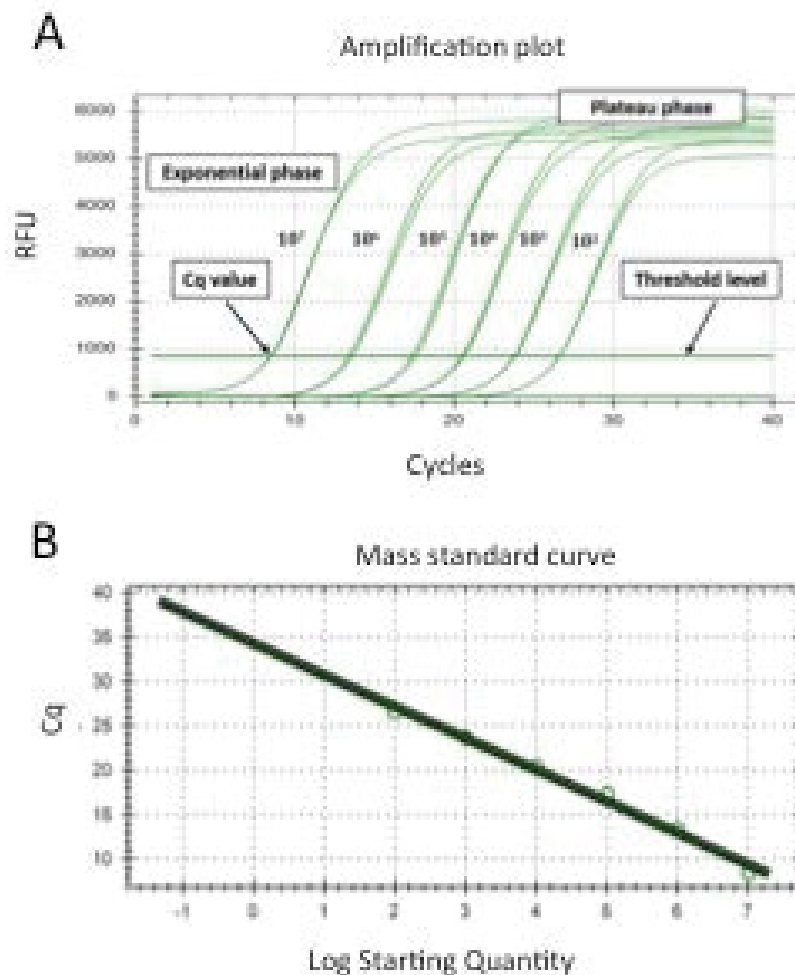


**Figure 1: Principles of qPCR using the mass standard curve method:**

A, Amplification plot of a mass standard dilution series. Relative fluorescence units (= RFU) were measured during the qPCR run at the end of each of 40 cycles. In the beginning of the exponential phase quantification cycle (=Cq) values are recorded as the time point when a set threshold level of RFU is reached. Later, the RFU reach a plateau phase. The numbers  $10^7$  to  $10^2$  indicate the starting quantity in molecules per reaction. The reactions were performed in duplicate technical replicates.

B, Linear mass standard curve derived from the data in A. Starting quantities of unknown samples are calculated based on the measured Cq values.

The images were produced with the CFX Manager software (Biorad).

## 2.2 General analysis of DNA and RNA:

- Regular PCR: REDTaq ReadyMix PCR Reaction Mix (Sigma).
- TAE DNA gel electrophoresis: 40 mM Tris, 20 mM acetic acid, 1 mM EDTA, pH 8.0. Prepare 50X TAE buffer stock and dilute to 1X TAE buffer ready to use. A 50X stock solution is prepared by dissolving 242 g Tris base in water, adding 57.1 mL glacial acetic acid, and 100 mL of 500 mM EDTA (pH 8.0) solution, and bringing the final volume up to 1 L. For a 1 % gel dissolve 1g agarose in 100 mL 1X TAE buffer by boiling, add 3  $\mu$ L DNA staining dye (GelRed, Biotium, or equivalent) and pour agarose gel. For all steps of the agarose gel electrophoresis set up and run consult the information provided by the agarose gel electrophoresis equipment supplier or molecular biology standard protocols (Green and Sambrook 2012). For size determination use a DNA molecular weight marker with an appropriate size range. DNA staining is visible under UV light (*see Note 1*) and documented with a gel documentation system.
- DNA gel extraction: GeneJET Gel Extraction Kit (Thermo Scientific).
- DNA/RNA quantification: Measure the nucleic acid concentration by UV spectrophotometry. The  $OD_{260} = 1$  corresponds to 50 ng double-stranded DNA or 40 ng single-stranded RNA per  $\mu$ L in a 1 cm cuvette. The ratios of the values for nucleic acid versus protein absorption peaks ( $OD_{260}/OD_{280}$ ) are indicative of purity and should be above 1.5. To reduce the amount of nucleic acid material needed for measuring, a micro volume spectrophotometric device, such as the NanoDrop (Thermo Scientific), Nano Quant plate of a micro plate reader (Tecan) or equivalent can be used.
- PCR oligonucleotide primers.

## 2.3 Reverse transcription-qPCR:

- RNA preparation: peqGOLD Plant RNA kit (Peqlab) or equivalent.
- DNase I, RNase-free.
- RNase- and DNase-free PCR grade water.
- Oligo dT<sub>18</sub>.
- cDNA synthesis: RevertAid First Strand cDNA synthesis kit (Thermo Scientific) or

equivalent.

- Ribolock RNase inhibitor (Thermo Scientific) or equivalent.
- qPCR: Dynamo Flash SYBR Green qPCR kit (Thermo Scientific) or equivalent.
- Oligonucleotide primers for PCR reactions can be ordered from multiple companies.
- Colored 200  $\mu$ L 8-tube PCR strips.
- Optical sealing tape for 96-well PCR plates.
- 96-well plates for qPCR, adapted for the available real-time PCR device.
- Real-time PCR cycler (CFX96, Bio-Rad or equivalent).

**3. Methods:** A flow chart of the RT-qPCR procedure is depicted in **Fig. 2A**. External calibration standards allow absolute quantification of template present at the start of the PCR (standard curve method) and serve as positive controls to monitor PCR assay variation over time.

Several points require special attention by the researchers when performing RT-qPCR and we address them in the following sections. These include the design of appropriate oligonucleotide primers for qPCR to achieve high PCR efficiency, the choice of reference genes for normalization of biological samples, a work plan for generation of suitable plant material in biological replicates prior to RT-qPCR, handling and pipetting, the quality of materials and consumables, and finally, thorough analysis of qPCR data.

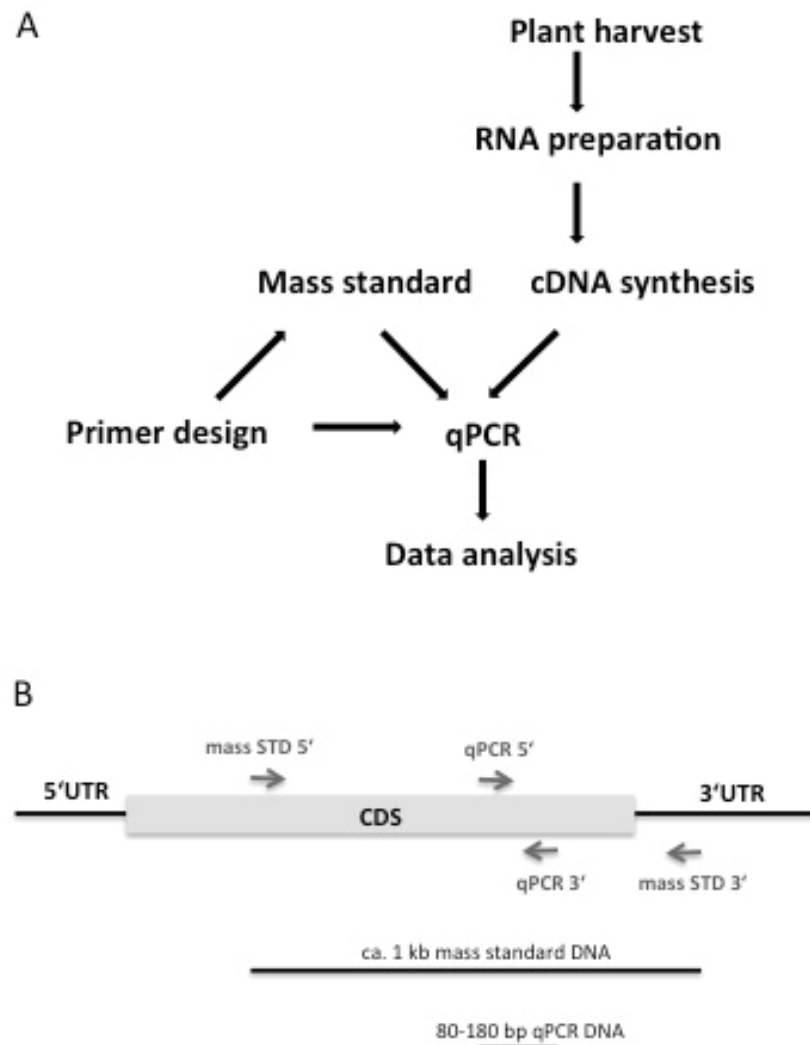


**Figure 2: Experimental flowchart and primer design :**

A, Experimental flowchart to determine gene expression levels using RT-qPCR and the mass standard curve method.

B, Primer design. A schematic representation of a cDNA is shown with coding sequence (CDS) and 5' and 3' untranslated regions (UTR). qPCR and mass standard (mass STD) oligonucleotide primer binding sites are indicated by arrows. The amplification products are depicted below. The qPCR fragment must be contained within the mass standard DNA fragment.

### 3.1. Design of qPCR strategy and oligonucleotide primers:

1. Select genes of interest and reference genes and obtain DNA sequence information (*see Note 2*). Use DNA analysis software tools and analyze cDNA sequence for translation start and stop codons and for conserved regions among related cDNA sequences obtained from the species to spot unique regions optimal for qPCR primer design, at best in the vicinity of the 3' end (**Fig. 2B**). Consider splicing and alternative splicing events.
2. Use the primer3 software tool to design qPCR 5' and 3' oligonucleotide primers in non-conserved regions of the cDNA with the following characteristics: amplification of ca. 80-180 bp cDNA fragments, 60°C annealing, low risk of hairpin and primer dimer formation (**Fig. 2B**). Conduct a BLAST search with the oligonucleotide primer sequences against all expressed sequences available from the species or a close relative to check that oligonucleotide primer binding sites are not present in transcribed sequences.
3. Use the primer3 software tool to design mass standard 5' and 3' oligonucleotide primers to produce external calibration standard DNA fragments. The mass standard oligonucleotide primer binding sites need to encompass the qPCR target regions and should allow production of linear ca. 1 kb mass standard DNA fragments (**Fig. 2B**).

### 3.2. Mass standard preparation for qPCR:

1. Amplify mass standard DNA fragments from 1  $\mu\text{L}$  template (*see Note 3*) with 1  $\mu\text{L}$  of 10  $\mu\text{M}$  5' and 3' mass standard oligonucleotide primers in a regular 20  $\mu\text{L}$  PCR reaction.
2. Use 15  $\mu\text{L}$  of the PCR reaction and separate the DNA fragments by TAE agarose gel electrophoresis (1 % gel). With a razor blade and under UV light dissect a small agarose cube containing the mass standard PCR fragment and purify the DNA using any of the commercially available gel extraction kits. The final volume of the purified mass standard DNA is typically 20-50  $\mu\text{L}$ . Measure the DNA concentration of the purified mass standard DNA fragment solutions and use 3-5  $\mu\text{L}$  to run a gel electrophoresis to confirm the correct size of the purified DNA fragments.

3. Determine the molar concentrations of the purified mass standard PCR fragment solutions and calculate the concentrations in number of DNA molecules/ $\mu\text{L}$  using the molar conversion tool at [http://molbiol.edu.ru/eng/scripts/01\\_07.html](http://molbiol.edu.ru/eng/scripts/01_07.html).
4. Dilute the purified mass standard DNA fragment solutions in an initial 1:100 and subsequent 1:10 steps to obtain a dilution series ranging from  $10^7$ ,  $10^6$ ,  $10^5$ ,  $10^4$ ,  $10^3$  to  $10^2$  DNA molecules per  $10 \mu\text{L}$ . Prepare 800-1000  $\mu\text{L}$  of each dilution in 1.5 mL reaction tubes.
5. Dispense 50  $\mu\text{L}$  of each of the six dilutions of the series into 8mer PCR strips and freeze until use (*see Note 4*).

### 3.3. Test of qPCR oligonucleotide primers by PCR:

1. Perform a regular 20  $\mu\text{L}$  PCR reaction (40 cycles) with qPCR 5' and 3' oligonucleotide primers and use 1  $\mu\text{L}$  of purified mass standard DNA ( $10^7$  molecules/ $10 \mu\text{L}$  dilution) as template
2. Check 15  $\mu\text{L}$  of the PCR reaction by TAE DNA agarose gel electrophoresis (using a 2.5 % gel) for the presence of a PCR fragment of the expected size. In case of absent PCR product or presence of unexpected PCR fragments, try to optimize PCR parameters (Mg and primer concentration, annealing temperature). If this fails you will need to design new primers.
3. Test PCR efficiency of the qPCR primers for amplification of the mass standard series using qPCR. This step can be combined with and is described in section 3.6 and 3.7.

### 3.4. Generation of plant material:

1. Grow plants to obtain three independent biological replicates of all sample conditions (*see Note 5*).
2. Harvest plant material, shock-freeze with liquid nitrogen and if needed store at  $-80^\circ\text{C}$  (*see Note 6*).

### 3.5. RNA preparation and reverse transcription:

A critical point in RNA preparation and reverse transcription is to avoid damage by active RNases (*see Note 7*). For all steps of reverse transcription prepare master mixes to achieve similar reaction conditions in all samples (*see Note 8*).

1. Grind the frozen material to fine powder (*see Note 9*).
2. Use a maximum of 100 mg ground plant material and isolate total RNA according to the supplier's protocol. This procedure usually results in 50  $\mu\text{L}$  purified RNA.
3. Determine RNA concentration (*see Note 10*).
4. Label individual 200  $\mu\text{L}$  PCR tubes (*see Note 11*).
5. In each 200  $\mu\text{L}$ -PCR tube combine 500-1000 ng RNA and RNase- and DNase-free PCR grade water in a maximum volume of 7  $\mu\text{L}$  to obtain similar RNA amounts in all samples. Include a negative cDNA control sample devoid of RNA.
6. For DNase I treatment, prepare a DNase I reaction master mix containing per reaction a total of 3  $\mu\text{L}$  (0.5  $\mu\text{L}$  DNase-free water, 1.0  $\mu\text{L}$  DNase I buffer, 1  $\mu\text{L}$  of 1 u/ $\mu\text{L}$  DNase I, 0.5  $\mu\text{L}$  of 40 u/ $\mu\text{L}$  Ribolock). Add 3  $\mu\text{L}$  of this DNase I reaction mix to the 7  $\mu\text{L}$  RNA and incubate at 37°C for 30min (total reaction volume 10  $\mu\text{L}$ ).
7. For denaturing and oligo dT primer annealing prepare an oligo dT primer annealing master mix containing per reaction 1  $\mu\text{L}$  of 100  $\mu\text{M}$  oligo dT<sub>18</sub> primer and 1  $\mu\text{L}$  of 25 mM EDTA. Add 2  $\mu\text{L}$  of this oligo dT primer annealing mix to the reactions from step 6 and incubate for 10 min at 65°C, then at 4°C until further use (total reaction volume 12  $\mu\text{L}$ ).
8. For cDNA synthesis prepare a cDNA synthesis master mix by combining per reaction 1.0  $\mu\text{L}$  DNase-free water, 4.0  $\mu\text{L}$  reverse transcription buffer, 2  $\mu\text{L}$  of 10 mM each dNTP, 0.5  $\mu\text{L}$  of 40 u/ $\mu\text{L}$  Ribolock and 0.5  $\mu\text{L}$  of 200 u/ $\mu\text{L}$  M-MuLV RTase, as according to the suppliers. Add 8  $\mu\text{L}$  of this cDNA synthesis mix to the reactions from step 7 and incubate for 2 h at 42°C, followed by 10 min at 70°C (total reaction volume 20  $\mu\text{L}$ ).
9. Add 180  $\mu\text{L}$  of RNase- and DNase-free PCR grade water to each cDNA sample and mix well. Store these cDNA stocks long-term at -20°C.
10. For qPCR, dilute each cDNA stock 1:10, e.g. by combining in a 1.5 mL reaction tube 350  $\mu\text{L}$  RNase- and DNase-free PCR grade water, 10  $\mu\text{L}$  yellow color indicator (from qPCR kit) and 40  $\mu\text{L}$  cDNA, mix well. Dispense 50  $\mu\text{L}$  of the cDNA dilutions into 8mer PCR strips and store at -20°C (*see Note 12*).

### 3.6. qPCR set up and run:

Prepare a master mix for qPCR and simultaneously perform the qPCR reactions for the cDNA samples, the cDNA negative control, a qPCR negative control and the mass standards in technical replicates (*see Note 13*).

1. Plan and program the plate set up and qPCR conditions using the qPCR software of the available real time PCR cycler (see example in **Fig. 3A, B**).
2. Prepare the qPCR master mix by combining per reaction 9.6  $\mu\text{L}$  qPCR commercial 2X mix (containing SYBR Green and blue color indicator; mix thoroughly before use), 0.2  $\mu\text{L}$  of each 15  $\mu\text{M}$  5' and 3' oligonucleotide primer, mix well.
3. Dispense 10  $\mu\text{L}$  of the qPCR master mix into the bottom of each well of the PCR plate (*see Note 14*). Check for even loading of the wells.
4. Transfer 10  $\mu\text{L}$  of the samples (diluted cDNA, cDNA control and mass standard dilution series) from the 8mer PCR strips into the plate using a 10  $\mu\text{L}$  multichannel pipet (*see Note 15*). Check even loading and color indicator change to green.
5. Tap the plates gently at the bench, seal with optical tape by slowly placing the tape from the middle to the edges of the plate, fix with sealing tool, and centrifuge the plate in a plate centrifuge. Ready PCR plates can be stored at 4°C in the dark for several hours.
6. Place the plate into the qPCR machine and start the run as programmed. Save the optical data in a file.

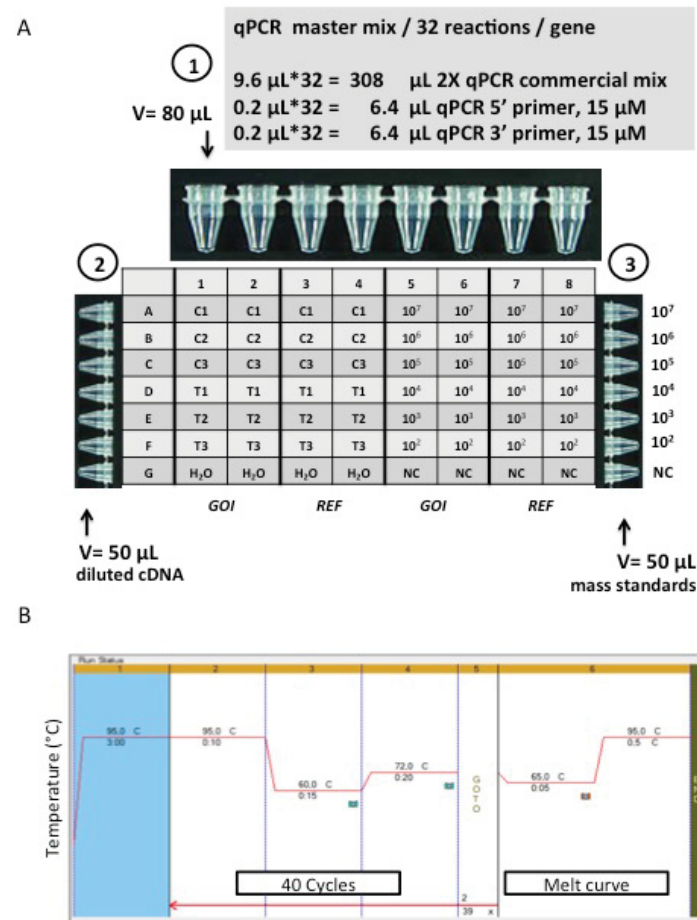


**Figure 3: Set up of qPCR:**

A, Plate set-up and pipetting scheme. The plate set-up shows the arrangement of samples in a qPCR micro plate, with three biological replicates of the control (C1-C3) and treated samples (T1-T3), the negative cDNA control (H<sub>2</sub>O), the mass standards 10<sup>7</sup> to 10<sup>2</sup> and a qPCR negative control (= NC). Two different qPCR reactions are to be performed (*GOI*, gene of interest, *REF*, reference gene). All reactions are to be conducted in technical duplicates. The preparation of a qPCR master mix is provided as an example. 80  $\mu\text{L}$  of the qPCR master mixes is transferred to the wells of an 8mer strip, with *GOI* qPCR master mix in positions 1, 2, 5, 6, and *REF* qPCR master mix in the positions 3, 4, 7, 8. The circled numbers indicate the order of pipetting steps to transfer 10  $\mu\text{L}$  of the qPCR master mixes, the diluted cDNA samples and the mass standards from 8mer strips into the plate using a 10  $\mu\text{L}$  multichannel pipet.

B, PCR program; step 1 is the initial denaturation (3:00 min, 95°C); steps 2-4 comprise denaturing (0:10 min; 95°C), annealing (0:15 min; 60°C) and elongation (0:20 min; 72°C) and are repeated 39 times with fluorescence data acquisition after each cycle indicated by a camera sign; step 6 serves the melt curve data collection (0:05 min; 65°C to 95°C with gradual increase of 0.5°C) with regular data acquisition at each increment. The image was produced with the CFX Manager software (Biorad).

### 3.7. qPCR data analysis and presentation of gene expression data:

1. Check qPCR data thoroughly by melt curve analysis (*see Note 16; Fig. 4C, D*), check for reliability of C<sub>q</sub> values and technical replicate amplification (*see Note 17; Fig. 4E*), check PCR efficiency and mass standard curve (*see Note 18; Fig. 1A, B*).
2. Export raw data into Excel. Name samples appropriately and remove unnecessary columns and rows to keep only the means of the technical replicate initial template numbers for the biological samples as the raw data (**Fig. 5**).
3. Perform the analysis steps by following the outline in **Fig. 5**. Briefly, proceed with subtraction of negative cDNA water control values (*see Note 19*). Calculate normalization factors based on the reference gene amplification data (*see Note 20*). Normalize gene of interest data using the normalization factors. Calculate average and standard deviation based on the biological replicate data. Subject the data to statistical analysis (*see Note 21*). Represent the final results in a bar diagram (*see Note 22*).

### 4. Notes:

1. UV light is dangerous. Wear eye and skin protection.
2. The choice of reference genes is critical for data interpretation. Generalizations about the number of reference genes needed for analysis is difficult. It is important to search for a reference gene whose expression does not vary across the experimental conditions that are studied. The probability of finding such a reference gene is highest when only one well-defined plant part or tissue is under investigation, e.g. roots. However, if there is high variation across the biological samples, e.g. when comparing expression in different parts of the plants or when comparing physiological situations that severely disturb development, the use of only one

## Manuscript 1

reference gene may not be reliable and there is a need for additional reference genes. In this case, the expression data of multiple reference genes are usually averaged for calculation of normalization factors. The selection of reference genes requires prior experiments or the mining of transcriptomic data. Typical reference genes are those encoding general cellular functions, like tubulin, ubiquitin and elongation factor. In Fig. 4A and B we present qPCR amplification plots for two reference genes across biological samples (treatment and control). It can be seen that reference gene #2 shows a lower degree of variability than reference gene #1 and should therefore be preferred (**Fig. 4A, B; see later Note 20**).

3. Mass standard templates can be cDNA, recombinant plasmid or genomic DNA.

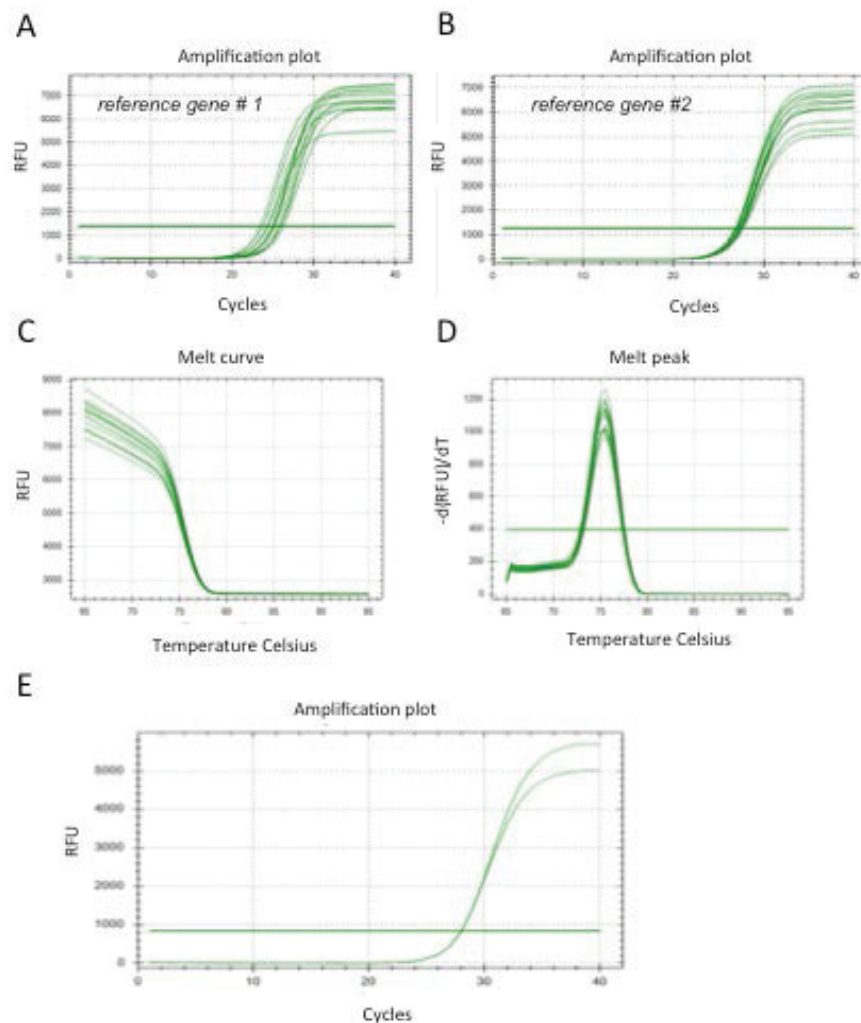


**Figure 4: qPCR data control:**

A, B, Amplification plots for reference genes #1 and #2 across multiple biological samples. Reference gene #2 would be selected due to low variation in the Cq values.

C, Melt curve analysis. The decrease of RFU with increasing temperature is caused by melting of double-stranded DNA and loss of SYBR Green fluorescence.

D, Melt peak analysis. A single peak indicates melting in a narrow temperature range indicating that a single DNA fragment was present in the samples.

E, Amplification plot of two technical replicates; due to  $Cq < 0.3$  an average Cq value is used for data analysis. A description of the amplification plots is provided in Fig. 1. The images were produced with the CFX Manager software (Biorad).

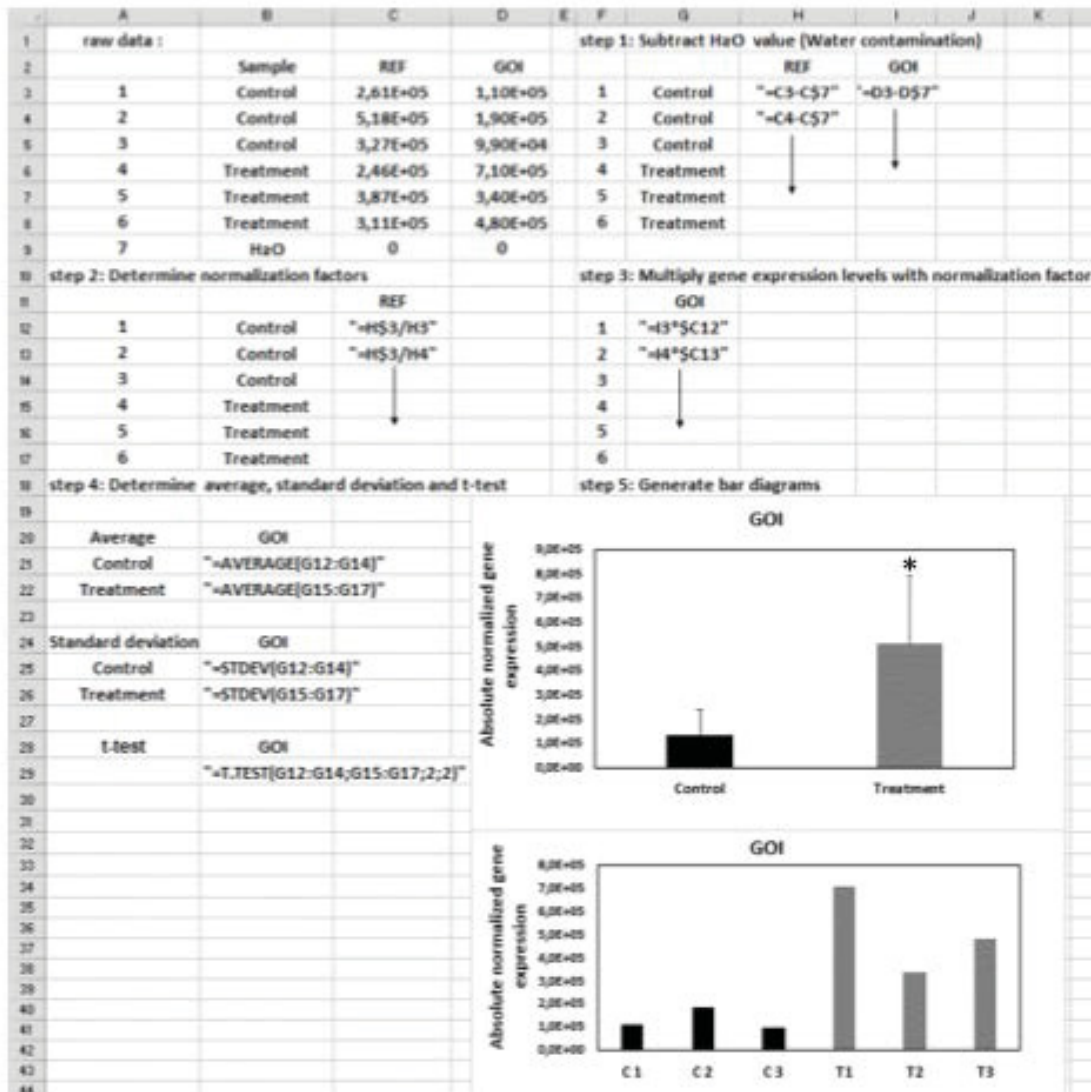


**Figure 5: Data interpretation using Excel:**

An Excel data sheet with calculation tools is shown. The raw data correspond to the initial starting quantities in the 10  $\mu$ L cDNA samples (control and treatment, three biological replicates) and the negative cDNA control (H<sub>2</sub>O), and are the average of two technical replicates for the gene of interest (GOI) and the reference gene (REF). The data are processed and normalized as indicated inside the figure. Mean and standard deviation values are calculated, and a t-test (unpaired, two-tailed) is performed. The final data are displayed in the form of bar diagrams reflecting the absolute normalized

gene expression of GOI in the two experimental conditions control and treatment, representing either the average values, standard deviation and \* indicating significant difference with  $p < 0.05$  or the individual values.

4. A volume of 50  $\mu\text{L}$  is sufficient to set up four 10  $\mu\text{L}$  qPCR reactions (**Fig. 3A**). For convenience prepare up to 15 mass standard strips per gene and store the unused ones at  $-20^{\circ}\text{C}$ . Discard unused solutions after thawing. Specifically colored PCR strips are useful to easily distinguish the mass standards corresponding to different genes.

5. The plant material itself accounts to a large extent for the variability in gene expression analyses. At least three independent biological replicates are required for publication and for statistical treatment of gene expression data. Try to minimize variation in the source of genetic material, growth conditions, harvesting time and age of plants and if possible pool material from 10 or more plants in a single biological replicate to achieve low levels of standard deviations among the three replicates. Repeat the entire experiment including biological replicates at least two or three times.

6. Note that storage at  $-80^{\circ}\text{C}$  may affect the stability of some RNA species.

7. Some types of RNases are very stable, omnipresent on hands and working materials and released upon cell disruption. RNase contamination can occur easily in laboratories where bacterial plasmid and genomic DNA preparations are conducted since some of the preparation solutions may contain added RNase. RNA extraction buffers may contain toxic substances like phenol, guanidinium thiocyanate (GTC), Beta-mercaptoethanol and/or other effective denaturing and reducing agents to block RNase activity (wear gloves). In some commercial RNA extraction kits the buffer composition is not described (e.g. peqGold kit). Generally, RNA is safeguarded in the deep-frozen state ( $-80^{\circ}\text{C}$  or lower) and inside RNA extraction buffer. For subsequent steps of RNA purification, RNA elution and reverse transcription, change gloves, use filter tips, clean the work surface area and materials (better reserve special equipment for RNA handling). Open and close the tubes at the very tip of the cap with two fingers without contaminating with RNase from the thumb.

8. When preparing master mixes take into account volume loss after multiple pipetting steps, e.g. prepare a master mix of 11 reactions for ten reactions.

9. A simple way to grind plant material in liquid nitrogen is to use either a mortar and pestle or an automated homogenizer stick fitting into a plastic reaction tube. Working with liquid nitrogen is dangerous and protection of hands, body, face and eyes is needed. Closing of tubes should be avoided while working with liquid nitrogen since evaporation of liquid nitrogen may cause explosion of tubes at room temperature. Plant material should never be allowed to thaw in the absence of RNA extraction buffer. If available, use the Precellys homogenizer machine (or equivalent) as it allows safe and more reproducible homogenization results. In this case, add 450  $\mu$ L RNA extraction buffer and ceramic Precellys beads (for Arabidopsis roots and leaves use 50 beads of 1.4 mm; testing of appropriate number and mix of e.g. 1.4 and 2.8 mm beads may be required for other plant species) to the 100 mg frozen intact tissue inside 2 mL Precellys tubes. Proceed immediately for cell disruption using the Precellys homogenizer (3x60 s, interrupted by 30 s breaks).

10. For unexperienced operators it is advisable to check the quality of the RNA by running 5  $\mu$ L in a TAE gel electrophoresis (1 % gel). Use only thoroughly cleaned electrophoresis materials and TAE buffer reserved for RNA electrophoresis purposes. Discrete bands for ribosomal and Rubisco RNA species indicate a high quality of RNA. If available use the Agilent Bioanalyzer or equivalent device to determine RNA quality and quantity. Note that different methods for determining nucleic acid concentrations have inherent sources of mistakes. It is therefore important for the subsequent steps of RT-qPCR that the concentrations of all biological RNA samples are determined in parallel with the same technique to ensure a low level of variation in the RNA input.

11. 8mer PCR strips are problematic for this step since vortexing is not possible and risk of cross-contamination is high. The cDNA samples can be kept long-term. Therefore, label reaction tubes with a tape stating "date", "cDNA sample name" and "number" and prepare for long-term storage a sealed plastic bag with a print-out of the experimental description, date and detailed description of the samples.

12. Dilution of the cDNA stocks is necessary for qPCR since it is more precise to dispense 10  $\mu$ L rather than 1  $\mu$ L. A volume of 50  $\mu$ L of diluted cDNA sample is sufficient for four qPCR reactions, namely two technical replicates x two genes (**Fig. 3A**). For convenience prepare up to 8 cDNA strips from the 400  $\mu$ L diluted cDNA samples and store the unused ones at -20°C

until needed. Stored strips should be allowed to thaw only once and then be discarded. Long-term storage of diluted cDNA samples beyond 6 months is not recommended. After the six months, prepare new diluted cDNA from the cDNA stocks. Specifically colored strips are convenient for handling in order to distinguish different cDNA samples (e.g. samples 1-8 in yellow, samples 9-16 in blue, etc.).

13. In case that the total number of samples exceeds the well number in a 96well plate, include interplate calibration standards (e.g. commercially available through TATAA Biocenter) to account for plate to plate qPCR variations and allow to integrate the results of multiple plates. At least two reliable technical replicates are required. Technical replicate variation is most frequently a consequence of inappropriate handling and imprecise pipetting. To ensure best repeatability of qPCR use only high-quality 10 or 20  $\mu$ L pipets and 10  $\mu$ L multichannel pipets and perform an initial training of pipet handling. Use thin pipetting tips for small volumes and carefully check upon every pipetting step the expected volume in the pipet tip. Check the expected volume also inside the PCR plate after transferring the solutions. Use only 2X qPCR reaction mixes since transferring 10  $\mu$ L introduces fewer errors than transferring smaller volumes.

14. Dispense the qPCR master mix either with a 10 or 20  $\mu$ L pipet sequentially into each well or transfer a higher volume into a 8mer PCR strip for dispensing with a 10  $\mu$ L multichannel pipet (shown in **Fig. 3A**).

15. Hold the pipet in an angle to dispense the template solution onto the top side of the wells, without touching the qPCR mix. This procedure allows using the same tips to load multiple wells or plates with the same templates.

16. The melt curve peak provides hints to the integrity and length of the PCR product. A single peak indicates melting of the PCR products at one specific temperature, suggesting that there is a single PCR product present. In case of multiple peaks the PCR conditions and primer design have to be improved prior to qPCR and any meaningful analysis.

17. Assess technical replicate amplification for all samples one by one by judging the  $\Delta$ C<sub>q</sub> values. For low C<sub>q</sub> values (< 20) a  $\Delta$ C<sub>q</sub> deviation up to 0.3 is acceptable. Higher C<sub>q</sub> values especially those above 25 may show per se a higher deviation between the technical replicates

and a  $\Delta C_q$  of 0.5 is acceptable and for  $C_q$  values above 30,  $\Delta C_q$  0.5-1.0 is acceptable. Samples with inappropriate amplification and high technical replicate deviations need to be removed from the analysis and the entire qPCR experiment repeated. Consistently large variations in  $C_q$  values between technical replicates will not allow to reach valid conclusions, qPCR has to be optimized and precision of pipetting improved (*see Note 13* for recommendations). In case that all gene expression data can only be based on high  $C_q$  values  $>30$ , a meaningful conclusion is drastically compromised. In this case, reconsider and improve RNA purification, and test alternative kits for cDNA synthesis and qPCR.

18. PCR efficiency is usually calculated with the mass standard curve. The mass standard curve shows an inverse linear correlation between  $C_q$  value and template input (**Fig. 1B**). This is usually the case during the linear dynamic range and when PCR efficiency is close to 1 (100 %). A 100 % PCR efficiency indicates full doubling of PCR fragments at each cycle. In case of a poor PCR efficiency below 90 % check different conditions for amplification with oligonucleotide primers. Most primer pairs function optimally in equimolar ratios of 150 nM in a qPCR. In case of low PCR efficiency, perform a primer matrix to find more optimal primer concentrations and ratios (Klatte and Bauer 2009) and test a temperature gradient for optimal annealing temperatures. Lack of success denotes the need to design new primers.

19. In case of a contamination that prevents proper interpretation of qPCR results, repeat qPCR and/or cDNA synthesis. In our experience, thorough working does not lead to contamination of the negative cDNA controls.

20. In the example (**Fig. 4A, B**), a low level of variation of expression was found for reference gene #2 resulting in low variation of the  $C_q$  values, in contrast to reference gene #1. Reference gene #2 is thus the preferred reference gene for qPCR data analysis.

21. In the presented outline (**Fig. 5**) we performed t-test (unpaired, two-tailed) for statistical analysis. Due to the low number of biological replicates it is also transparent and acceptable to present the data for individual biological replicates instead. In case of many different biological samples and multiple genes to be studied it is convenient to use an ANOVA-based statistical tool, e.g. (Sharov et al. 2005). Further considerations about statistical analysis are discussed at <http://www.nature.com/collections/qghhqm>.

22. We suggest representing the data as absolute normalized gene expression rather than normalized initial transcript amounts. Application of the standard curve method for deducing initial template amounts in the cDNA samples is based on the assumption of accurate reverse transcription and qPCR. This accuracy can be determined during the RT-qPCR procedure by adding internal RNA and DNA spikes to the samples, commercially available through TATAA Biocenter or equivalent.

**Acknowledgement:** H.B.A. was supported through internship and STIBET fellowships from the DAAD and the Tunisian government.

## 5. References:

- Bustin SA, Benes V, Garson JA, Hellemans J, Huggett J, Kubista M, Mueller R, Nolan T, Pfaffl MW, Shipley GL, Vandesompele J, Wittwer CT (2009) The MIQE guidelines: minimum information for publication of quantitative real-time PCR experiments. *Clin Chem* 55: 611-622.
- Green MR, Sambrook J (2012) *Molecular Cloning: A Laboratory Manual*, Cold Spring Harbor.
- Klatte M, Bauer P (2009) Accurate real-time reverse transcription quantitative PCR. *Meth Mol Biol* 479: 61-77.
- Lingam S, Mohrbacher J, Brumbarova T, Potuschak T, Fink-Straube C, Blondet E, Genschik P, Bauer P (2011) Interaction between the bHLH transcription factor FIT and ETHYLENE INSENSITIVE3/ETHYLENE INSENSITIVE3-LIKE1 reveals molecular linkage between the regulation of iron acquisition and ethylene signaling in *Arabidopsis*. *The Plant cell* 23: 1815-1929.
- Ronfort J, Bataillon T, Santoni S, Delalande M, David JL, Prospero J-M (2006) Microsatellite diversity and broad scale geographic structure in a model legume: building a set of nested core collection for studying naturally occurring variation in *Medicago truncatula*. *BMC Plant Biology* 6: 28.
- Schuler M, Rellán-Álvarez R, Fink-Straube C, Abadía J, Bauer P (2012) Nicotianamine functions in the Phloem-based transport of iron to sink organs, in pollen development and pollen tube growth in *Arabidopsis*. *The Plant cell* 24: 2380-23400.
- Sharov AA, Dudekula DB, Ko MSH (2005) A web-based tool for principal component and significance analysis of microarray data. *Bioinformatics* 21: 2548-2549.

**Author contribution to Manuscript 1:**

Quantitative reverse transcription-qPCR-based gene expression analysis in plants (**published**). (Abdallah and Bauer 2016).

Heithem Ben Abdallah

Prepared the figures, reviewed and wrote some text sections.

Petra Bauer

Designed the outline of the manuscript, supervised the study, provided funding, wrote and corrected the manuscript.

Abdallah HB, Bauer P (2016) Quantitative reverse transcription-qPCR-based gene expression analysis in plants. *Plant Signal Transduction*. Springer.

# Manuscript 2

**Natural variation of physiological and molecular  
responses of Tunisian *Hedysarum carnosum*  
subjected to iron deficiency**

1 **Natural variation of physiological and molecular responses of Tunisian *Hedysarum***  
2 ***carnosum* subjected to iron deficiency**

3 Heithem Ben Abdallah<sup>1</sup>, Hans Jörg Mai<sup>1</sup>, Tarek Slatni<sup>2</sup>, Claudia Fink-Straube<sup>3</sup>, Chedly  
4 Abdelly<sup>2</sup>, Petra Bauer<sup>1, 4</sup>

5 <sup>1</sup> Institute of Botany, Heinrich Heine University Düsseldorf, Universitätsstrasse 1, D-40225,  
6 Düsseldorf, Germany.

7 <sup>2</sup> Laboratory of Extremophiles Plant, Center of Biotechnology of Borj Cedria (CBBC) BP 901,  
8 2050 Hammam-Lif, Tunisia.

9 <sup>3</sup> INM-Leibniz Institute for New Materials, Campus D2 2, 66123 Saarbrücken, Germany

10 <sup>4</sup> CEPLAS Cluster of Excellence on Plant Sciences Heinrich Heine University,  
11 Universitätsstraße 1, D-40225 Düsseldorf.

12

13

14

15 **Corresponding Author:** Petra Bauer, Institute of Botany, Heinrich Heine University  
16 Düsseldorf, Universitätsstrasse 1, D-40225 Düsseldorf, Germany

17

18

19 **Email:** [petra.bauer@uni-duesseldorf.de](mailto:petra.bauer@uni-duesseldorf.de)

20 **Tel:** +49 211 81-13479

21 **Fax:** +49 211 81-12881

22

23 **Running title:** Iron deficiency in *Hedysarum carnosum*

1

### 2 **ABSTRACT**

3 Iron (Fe) is an essential element for plant growth and development. The cultivation of  
4 leguminous plants has generated strong interest because of their growth even on poor soils. In  
5 this study we characterized Fe deficiency responses of three different isolates of the fodder  
6 crop *Hedysarum carnosum*, an endemic Tunisian extremophile species growing in native  
7 stands in salt and calcareous soil conditions. *H. carnosum* is a non-model crop. The three  
8 isolates, named according to their habitats Karkar, Thelja and Douiret, differed in the  
9 expression of Fe deficiency symptoms like altered morphology, leaf chlorosis with  
10 compromised leaf chlorophyll content and photosynthetic capacity and altered leaf metal  
11 contents. Across these parameters Thelja was found to be tolerant, while Karkar and Douiret  
12 were susceptible to Fe deficiency stress. The three physiological and molecular indicators of  
13 the iron deficiency response in roots, Fe reductase activity, growth medium acidification and  
14 induction of the *IRON-REGULATED TRANSPORTER1* homolog, indicated that all lines  
15 responded to -Fe, however, varied in the strength of the different responses.

16 We suggest that the individual lines have distinct adaptation capacities to react to iron  
17 deficiency, presumably involving mechanisms of whole-plant iron homeostasis and internal  
18 metal distribution. The Fe deficiency tolerance of Thelja might be linked with adaptation to its  
19 natural habitat on calcareous soil.

20 **Key words:** *Hedysarum carnosum*, legume, natural diversity, iron deficiency, chlorophyll,  
21 acidification, Fe reductase activity, *IRT1*, TAIL-PCR

22

## 1 INTRODUCTION

2 The *Hedysarum* (sweetvetch) genus belongs to the Fabaceae plant family, which contains  
3 many of the very important crops. Species of this genus have arisen in a non-monophyletic  
4 manner, as recently established based on multiple sequence alignments and phylogenetic tree  
5 constructions of 58 accessions accounted to this genus using nuclear and plastid gene  
6 sequences (Liu et al., 2017). *Hedysarum carnosum* (also known as *Sulla carnosa*) that is  
7 subject of this study is most related to *H. coronarium* (also known as *S. coronaria*) (Liu et al.,  
8 2017). *H. coronarium* is wide-spread around the Mediterranean basin. In contrast, *H.*  
9 *carnosum* is endemic in Tunisia where it grows in different climates, ranging from semi-arid  
10 (Karkar) to arid regions (Thelja and Douiret). This species prefers slightly acid to alkaline  
11 soils (pH 5.5-8.5), sandy loams and clays, and good growth is achieved on alkaline soils. As  
12 an extremophile, *H. carnosum* also grows on Tunisian saline sodic soils, represented  
13 especially by Chotts and Sebkhass (Dallali et al., 2012). This species plays important roles in  
14 animal feed due to its high protein contents and tannins (Aissa et al., 2016).

15 Iron (Fe) is an essential micronutrient with numerous cellular functions, e.g. in  
16 photosynthesis, respiration, DNA synthesis and N<sub>2</sub> fixation. Plants are frequently challenged  
17 by Fe deficiency, especially on alkaline and calcareous soils due to poor Fe solubility under  
18 these conditions. In Tunisia, the exploration of such kinds of natural habitats and saline  
19 environments revealed that they are colonized by a native leguminous vegetation which might  
20 have specific adaptations to both, salinity and nutrient deficiencies, especially Fe (Ben  
21 Abdallah et al., 2017). Leguminous plants take up reduced Fe using mainly the so-called  
22 Strategy I. The main feature of Strategy I plants, e.g. in *Arabidopsis* and leguminous plants, is  
23 that they acidify the soil via proton extrusion through an ATPase, reduce ferric to ferrous Fe  
24 by a ferric chelate reductase and take up the divalent Fe via divalent metal IRON-  
25 REGULATED TRANSPORTER1 (Brumbarova et al., 2015), being a member of the ancient  
26 ZIP (= ZRT/IRT1) protein family (Eng et al., 1998). *IRT1* homologs were found Fe-regulated  
27 in roots of multiple legumes like *Pisum sativum* (Cohen et al., 2004), *Medicago*  
28 *truncatula* (Lopez-Millan et al., 2004), *Arachis hypogaea* (Ding et al., 2010), *Glycine max*  
29 (Brear et al., 2013) and *Vigna radiata* (Muneer et al., 2014).

30 Natural variation studies make use of the existing natural allelic diversity in plant populations  
31 as a source to pinpoint the adaptive alleles for relevant traits. Natural variation was  
32 successfully applied in model plants to identify causal alleles by genome-wide association

1 studies for such different traits as environmental adaptation in *Arabidopsis* (Li et al., 2010), or  
2 nutritional quality and agronomic traits in maize (Diepenbrock et al., 2017) and rice (Si et al.,  
3 2016). The three model legumes *M. truncatula* and *G. max* are particularly suited for natural  
4 biodiversity studies (Gentzbittel et al., 2015). Prerequisites for association studies are existing  
5 genome sequence variation reflected by a broad collection of ecotypes demonstrating  
6 phenotypic diversity for given traits. However, alternative procedures are available for  
7 studying natural diversity of small population collections in the absence of large genome  
8 sequence data, e.g. by making use of recombinant or near-isogenic inbred lines suitable for  
9 mapping and gene identification (Yan et al., 2017), by isolating candidate genomic regions  
10 and genes based on comparative genomics (Friesen et al., 2010; Turner et al., 2010; Friesen et  
11 al., 2014) and transcriptomics or proteomics of genetically divergent lines (Voelckel et al.,  
12 2017).

13 The objective of this work was to investigate the effect of Fe deficiency at the physiological  
14 and molecular level of the non-model extremophile species *H. carnosum* and to compare the  
15 responses in three different isolates collected from different natural sites. The identified  
16 tolerant Thelja isolate will be useful in future genetic and RNAseq studies to identify the  
17 natural basis for calcareous soil-induced Fe deficiency.

## 18 MATERIAL AND METHODS

### 19 Plant material and growth condition

20 Three isolates of *H. carnosum* were acquired by collecting seeds from Karkar, Thelja and  
21 Douiret in Tunisia (see Supplementary Figure 1 for species characteristics and geographic  
22 repartition of collected isolates). About 300 seeds per isolate were collected from an average  
23 of 10 plants distributed in a diameter of 100 m. Seeds of the three isolates were germinated  
24 and grown in separate green houses. Due to allogamy plants were multiplied by cross-  
25 fertilization of plants within each isolate. The F3 generation was used for analyses.

26 Seeds were mechanically scarified by rubbing in between fine grit sand paper sheets. The  
27 seeds were sterilized in 10 % sodium hypochlorite for 8 min and then abundantly rinsed with  
28 distilled water. After a 10 min imbibition phase, they were germinated for 4 days at 20 °C in  
29 Petri dishes on constantly moistened filter paper.

1 Four day-old seedlings were transferred to a half strength aerated liquid nutrient solution for  
2 two days. Similarly sized seedlings were then selected and cultured in groups of 4 or 10 plants  
3 in 1 or 10 l of full strength aerated nutrient solution (1.5 mM  $\text{Ca}(\text{NO}_3)_2$ , 1.25 mM  $\text{KNO}_3$ ,  
4 0.75 mM  $\text{MgSO}_4$ , 0.5 mM  $\text{KH}_2\text{PO}_4$  and 10  $\mu\text{M}$   $\text{H}_3\text{BO}_3$ , 1  $\mu\text{M}$   $\text{MnSO}_4$ , 0.5  $\mu\text{M}$   $\text{ZnSO}_4$ , 3  $\mu\text{M}$   
5  $\text{M}_2\text{O}_4\text{Na}_2$ , 0.5  $\mu\text{M}$   $\text{CuSO}_4$  and 50  $\mu\text{M}$  Fe-EDTA). At day 6, the following treatments were  
6 conducted for the amount of time indicated in the text and figure legends: +Fe, control (Fe-  
7 sufficient medium with 50  $\mu\text{M}$  Fe) and -Fe, Fe deficiency (medium without Fe). The pH was  
8 adjusted to 6.0 with NaOH for both, the +Fe (control) and -Fe (iron deficiency) treatments.  
9 Aerated hydroponic cultures were maintained in a growth chamber with a day/night regime of  
10 16/8 h light-dark-cycle, a 24/18 °C temperature cycle and a constant relative humidity of  
11 70%. The solution was renewed every 4 days. The standard experiment was conducted using  
12 ten-day Fe sufficiency and deficiency treatments.

### 13 **Morphological root and shoot phenotypes**

14 Roots and shoots were harvested, dried in an oven at 70 °C for 48 h and the dry weights  
15 determined per plant. The main root lengths were measured. The degree of leaf chlorosis was  
16 assessed in the youngest expanded leaves. The leaf chlorosis scale is described in the text and  
17 figure legend, ranging from 1 = green, 2 = light green, partially yellow, 3 = yellow-green, 4 =  
18 yellow to 5 = white-yellow.

### 19 **Chlorophyll measurements**

20 Total chlorophyll was extracted from fresh leaves in 80 % acetone and assayed  
21 photometrically at 645 nm and 663 nm. The OD values were used to calculate the total  
22 chlorophyll content in mg/g fresh weight of the leaves as published (Arnon, 1949).

### 23 **Pulse Amplitude Measurements (PAM)**

24 PAM was determined with the FluorCam FC 800-C machine (Photon Systems  
25 Instruments™). Plants were adapted to darkness for about 15 minutes. Then single leaves  
26 were harvested and measured for  $F_0$  (minimal fluorescence) up to  $F_m$  (maximal fluorescence).  
27 To analyze photosystem II activity,  $F_v/F_m$  values and  $F_v/F_0$  values were calculated (Murchie  
28 and Lawson, 2013).  $F_0$  and  $F_m$  present the minimum and maximum values of chlorophyll  
29 fluorescence, while  $F_v$  is the variable fluorescence.

### 1 **Acidification of the growth medium**

2 The acidification capacity was determined after placing plants into 1 l nutrient solution (at pH  
3 6.2), respectively, and measuring the pH of the nutrient solution in the subsequent days as  
4 indicated in the text and figure legend.

### 5 **Measurements of root Fe reductase activity**

6 Intact root systems were washed with 100 mM Ca(NO<sub>3</sub>)<sub>2</sub> solution and submerged in the Fe  
7 reductase assay solution containing 0.1 mM Fe<sup>3+</sup>-NaEDTA and 0.3 mM ferrozine at pH 5.0  
8 for 1 h in the dark. Then the absorbance was determined at 562 nm. The concentration of the  
9 Fe<sup>2+</sup>-ferrozine complex was calculated using the molar extinction coefficient of  
10 28.6 mM<sup>-1</sup> cm<sup>-1</sup>. The amount of Fe<sup>2+</sup> was normalized to the root weight in the assay and Fe  
11 reductase activity was calculated.

### 12 **Mineral element analysis:**

13 To determine the metal ion content the youngest expanded leaves of *H. carnosum* were  
14 harvested and dried over 72 h at 70 °C. After drying, the harvested leaves were finely  
15 powdered with an achat mortar and pestle. Metal contents (Zn, Fe, Cu) were determined using  
16 inductively-coupled plasma optical emission spectrometry (ICP-OES) at the Leibniz Institute  
17 for New Materials (INM, Saarbrücken).

### 18 **Obtention of *H. carnosum* cDNA sequences and multiple sequence alignment of amino 19 acid sequences**

20 Obtention of *H. carnosum* cDNA sequences is outlined in Supplementary Figure 2A. *A.*  
21 *thaliana*, *M. truncatula*, *Glycine max.*, *L. japonicus* sequences of *IRT1* and  $\beta$ -*ACTIN* (*ACT*)  
22 were aligned. Conserved regions near the start and stop codons were identified and primers  
23 matching 100 % the *M. truncatula* sequences were designed (Mt primers, Supplementary  
24 Figure 3). With these Mt primers 1  $\mu$ l of template root cDNA of *H. carnosum* was used to  
25 amplify the *IRT1* and *ACT* internal coding sequences in a standard PCR. PCR amplicon bands  
26 were purified from agarose gels according to standard procedures and sequenced.

27 Next, TAIL-PCR (Supplementary Figure 2B) was used to identify the unknown upstream 5'  
28 and downstream 3' cDNA sequences adjacent to the determined *HcIRT1* and *HcACT* partial  
29 sequences. We used three nested specific primers (S1-S3) that aligned near the edge of the

1 known cDNA (Supplementary Figure 3). For extension in the opposite direction AD (arbitrary  
2 degenerate) primers were used. The AD primers were 64x-256x degenerate and designed to  
3 be relatively short (15-16 nt) with a low melting temperature (ca. 40-50 °C) (Supplementary  
4 Figure 3). Three consecutive TAIL-PCR reactions were conducted as described (Liu et al.,  
5 1995). The third step PCR products were sequenced and *HcIRT1* and *HcACT* sequences  
6 assembled and provided to Genbank (accession numbers will be provided prior to  
7 publication).

8 Multiple sequence alignment and construction of neighbor-joining trees using amino acid  
9 sequences was performed using the Clustal Omega tool at <https://www.ebi.ac.uk>.

### 10 **RNA isolation and quantitative real-time PCR**

11 RNA isolation and reverse transcription-quantitative PCR were carried out as described  
12 previously (Ben Abdallah and Bauer, 2016). Briefly, total RNA prepared from 100 mg  
13 *H. carnosum* root tissue was used for cDNA synthesis using an oligo-dT primer. qPCR was  
14 conducted using the SYBR Green detection method. RT-qPCR primers were used for qPCR.  
15 The absolute quantity of initial transcripts was determined for the genes *IRT1* and *ACT* by  
16 standard curve analysis using mass standards prepared from *H. carnosum* cDNA PCR  
17 products amplified with Mt primers. Absolute expression data of *IRT1* was obtained after  
18 normalization to the internal control *ACT* gene. Each biological cDNA sample was tested in  
19 two technical replicates. The absolute expression values of three biological replicates were  
20 averaged.

### 21 **Statistical analysis**

22 Morphological, physiological and molecular data were obtained in at least three biological  
23 replicates, as detailed in the figure legends. Data of biological replicates were used to  
24 calculate mean values and standard deviations. Statistical significance was determined by  
25 applying t-tests (for two sample comparisons) and ANOVA followed by Tukey's HSD test  
26 (for more than two sample comparisons) as indicated in the figure legends.

27

28

29

## 1 RESULTS

### 2 Morphological and physiological shoot responses to Fe deficiency

3 Seeds from *H. carnosum* plants were collected in three different locations in Tunisia  
4 characterized by semi-arid, arid and Saharan conditions, named Karkar, Thelja and Douiret,  
5 with saline-sodic, calcareous and sandy soil characteristics (Supplementary Figure 1). After  
6 seeds were multiplied for three generations, morphological and physiological experiments  
7 were carried out. We were interested in obtaining an ecotype with high tolerance to prolonged  
8 Fe deficiency growth conditions, a trait expected to be beneficial upon growth on calcareous  
9 soil. We therefore hypothesized that the three isolates might show different adaptation and  
10 respond differently to Fe deficiency conditions. Plant seedlings were grown in controlled  
11 hydroponic conditions and exposed to sufficient iron (+Fe) or deficient iron supply (-Fe) for  
12 ten days. At first, we compared the tolerance/sensitivity of the lines to -Fe by measuring  
13 different growth parameters. The three isolates did not behave any different from each other  
14 in terms of root biomass production under + and -Fe (Figure 1A). Also in terms of shoot  
15 biomass production, the ecotypes were very similar (Figure 1B). Only one comparison  
16 resulted in a significant difference in biomass, which was the fourfold higher shoot dry weight  
17 of Douiret versus Karkar at -Fe (Figure 1B). However, none of the lines showed lower root or  
18 shoot biomass when grown at - compared to +Fe (Figures 1A, B). Karkar displayed a shorter  
19 main root compared to Douiret at +Fe. When comparing the main root length at -Fe versus  
20 +Fe, there was a significant decrease only in the case of Douiret but not Karkar and Thelja  
21 (Figure 1C).

22 Fe is required in high amounts during plant growth in the leaves to sustain photosynthesis and  
23 for chlorophyll synthesis. Fe can also be stored in chloroplasts in the form of ferritin. Lack of  
24 Fe results in the typical leaf chlorosis symptoms especially in the expanding leaves. Leaf  
25 chlorosis is caused by low chlorophyll contents under Fe deficiency. Karkar and Douiret had  
26 higher total chlorophyll contents at + than at -Fe (Figure 1D). Thelja, on the other hand,  
27 displayed no significant difference at + versus -Fe (Figure 1D). No significant differences  
28 were detectable between the lines at either + or -Fe (Figure 1D). PAM measurements based  
29 on chlorophyll fluorescence are an indicator for the photosynthetic performance under stress  
30 conditions. Low  $F_v/F_m$  and  $F_v/F_0$  ratios are indicative of stress affecting negatively the  
31 photosystem activity. We found that Karkar had lower  $F_v/F_m$  and  $F_v/F_0$  ratios at - versus +Fe,  
32 while no significant differences were found in Thelja and Douiret (Figures 1E, F). When

1 comparing the lines with each other, Karkar had a lower Fv/Fm ratio than Thelja and Douiret  
 2 and Thelja had a higher Fv/F<sub>0</sub> ratio than Karkar and Douiret (Figures 1E, F). We were also  
 3 interested in comparing the development of the leaf chlorosis during the ten days of exposure  
 4 to -Fe. Leaf chlorosis started two days earlier in Douiret than in Karkar and Thelja, but after  
 5 ten days the chlorosis had reached similar levels, as determined above from the chlorophyll  
 6 measurements (Figures 1D, G).

7 Next, we investigated whether the observed leaf chlorosis and impact on photosynthesis could  
 8 be related to the amount of Fe taken up into the expanding leaves. In addition to Fe we  
 9 measured Zn and Cu contents. Arabidopsis IRT1 can take up Zn but not Cu (Vert et al., 2002)  
 10 and MtZIP6 can also transport Zn (Lopez-Millan et al., 2004). Karkar and Douiret had lower  
 11 Fe contents upon -Fe than under +Fe, but not Thelja, which had comparable levels under both  
 12 conditions (Figure 2A). Thelja also had higher Fe contents upon -Fe compared to Karkar and  
 13 Douiret (Figure 2A). The Zn content was decreased at - versus +Fe growth conditions only in  
 14 Douiret (Figure 2B). However, Thelja had a higher Zn content than Karkar and Douiret at -  
 15 but not +Fe (Figure 2B). The Cu content was decreased at - versus +Fe in Karkar and Douiret,  
 16 but again not in Thelja (Figure 2C). When comparing the lines with each other, a significant  
 17 difference of Cu was only found in the comparison of Thelja versus Karkar at -Fe (Figure  
 18 2C).

19 To conclude from this physiological and growth analysis of the three lines exposed to +  
 20 and -Fe, we summarized the comparative outcomes for the parameters measured at + versus -  
 21 Fe for each line and designated a significant decrease at - versus +Fe as "sensitive" and no  
 22 decrease as "tolerant" behavior (Figure 3). Karkar received four sensitivity and five tolerance  
 23 labels, Douiret six sensitivity and three tolerance labels, and Thelja nine tolerance labels. Root  
 24 and shoot biomass were not identified as parameters that could be used to discriminate the  
 25 behavior of the lines at + and -Fe, while leaf chlorosis, photosystem activity and metal  
 26 contents were well suited to do so. Taken together, it can be deduced that Thelja shows  
 27 tolerance to -Fe in contrast to the other two lines.

## 28 **Physiological and molecular root responses to Fe deficiency**

29 Roots of strategy I plants show typical Fe deficiency symptoms like enhanced soil  
 30 acidification, Fe reduction and increased *IRT1* gene expression. Quantification of these  
 31 responses is used to judge the degree of Fe deficiency (Brumbarova et al., 2015). Therefore,

1 we tested next for potential differences in the level of Fe deficiency responses in the root.  
2 None of the plants subjected to Fe deficiency showed a significant increase in root Fe  
3 reductase activity (Figure 4A). In a time-course experiment we found that the growth medium  
4 was acidified significantly starting as early two days after exchange to Fe deficiency and  
5 continued until 10 days in all three lines (Figure 4B). To conduct *IRT1* gene expression  
6 analysis by the RT-qPCR method, we first identified homologs of *IRT1* and *ACT* and of the  
7 reference gene  $\beta$ -*ACTIN* (*ACT*) from *H. carnosum* using PCR and TAIL-PCR by exploiting  
8 sequence similarities among leguminous plant IRT1 sequences and available microarray-  
9 based gene expression data for *M. truncatula* (see Materials and Methods; outline in  
10 Supplementary Figure 2). The full-length HcIRT1 amino acid sequence was found most  
11 related to MtZIP6 in a neighbor-joining tree derived from a multiple sequence alignment of  
12 the entire families of *A. thaliana*, *M. truncatula*, *G. max* and *L. japonicus* ZIP protein  
13 sequences (Figure 5). MtZIP6 was the only *M. truncatula* ZIP protein with high sequence  
14 similarity to HcIRT1 and AtIRT1 (Figure 5). MtZIP6 is up-regulated by -Fe in roots (He et  
15 al., 2009; Benedito et al., 2010) and it was characterized as Fe transporter (Lopez-Millan et al.,  
16 2004). All other *M. truncatula* ZIP proteins group along with other branches of *A. thaliana*  
17 ZIP proteins (Figure 5), indicating that these other MtZIP proteins have different functions in  
18 metal homeostasis. Interestingly, this analysis also shows that *A. thaliana* seems to have a  
19 high expansion of four IRT1-like proteins (IRT1, IRT2, ZIP8, ZIP10), while legumes had on  
20 the same branch of the tree (highlighted by a red box in Figure 5) besides a single *M.*  
21 *truncatula* ZIP, only two *G. max* and two *L. japonicus* ZIP sequences. HcIRT1 and MtZIP6  
22 share two important functional sequence features in the predicted variable cytoplasmic loop  
23 region with AtIRT1, namely two conserved lysine positions used for ubiquitination in metal-  
24 directed IRT1 turnover (Kerkeb et al., 2008) and the histidine-rich stretch for metal-binding  
25 relevant for metal import by ZIPs into the cell (Zhang et al., 2017) (Figure 6A). Hence, the  
26 sequence analysis convincingly suggests that *HcIRT1* encodes a functional IRT1 homolog.  
27 *HcIRT1* gene expression was found significantly induced by -Fe in Karkar, Thelja and  
28 Douiret (Figure 6B). Thelja displayed a higher base level of *HcIRT1* expression in the +Fe  
29 control situation compared to Karkar and Douiret (Figure 6B). Thelja and Douiret had a  
30 higher *HcIRT1* expression level at -Fe versus Karkar (Figure 6B).

31 In summary, the three lines displayed root Fe deficiency response reactions which were most  
32 pronounced in case of *HcIRT1* induction and medium acidification, while Fe reductase  
33 activity increases were not found to be significant. Perhaps the constitutively elevated *IRT1*

1 expression level of *Thelja* is linked with its higher Fe content under -Fe as an adaptation to  
2 growth on calcareous soil.

3

#### 4 **DISCUSSION**

5 Here, we show that the extremophile *H. carnosum* shows natural variation and phenotypic  
6 plasticity with regard to Fe deficiency responses. This species is an endemic growing on  
7 Tunisian saline and calcareous soil conditions that are known to affect micronutrient use  
8 efficiency. Overall, *Thelja* is the most tolerant isolate to Fe deficiency, perhaps a consequence  
9 of its adaptation to calcareous soils.

10 All *H. carnosum* isolates sensed Fe deficiency and responded to this stress, while the outcome  
11 of -Fe stress was different among the ecotypes. The common -Fe responses elicited by all  
12 three lines were the development of a leaf chlorosis, acidification of the plant medium and the  
13 induced expression of *HcIRT1* under -Fe versus +Fe. This shows that all plant lines had been  
14 exposed to + and -Fe. Several other -Fe symptoms were however only displayed by Karkar  
15 and Douiret, but not by *Thelja*. Karkar and Douiret exhibited quite drastic leaf chlorosis at -  
16 Fe. This was evident from accelerated leaf chlorosis and the low chlorophyll contents at -  
17 versus +Fe after ten days of -Fe. Leaf chlorosis is a frequently occurring stress symptom in  
18 plants since under unfavorable conditions plants tend to reduce photosystem activity by  
19 removing chlorophyll and degrading chloroplasts to avoid additional stress caused by the  
20 light. This phenomenon can be measured by PAM chlorophyll fluorescence, which was lower  
21 in Karkar and Douiret and fits to the leaf chlorosis observations. Moreover, several steps in  
22 photosynthetic pigment metabolism and chloroplast ultrastructure are dependent on Fe, which  
23 explains the leaf chlorosis in the young expanding leaves after transfer of the plants to -Fe  
24 conditions. Fe deficiency resulted in a decrease of Fe contents in Karkar and Douiret  
25 expanding leaves, and hence the low Fe status can be regarded as reason for the leaf chlorosis.  
26 It is surprising that biomass production was not affected by -Fe in our experiments. We  
27 explain this partly by the fact that with ANOVA and Tukey HSD we applied the appropriate  
28 but comparably conservative statistical test for multiple comparisons that keeps the family-  
29 wise error rate (FWER) at 0.05. Hence, an increasing number of comparisons increases the  
30 Type II error (false negative) rate and thus decreases the power for the single comparisons.  
31 Perhaps, less conservative tests such as Fisher LSD or two-sample t-tests would have resulted

1 in statistically significant differences. The data indicate that there was a tendency for lower  
 2 values at - versus +Fe for many parameters even in Thelja, but the differences were not  
 3 significant according to ANOVA/Tukey HSD.

4 Zn and Cu contents were affected by -Fe in Karkar and Douiret in addition to Fe contents, but  
 5 not in Thelja. The reduced Fe contents are explained as primary reaction by the low amount of  
 6 Fe to which the plants were exposed. However, the reduced Zn and Cu contents must have  
 7 been a secondary reaction of the plant to -Fe. Normally, it would be expected that Zn contents  
 8 might increase upon -Fe, because increased IRT1 would take up Zn (Li et al., 2014). Perhaps,  
 9 Hedysarum plants have different capacities to regulate metal homeostasis, and this capacity  
 10 differs between Thelja, Douiret and Karkar. Differences in the regulation of Fe reductase  
 11 activity, *IRT1* gene expression and metal contents between different ecotypes were also found  
 12 for *M. truncatula* (Li et al., 2014). Under Fe deficiency, plants can suffer from oxidative  
 13 stress (Ranieri et al., 2001; Zaharieva and Abadia, 2003; Waters et al., 2012; Ramirez et al.,  
 14 2013). In *A. thaliana*, the CuSOD (copper/zinc superoxide dismutase) genes *CSD1* and *CSD2*  
 15 are induced under Fe deficiency and have been suggested to replace FeSOD's (iron  
 16 superoxide dismutases) to cope with oxidative stress under iron deficient conditions (Waters  
 17 et al., 2012). It can be assumed that a similar mechanism exists in leguminous plants and  
 18 elevated Cu and Zn contents could contribute to the effectiveness of this mechanism. Our  
 19 observation of higher Cu and Zn levels in Thelja could be one possible explanation for the  
 20 increased resistance of Thelja to iron deficiency compared to Karkar and Douiret. Hence, the  
 21 different efficiencies of Cu and Zn uptake under Fe deficiency in Thelja, Karkar and Douiret  
 22 could be an important distinctive factor with respect to Fe deficiency tolerance.

23 The stronger -Fe leaf symptoms of Karkar and Douiret suggest that these lines should sense -  
 24 Fe stress stronger than Thelja. But the two lines did not activate their root Fe mobilisation in a  
 25 stronger manner than Thelja. Karkar reduced more Fe in the root than did Douiret and Thelja.  
 26 On the other hand, medium acidification capacities were similar between the lines. Thelja and  
 27 Douiret displayed higher *HcIRT1* gene expression than did Karkar. An interesting regulatory  
 28 phenomenon could be seen for Thelja *HcIRT1* gene expression, which was higher at +Fe  
 29 compared to Karkar and Douiret. One possible explanation is that Thelja might take up more  
 30 Fe at +Fe than Karkar and Douiret, but store this Fe in the root. Upon Fe deficiency the Fe  
 31 stores could be remobilized and effectively transported to the shoots. Hence, Thelja could  
 32 survive better upon -Fe conditions and maintain Fe levels. Since Thelja was collected in a

1 region with calcareous soil condition it is tempting to speculate that the constitutive *HcIRT1*  
2 expression might contribute to adaptation. On the other hand, Karkar might profit from an  
3 inefficient Fe usage, perhaps caused by ineffective internal mobilisation and transport in its  
4 natural habitat with saline-sodic soil. Some abiotic stress factors induced for example by salt  
5 stress affect Fe uptake negatively, which can be explained by the toxicity of metals under  
6 water loss and the increased risk of oxidative stress (Le et al., 2016).

7 Future studies should focus on the internal iron homeostasis regulation and allocation upon -  
8 Fe in *H. carnosum*. One possibility would be to conduct comparative RNAseq using Thelja  
9 and Karkar as extreme pairs to better characterize the internal Fe homeostasis responses in  
10 different plant organs. Genome sequence variation of metal homeostasis-relevant genes might  
11 account for differences in the gene expression levels or functional SNPs in coding regions.  
12 Comparing stress and -Fe responses between young and adult stages as well as under double  
13 stress may lead to better understanding of the mechanism of -Fe regulation in this leguminous  
14 species.

15  
16  
17

### 1 **ACKNOWLEDGEMENTS**

2 This work was supported through an internship and STIBET fellowships from the DAAD and  
3 the Tunisian Ministry of Higher Education, Scientific Research (LR10CBBC02).

4

### 5 **AUTHOR CONTRIBUTIONS STATEMENT**

6 PB, TS and CA designed experiments. HBA carried out experiments. PB, HBA and HJM  
7 analyzed data. CFS performed metal determination. PB wrote the manuscript. HBA and HJM  
8 commented on the manuscript.

9

### 10 **CONFLICT OF INTEREST STATEMENT**

11 The authors declare that the submitted work was not carried out in the presence of any  
12 personal, professional or financial relationships that could potentially be construed as a  
13 conflict of interest.

14

1 **LIST OF FIGURES**

2 **Figure 1: Effect of Fe deficiency stress on Karkar, Thelja and Douiret lines**

3 (A) Root dry weight (RDW), n = 3; (B) Shoot dry weight (SDW), n = 3; (C) Main root length,  
 4 n= 4-5; (D) Total chlorophyll (Chl) content, n = 3; (E, F) Photon yield of PSII calculated by  
 5 Fv/Fm and Fv/F<sub>0</sub>, n = 4; (G) Chlorosis phenotype symptoms of young leaves calculated  
 6 according to the indicated scale from 1,green leaves up to 5,white-yellow leaves, n = 4.  
 7 *H. carnosum* plants were exposed for 10 days (A-F) or up to 10 days (G) to Fe-sufficient  
 8 (+Fe) and Fe-deficient (-Fe) hydroponic growth conditions. Data are means ± SD; means with  
 9 the same letter are not significantly different with P≤ 0.05 according to ANOVA and Tukey's  
 10 HSD test.

11

12 **Figure 2: Metal contents of Karkar, Thelja and Douiret**

13 (A) Fe; (B) Zn; (C) Cu contents of the youngest expanded leaves.  
 14 *H. carnosum* plants were exposed for 10 days to Fe-sufficient (+Fe) and Fe-deficient (-Fe)  
 15 hydroponic growth conditions. Data are means ± SD; n= 4; means with the same letter are not  
 16 significantly different with P≤ 0.05 according to ANOVA and Tukey's HSD test.

17

18 **Figure 3: Summary assessment of Karkar, Thelja and Douiret for Fe deficiency stress**  
 19 **responses and metal contents**

20 The investigated parameters are root and shoot dry weights (RDW, SDW), total chlorophyll  
 21 (Chl), photon yield, chlorosis score (see Figure 1) and Fe, Zn and Cu contents (see Figure 2).  
 22 Responses that showed a decrease at - versus +Fe are designated by light grey color (S,  
 23 sensitive) and no decrease by dark grey color (T, tolerant).

24 **Figure 4: Physiological Fe deficiency responses of Karkar, Thelja and Douiret**

25 (A) Root Fe reductase activity, n= 4-5; (B) pH changes in the growth medium, n = 4.  
 26 *H. carnosum* plants were exposed for 10 days (A) or up to 10 days (B) to Fe-sufficient (+Fe)  
 27 and Fe-deficient (-Fe) hydroponic growth conditions. Data are means ± SD; means with the  
 28 same letter are not significantly different with P≤ 0.05 according to ANOVA and Tukey's HSD  
 29 test, means with \* label in B show a significant difference of + versus -Fe with P≤ 0.05  
 30 according to a t-test.

1

2 **Figure 5: Neighbor-joining tree of HcIRT1 and ZIP protein sequences from selected**  
3 **legumes and Arabidopsis**

4 The multiple amino acid sequence alignment was produced with *H. carnosum* IRT1 and all  
5 identified ZIP protein sequences from *A. thaliana*, *M. truncatula*, *G. max* and *L. japonicus*.  
6 The box indicates the closest relatives of AtIRT1. The star indicates HcIRT1.

7

8 **Figure 6: Conservation of functional IRT1 sequences and IRT1 gene expression in**  
9 **Karkar, Thelja and Douiret**

10 (A) Multiple amino acid sequence alignment of the variable cytoplasmic loop region of  
11 AtIRT1, HcIRT1 and MtZIP6, containing relevant functional residues involved in  
12 ubiquitination (lysines) and metal binding (histidine stretch). (B) Normalized gene expression  
13 of *IRT1*. *H. carnosum* plants were exposed for 10 days to Fe-sufficient (+Fe) and Fe-deficient  
14 (-Fe) hydroponic growth conditions. Data are means  $\pm$  SD; n= 3; means with the same letter  
15 are not significantly different with  $P \leq 0.05$  according to ANOVA and Tukey's HSD test.

16

17

18 **Supplementary Figure 1: Overview of *Hedysarum carnosum* plant material**

19 (A) Morphology of *H. carnosum*; (B) Geographic distribution of collected Tunisian *H.*  
20 *carnosum* lines.

21

22 **Supplementary Figure 2: Overview of *HcIRT1* and *HcACT* cDNA sequence obtention**

23 (A) Flowchart for obtaining *H. carnosum* *IRT1* and *ACT* cDNA sequences; (B) Flowchart of  
24 TAIL-PCR steps.

25

26 **Supplementary Figure 3: List of primers used in the study**

27

28

29

## 1 REFERENCES

- 2 Aissa, A., Manolaraki, F., Ben Salem, H., Hoste, H., and Kraiem, K. (2016). In vitro assessment of the  
3 anthelmintic activity of *Hedysarum carnosum* Desf. at different phenological stages and from  
4 six locations in Tunisia. *Parasitology* 143, 778-786.
- 5 Arnon, D.I. (1949). Copper enzymes in isolated chloroplasts. Polyphenoloxidase in *Beta vulgaris*. *Plant*  
6 *Physiology* 24, 1-15.
- 7 Ben Abdallah, H., and Bauer, P. (2016). Quantitative Reverse Transcription-qPCR-Based Gene  
8 Expression Analysis in Plants. *Methods in Molecular Biology* 1363, 9-24.
- 9 Ben Abdallah, H., Mai, H.J., Alvarez-Fernandez, A., Abadia, J., and Bauer, P. (2017). Natural variation  
10 reveals contrasting abilities to cope with alkaline and saline soil among different *Medicago*  
11 *truncatula* genotypes. *Plant and Soil* 418, 45-60.
- 12 Benedito, V.A., Li, H., Dai, X., Wandrey, M., He, J., Kaundal, R., Torres-Jerez, I., Gomez, S.K., Harrison,  
13 M.J., Tang, Y., Zhao, P.X., and Udvardi, M.K. (2010). Genomic inventory and transcriptional  
14 analysis of *Medicago truncatula* transporters. *Plant Physiol* 152, 1716-1730.
- 15 Brear, E.M., Day, D.A., and Smith, P.M. (2013). Iron: an essential micronutrient for the legume-  
16 rhizobium symbiosis. *Front Plant Sci* 4, 359.
- 17 Brumbarova, T., Bauer, P., and Ivanov, R. (2015). Molecular mechanisms governing Arabidopsis iron  
18 uptake. *Trends Plant Sci.* 20, 124-133.
- 19 Cohen, C.K., Garvin, D.F., and Kochian, L.V. (2004). Kinetic properties of a micronutrient transporter  
20 from *Pisum sativum* indicate a primary function in Fe uptake from the soil. *Planta* 218, 784-  
21 792.
- 22 Dallali, H., Maaley, E.M., Boughanmi, N.G., and Haouala, R. (2012). Salicylic acid priming in  
23 *Hedysarum carnosum* and *Hedysarum coronarium* reinforces NaCl tolerance at germination  
24 and the seedling growth stage. *Australian Journal of Crop Science* 6, 407-404.
- 25 Diepenbrock, C.H., Kandianis, C.B., Lipka, A.E., Magallanes-Lundback, M., Vaillancourt, B., Gongora-  
26 Castillo, E., Wallace, J.G., Cepela, J., Mesberg, A., Bradbury, P.J., Ilut, D.C., Mateos-  
27 Hernandez, M., Hamilton, J., Owens, B.F., Tiede, T., Buckler, E.S., Rocheford, T., Buell, C.R.,  
28 Gore, M.A., and Dellapenna, D. (2017). Novel Loci Underlie Natural Variation in Vitamin E  
29 Levels in Maize Grain. *Plant Cell* 29, 2374-2392.
- 30 Ding, H., Duan, L., Li, J., Yan, H., Zhao, M., Zhang, F., and Li, W.X. (2010). Cloning and functional  
31 analysis of the peanut iron transporter AhIRT1 during iron deficiency stress and intercropping  
32 with maize. *J Plant Physiol* 167, 996-1002.
- 33 Eng, B.H., Guerinot, M.L., Eide, D., and Saier, M.H. (1998). Sequence analyses and phylogenetic  
34 characterization of the ZIP family of metal ion transport proteins. *J. Membr. Biol.* 166, 1-7.

- 1 Friesen, M.L., Cordeiro, M.A., Penmetsa, R.V., Badri, M., Huguet, T., Aouani, M.E., Cook, D.R., and  
 2 Nuzhdin, S.V. (2010). Population genomic analysis of Tunisian *Medicago truncatula* reveals  
 3 candidates for local adaptation. *Plant J* 63, 623-635.
- 4 Friesen, M.L., Von Wettberg, E.J., Badri, M., Moriuchi, K.S., Barhoumi, F., Chang, P.L., Cuellar-Ortiz, S.,  
 5 Cordeiro, M.A., Vu, W.T., Arraouadi, S., Djebali, N., Zribi, K., Badri, Y., Porter, S.S., Aouani,  
 6 M.E., Cook, D.R., Strauss, S.Y., and Nuzhdin, S.V. (2014). The ecological genomic basis of  
 7 salinity adaptation in Tunisian *Medicago truncatula*. *BMC Genomics* 15, 1160.
- 8 Gentzbittel, L., Andersen, S.U., Ben, C., Rickauer, M., Stougaard, J., and Young, N.D. (2015). Naturally  
 9 occurring diversity helps to reveal genes of adaptive importance in legumes. *Front Plant Sci* 6,  
 10 269.
- 11 He, J., Benedito, V.A., Wang, M., Murray, J.D., Zhao, P.X., Tang, Y., and Udvardi, M.K. (2009). The  
 12 *Medicago truncatula* gene expression atlas web server. *BMC Bioinformatics* 10, 441.
- 13 Kerkeb, L., Mukherjee, I., Chatterjee, I., Lahner, B., Salt, D.E., and Connolly, E.L. (2008). Iron-induced  
 14 turnover of the Arabidopsis IRON-REGULATED TRANSPORTER1 metal transporter requires  
 15 lysine residues. *Plant Physiol.* 146, 1964-1973.
- 16 Le, C.T., Brumbarova, T., Ivanov, R., Stoof, C., Weber, E., Mohrbacher, J., Fink-Straube, C., and Bauer,  
 17 P. (2016). ZINC FINGER OF ARABIDOPSIS THALIANA12 (ZAT12) Interacts with FER-LIKE IRON  
 18 DEFICIENCY-INDUCED TRANSCRIPTION FACTOR (FIT) Linking Iron Deficiency and Oxidative  
 19 Stress Responses. *Plant Physiol* 170, 540-557.
- 20 Li, G., Wang, B., Tian, Q., Wang, T., and Zhang, W.H. (2014). *Medicago truncatula* ecotypes A17 and  
 21 R108 differed in their response to iron deficiency. *J Plant Physiol* 171, 639-647.
- 22 Li, Y., Huang, Y., Bergelson, J., Nordborg, M., and Borevitz, J.O. (2010). Association mapping of local  
 23 climate-sensitive quantitative trait loci in *Arabidopsis thaliana*. *Proc Natl Acad Sci U S A* 107,  
 24 21199-21204.
- 25 Liu, P.L., Wen, J., Duan, L., Arslan, E., Ertugrul, K., and Chang, Z.Y. (2017). *Hedysarum* L. (Fabaceae:  
 26 Hedysareae) Is Not Monophyletic - Evidence from Phylogenetic Analyses Based on Five  
 27 Nuclear and Five Plastid Sequences. *PLoS One* 12, e0170596.
- 28 Lopez-Millan, A.F., Ellis, D.R., and Grusak, M.A. (2004). Identification and characterization of several  
 29 new members of the ZIP family of metal ion transporters in *Medicago truncatula*. *Plant Mol  
 30 Biol* 54, 583-596.
- 31 Muneer, S., Jeong, B.R., Kim, T.H., Lee, J.H., and Soundararajan, P. (2014). Transcriptional and  
 32 physiological changes in relation to Fe uptake under conditions of Fe-deficiency and Cd-  
 33 toxicity in roots of *Vigna radiata* L. *J Plant Res* 127, 731-742.
- 34 Murchie, E.H., and Lawson, T. (2013). Chlorophyll fluorescence analysis: a guide to good practice and  
 35 understanding some new applications. *J Exp Bot* 64, 3983-3998.

- 1 Ramirez, L., Bartoli, C.G., and Lamattina, L. (2013). Glutathione and ascorbic acid protect Arabidopsis  
2 plants against detrimental effects of iron deficiency. *J Exp Bot* 64, 3169-3178.
- 3 Ranieri, A., Castagna, A., Baldan, B., and Soldatini, G.F. (2001). Iron deficiency differently affects  
4 peroxidase isoforms in sunflower. *J Exp Bot* 52, 25-35.
- 5 Si, L., Chen, J., Huang, X., Gong, H., Luo, J., Hou, Q., Zhou, T., Lu, T., Zhu, J., Shangguan, Y., Chen, E.,  
6 Gong, C., Zhao, Q., Jing, Y., Zhao, Y., Li, Y., Cui, L., Fan, D., Lu, Y., Weng, Q., Wang, Y., Zhan, Q.,  
7 Liu, K., Wei, X., An, K., An, G., and Han, B. (2016). OsSPL13 controls grain size in cultivated  
8 rice. *Nat Genet* 48, 447-456.
- 9 Turner, T.L., Bourne, E.C., Von Wettberg, E.J., Hu, T.T., and Nuzhdin, S.V. (2010). Population  
10 resequencing reveals local adaptation of Arabidopsis lyrata to serpentine soils. *Nat Genet* 42,  
11 260-263.
- 12 Vert, G., Grotz, N., Dedaldechamp, F., Gaymard, F., Guerinot, M.L., Briat, J.F., and Curie, C. (2002).  
13 IRT1, an Arabidopsis transporter essential for iron uptake from the soil and for plant growth.  
14 *Plant Cell* 14, 1223-1233.
- 15 Voelckel, C., Gruenheit, N., and Lockhart, P. (2017). Evolutionary Transcriptomics and Proteomics:  
16 Insight into Plant Adaptation. *Trends Plant Sci* 22, 462-471.
- 17 Waters, B.M., Mcinturf, S.A., and Stein, R.J. (2012). Rosette iron deficiency transcript and microRNA  
18 profiling reveals links between copper and iron homeostasis in Arabidopsis thaliana. *J Exp Bot*  
19 63, 5903-5918.
- 20 Yan, G., Liu, H., Wang, H., Lu, Z., Wang, Y., Mullan, D., Hamblin, J., and Liu, C. (2017). Accelerated  
21 Generation of Selfed Pure Line Plants for Gene Identification and Crop Breeding. *Front Plant*  
22 *Sci* 8, 1786.
- 23 Zaharieva, T.B., and Abadia, J. (2003). Iron deficiency enhances the levels of ascorbate, glutathione,  
24 and related enzymes in sugar beet roots. *Protoplasma* 221, 269-275.
- 25 Zhang, T., Liu, J., Fellner, M., Zhang, C., Sui, D., and Hu, J. (2017). Crystal structures of a ZIP zinc  
26 transporter reveal a binuclear metal center in the transport pathway. *Sci Adv* 3, e1700344.
- 27

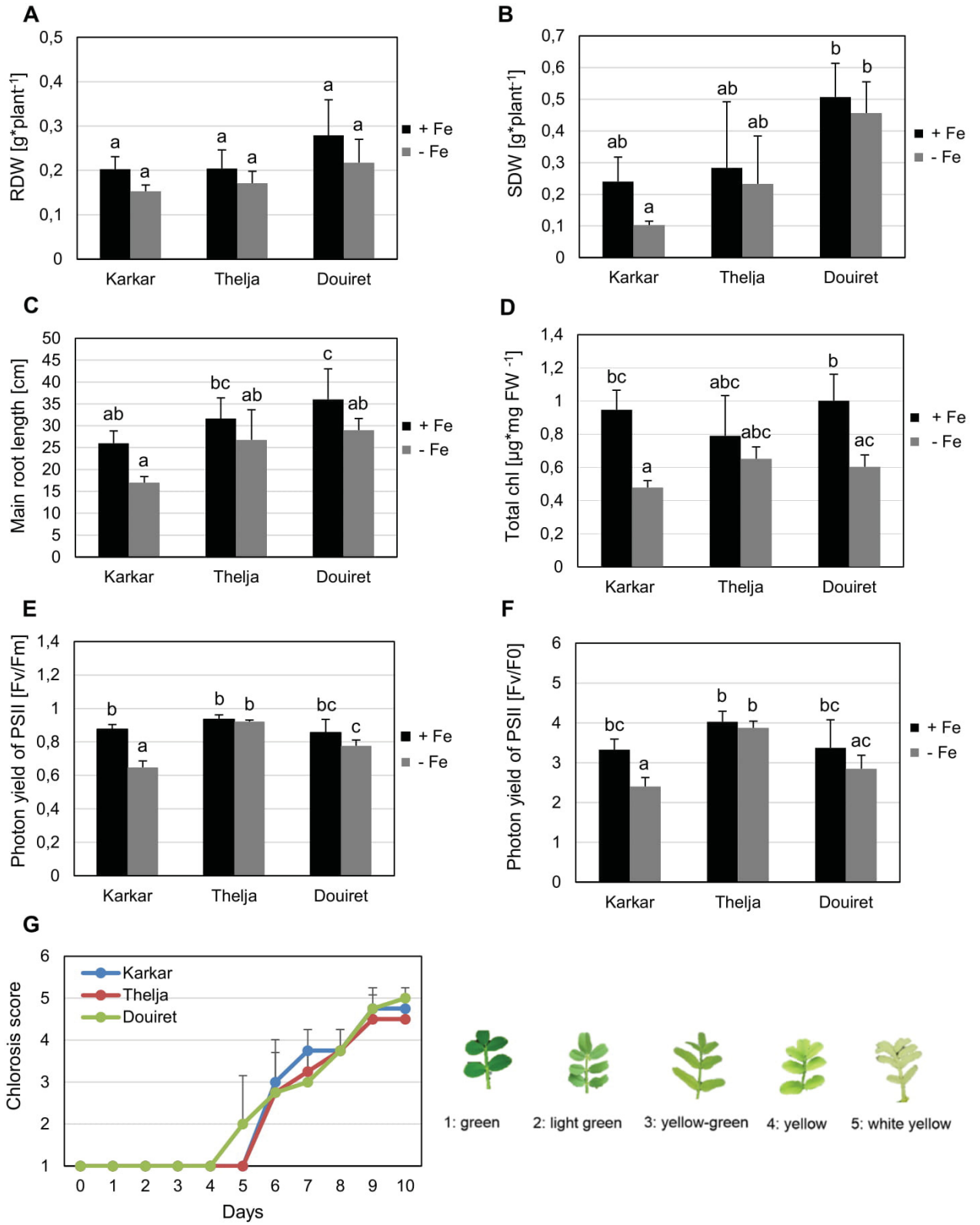


**Figure 1: Effect of Fe deficiency stress on Karkar, Thelja and Douiret lines**

(A) Root dry weight (RDW), n= 3; (B) Shoot dry weight (SDW), n= 3; (C) Main root length, n= 4-5; (D) Total chlorophyll (Chl) content, n= 3; (E, F) Photon yield of PSII calculated by Fv/Fm and Fv/F0, n= 4; (G) Chlorosis phenotype symptoms of young leaves calculated according to the indicated scale from 1, green leaves up to 5, white-yellow leaves, n = 4.

*H. carnosum* plants were exposed for 10 days (A-F) or up to 10 days (G) to Fe-sufficient (+Fe) and Fe-deficient (-Fe) hydroponic growth conditions. Data are means  $\pm$  SD; means with the same letter are not significantly different with  $P \leq 0.05$  according to ANOVA and Tukey's HSD test.

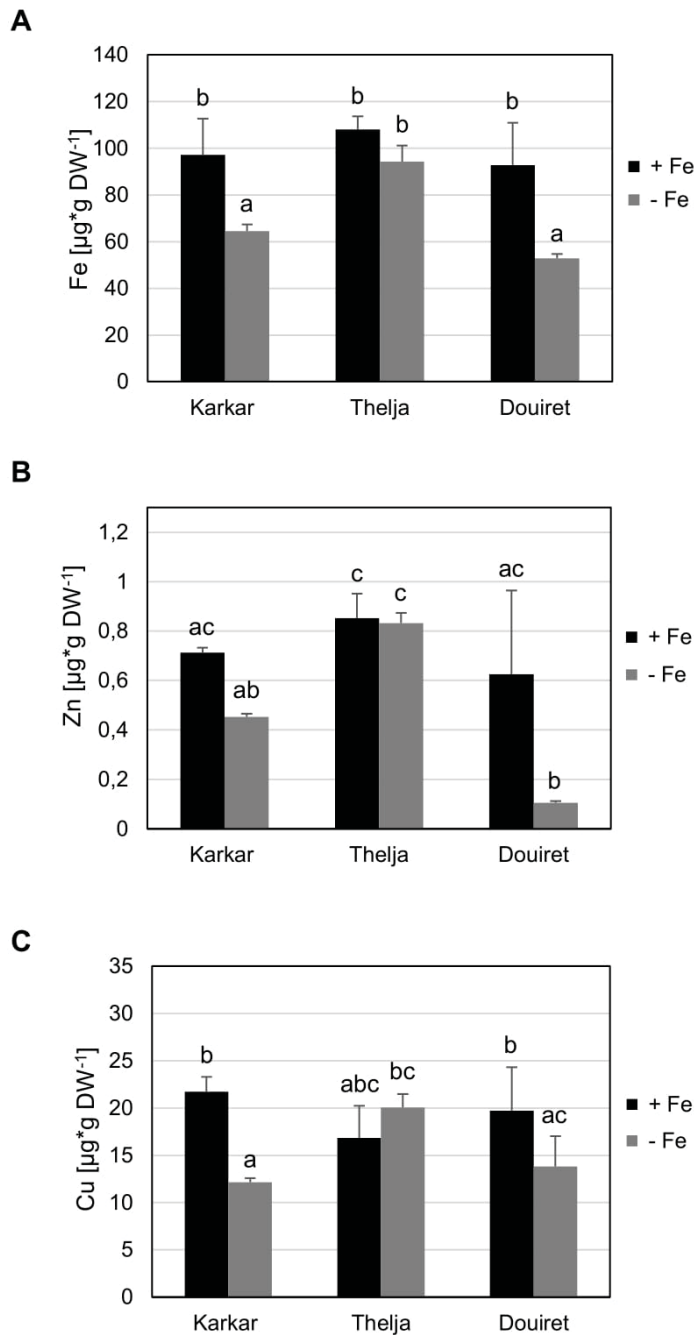


**Figure 2: Metal contents of Karkar, Thelja and Douiret**

(A) Fe; (B) Zn; (C) Cu contents of the youngest expanded leaves.

*H. carnosum* plants were exposed for 10 days to Fe-sufficient (+Fe) and Fe-deficient (-Fe) hydroponic growth conditions. Data are means  $\pm$  SD; n= 4; means with the same letter are not significantly different with  $P \leq 0.05$  according to ANOVA and Tukey's HSD test.

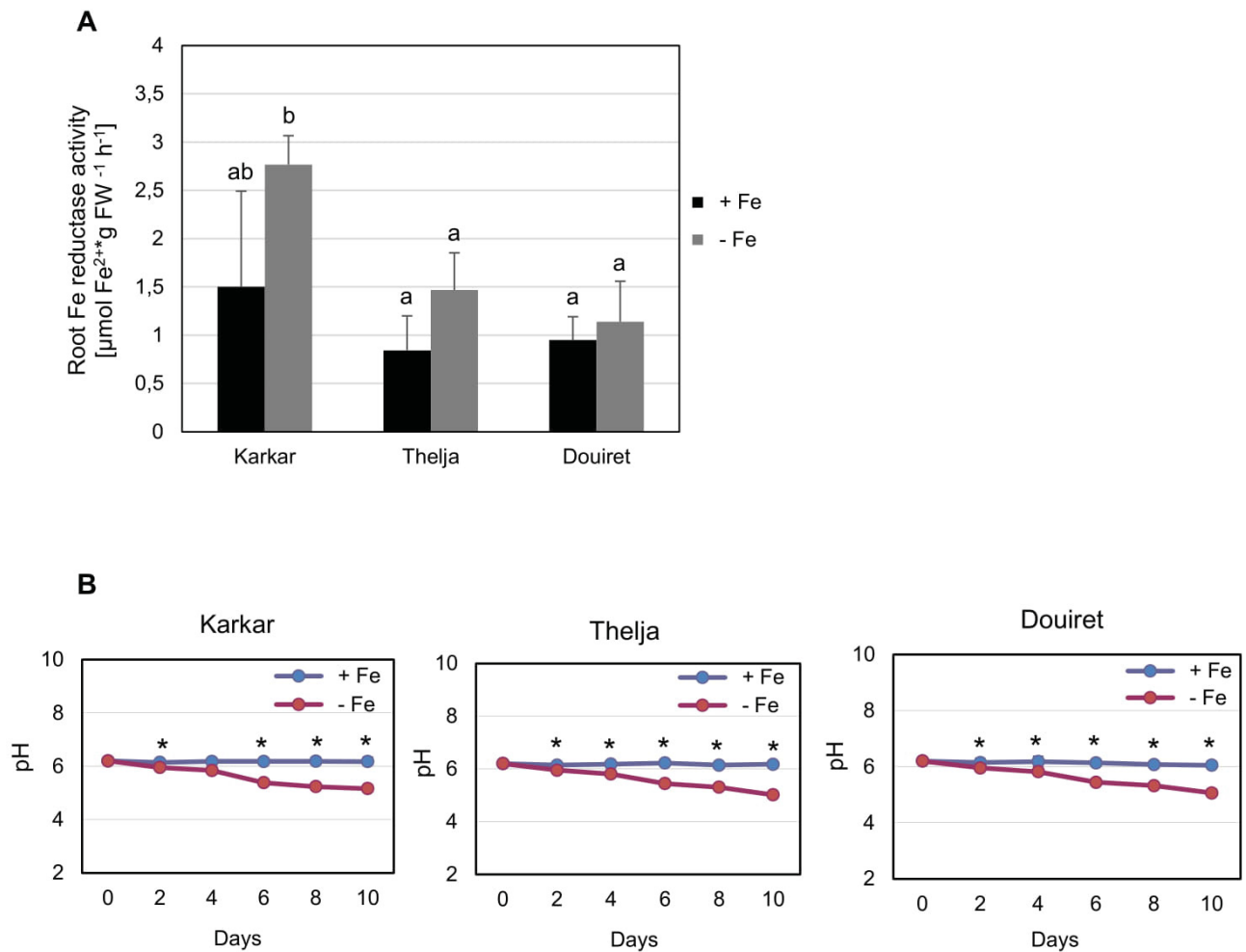
Lines	Parameters								
	RDW	SDW	MRL	Total chl	Photon yield	Chlorosis score	Fe	Zn	Cu
Karkar									
Thelja									
Douiret									

S	
T	

**Figure 3: Summary assessment of Karkar, Thelja and Douiret for Fe deficiency stress responses and metal contents**

The investigated parameters are root and shoot dry weights (RDW, SDW), total chlorophyll (Chl), photon yield, chlorosis score (see Figure 1) and Fe, Zn and Cu contents (see Figure 2). Responses that showed a decrease at - versus + Fe are designated by light gray color (S, sensitive) and no decrease by dark gray color (T, tolerant).



**Figure 4: Physiological Fe deficiency responses of Karkar, Thelja and Douiret**

(A) Root Fe reductase activity, n = 4-5; (B) pH changes in the growth medium, n = 4.

*H. carnosum* plants were exposed for 10 days (A) or up to 10 days (B) to Fe-sufficient (+Fe) and Fe-deficient (-Fe) hydroponic growth conditions. Data are means  $\pm$  SD; means with the same letter are not significantly different with  $P \leq 0.05$  according to ANOVA and Tukey's HSD test, means with \* label in B show a significant difference of + versus -Fe with  $P \leq 0.05$  according to a t-test.

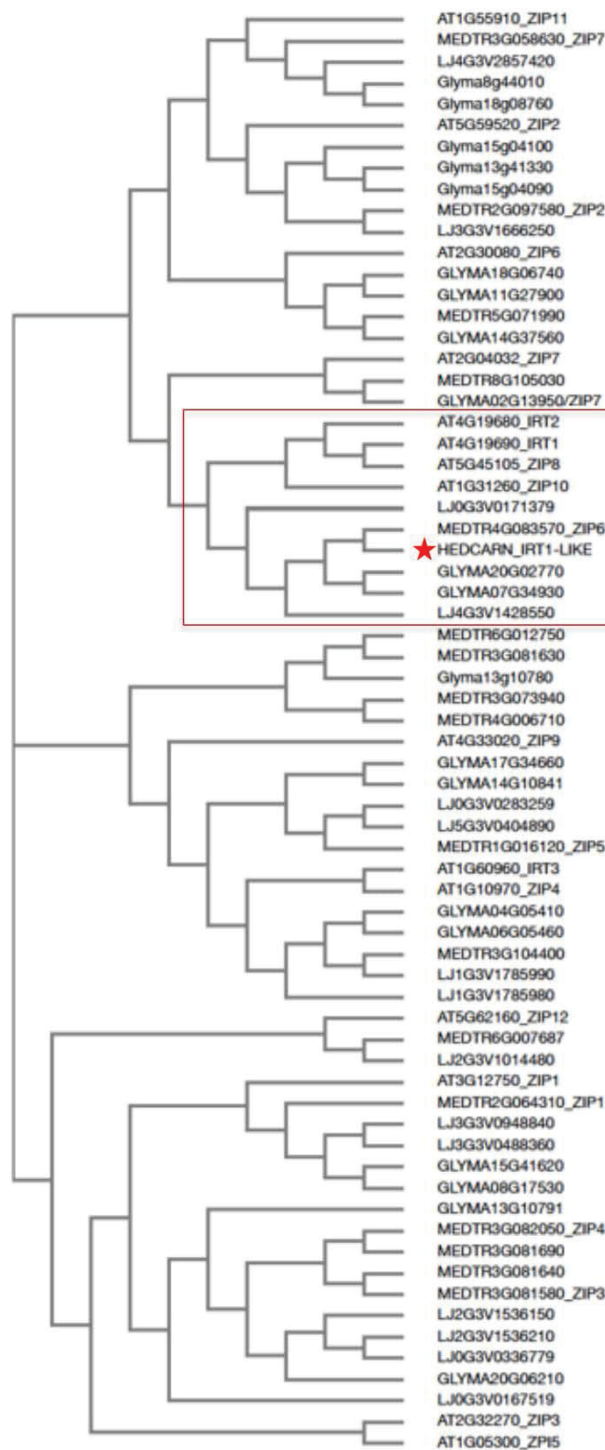
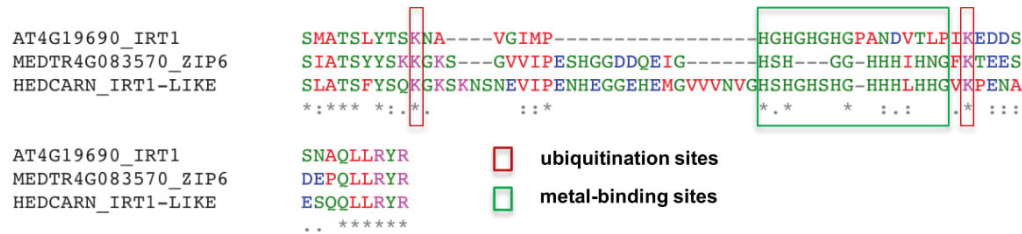


**Figure 5: Neighbor-joining tree of HcIRT1 and ZIP protein sequences from selected legumes and Arabidopsis**

The multiple amino acid sequence alignment was produced with *H. carnosum* IRT1 and all identified ZIP protein sequences from *A. thaliana*, *M. truncatula*, *G. max* and *L. japonicus*. The box indicates the closest relatives of AtIRT1. The star indicates HcIRT1.

A



B

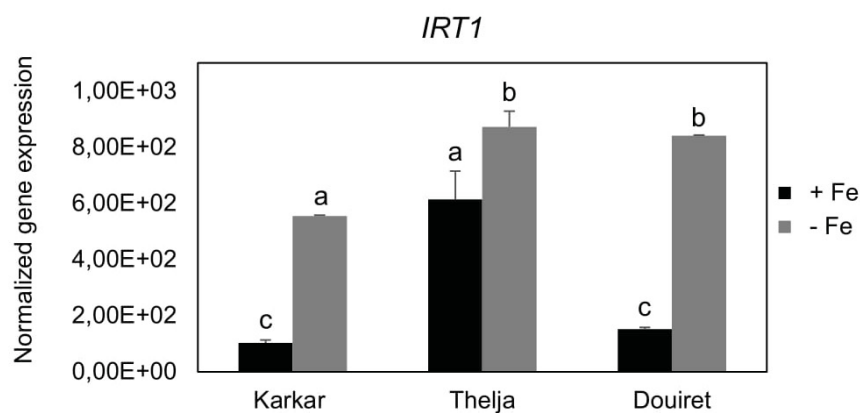


**Figure 6: Conservation of functional IRT1 sequences and *IRT1* gene expression in Karkar, Thelja and Douiret**

(A) Multiple amino acid sequence alignment of the variable cytoplasmic loop region of AtIRT1, HcIRT1 and MtZIP6, containing relevant functional residues involved in ubiquitination (lysines) and metal binding (histidine stretch). (B) Normalized gene expression of *IRT1*. *H. carnosum* plants were exposed for 10 days to Fe-sufficient (+Fe) and Fe-deficient (-Fe) hydroponic growth conditions. Data are means  $\pm$  SD; n= 3; means with the same letter are not significantly different with  $P \leq 0.05$  according to ANOVA and Tukey's HSD test.

A



B

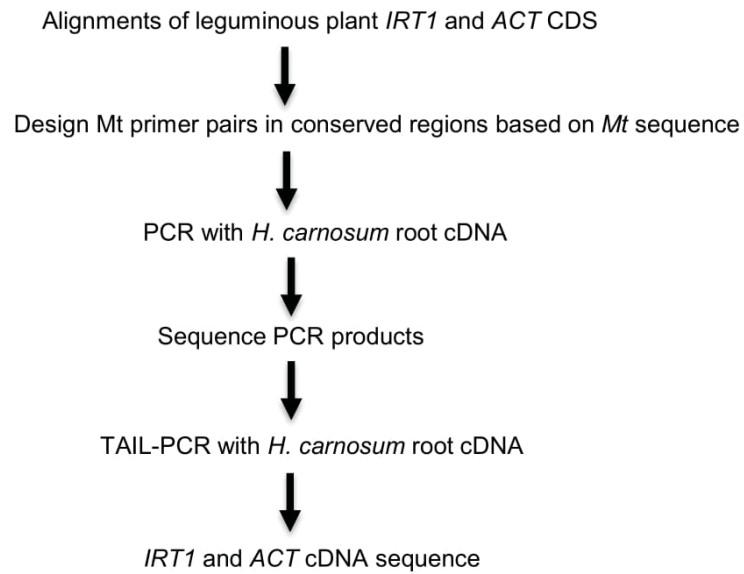
The map shows Tunisia with three collection localities marked: 1 (Karkar) in the north, 2 (Thelja) in the west, and 3 (Douiret) in the south. Neighboring countries Algeria and Libya are also labeled.

	Locality and name of line	Climate	Altitude (m)	Longitude (E)	Latitude (N)	Soil characteristics
1	Karkar	semi-arid	33	10°62'52"	35°47'34"	saline-sodic
2	Thelja	arid	195	8°19'24.2"	34°19'32.4"	calcareous
3	Douiret	saharan	434	10°17'13.1"	32°50'58.0"	sandy

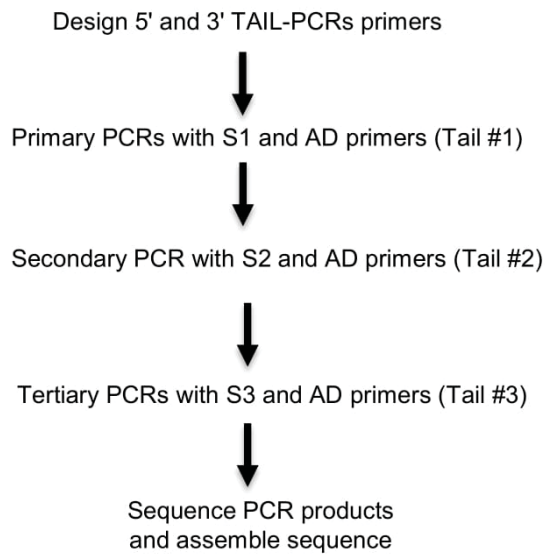
**Supplementary Figure 1: Overview of *Hedysarum carnosum* plant material**

(A) Morphology of *H. carnosum*; (B) Geographic distribution of collected Tunisian *H. carnosum* lines.

A



B



**Supplementary Figure 2: Overview of *HcIRT1* and *HcACT* cDNA sequence obtention**

(A) Flowchart for obtaining *H. carnosum* *IRT1* and *ACT* cDNA sequences; (B) Flowchart of TAIL-PCR steps.

**Primers used in this study**

**1/ Mt Primers**

Gene name/ Gene ID	Primer sequences (forward/reverse): ( 5'-3')	T <sub>m</sub> (°C)
MtIRT1(ZIP6)/ Mt4g083570.1	TTTAACATCACAAGCCCTAGCT GCCCATTTAGCCATGAGAGA	56
MtβACT/ Mt7g093260.1	TTGCAGGAGATGATGCA GTACACAGGAAATGCTTCTAA	59

**2/ qRT PCR Primers**

Gene name	Primer sequences (forward/reverse):( 5'-3')	T <sub>m</sub> (°C)
HcIRT1	AGTTTCCATTTTCAGGGCTTG TCTCATGTTCCACCTTCA	55
HcβACT	GCTACGTGGCTCCTGAAG GGTCTCAAACATGATCTGAGTCA	55

**3/ TAIL-PCR primers (gene IRT1)**

Gene name	Primer name	Primer sequences (forward/reverse): ( 5'-3')	T <sub>m</sub> (°C)
IRT1 5'	S1	CTCCATCTTAGCAACCAGCAT	58
	S2	CGGGTTCATGCATGTCTTCC	61
	S3	TGGTCTGATTGCTGGATGA	59
IRT1 3'	S1	TACAGCTTGAATTGTTGTTC	59
	S2	CCCCACTTGAATTGCCATAG	62
	S3	GAGTCCAAGGCTGCAGGTAG	60

**4/ TAIL-PCR primers (gene Beta actin)**

Gene name	Primer name	Primer sequences (forward/reverse): ( 5'-3')	T <sub>m</sub> (°C)
βACT 5'	S1	TGTGATGGTTGGTATGGGAC	59
	S2	TCTTCTAACCGAAGCACCAC	59
	S3	TGAGACCTTCAATACTCCAGC	58
βACT 3'	S1	GGAAACATTGCTTGAGTGGTG	58
	S2	GGAGATTTCTGCATTGGCAC	59
	S3	CCACCTGAGAGGAAGTACAG	59

**5/ Arbitrary degenerated Primers (AD) for TAIL-PCR**

Gene name	Concentration (μM )	Primer sequences (forward/reverse): ( 5'-3')	T <sub>m</sub> (°C)
AD1	24	NGTCGASWGANAWGAA	43-48
AD2	24	TGWNAGSANCASAGA	46-51
AD3	24	AGWGNAGWANCAWAGG	43-48
AD4	32	STTGNTASTNCTNTGC	43-51
AD5	16	NTCGASTWTSWGTGTT	41-44
AD6	32	WGTGNAGWANCANAGA	40-48

**Supplementary Figure 3:**  
List of primers used in the study

**Author contribution to Manuscript 2:** Natural variation of physiological and molecular responses of Tunisian *Hedysarum carnosum* subjected to iron deficiency (**submitted**).

Heithem Ben Abdallah

Performed and carried out experiments, prepared final figures, performed statistical analysis and commented on the manuscript.

Hans-Jörg Mai

Helped in analyzing experiments, statistical analysis and commented on the manuscript.

Tarek Slatni

Helped in designing experiments (Figure 4).

Claudia Fink-Straube

Performed metal measurements.

Chedly Abdelly

Helped in designing experiment (Figure 4).

Petra Bauer

Designed the outline of the manuscript, supervised the study, provided funding, wrote and corrected the manuscript.

## Manuscript 3

**Natural variation reveals contrasting abilities to cope with alkaline and saline soil among different *Medicago truncatula* genotypes**



## Natural variation reveals contrasting abilities to cope with alkaline and saline soil among different *Medicago truncatula* genotypes

Heithem Ben Abdallah · Hans-Jörg Mai · Ana Álvarez-Fernández · Javier Abadía · Petra Bauer

Received: 9 May 2017 / Accepted: 8 August 2017  
© Springer International Publishing AG 2017

### Abstract

**Background and Aims** Abiotic stress conditions cause extensive losses to agricultural production worldwide. Salinity and alkalinity affect plant growth, photosynthesis and availability of nutrients including Fe. Many studies have described the response mechanisms of plants to single abiotic stress conditions. However, in the field, crops and other plants are routinely subjected to a combination of different abiotic stresses. Salinity and alkalinity are wide-spread in Tunisia, where *Medicago truncatula* occurs as a native species.

**Methods** We established a growth system to study the combined effects of salinity and alkalinity conditions in laboratory conditions. We screened 11 Tunisian *M. truncatula* lines from the SARDI collection based on their phenotypic responses to the double stress.

**Results** Salinity and alkalinity affected germination rates, shoot and root dry weights, pigment contents and root morphology parameters. We were able to select among the 11 investigated lines four sensitive and tolerant lines with different abilities to respond to the double stress. Tolerant and sensitive genotypes (two lines each) differed in root flavin contents, root flavin staining patterns and concentrations of root flavins in the nutrient solution.

**Conclusions** Root architecture, flavin root localization in epidermal cells and flavin secretion are relevant tolerance mechanisms for salt and alkaline stress in *M. truncatula*. Pairs of contrasting lines from close origins were identified that will be useful tools to identify genes for the tolerance mechanisms.

**Keywords** *Medicago truncatula* · Root · Iron deficiency · Alkalinity · Salinity · Natural variation · Flavin

**Electronic supplementary material** The online version of this article (doi:10.1007/s11104-017-3379-6) contains supplementary material, which is available to authorized users.

H. Ben Abdallah · H.-J. Mai · P. Bauer  
Institute of Botany, University of Düsseldorf,  
D-40225 Düsseldorf, Germany

A. Álvarez-Fernández · J. Abadía  
Department of Plant Nutrition, Aula Dei Experimental Station,  
Consejo Superior de Investigaciones Científicas (CSIC),  
P.O. Box 13034, E-50080 Zaragoza, Spain

P. Bauer (✉)  
Institute of Botany, Heinrich-Heine University, Universitätsstrasse  
1, D-40225 Düsseldorf, Germany  
e-mail: petra.bauer@uni-duesseldorf.de

### Abbreviations

*Chl* chlorophyll  
*Rbfl* riboflavin

### Introduction

Soil salinity is a global environmental issue affecting an area of approximately 830 million ha worldwide (Rengasamy 2016). Plant growth in saline soils is usually hampered due to osmotic and oxidative stress and also to toxic effects resulting from high ion

concentrations (Rengasamy 2016). In sodic soils, clay dispersion and soil structural degradation result from high  $\text{Na}^+$  cation amounts and affect negatively plant growth (Rengasamy 2016). Moreover, sodic soils with a dominating presence of Na carbonate and calcareous soils are very alkaline (Rengasamy 2016). Alkalinity causes a low solubility of several other ions, including Fe. Many plant species display Fe deficiency symptoms, including leaf chlorosis and reduced biomass, when grown in a medium at neutral or alkaline pH, since Fe is essential for many enzymes involved in electron transfer processes in respiration, photosynthesis and N fixation (Briat et al. 2015). Iron deficiency also represents a serious problem in human nutrition worldwide (Naranjo-Arcos and Bauer 2016). Salinity and alkalinity are widespread in Tunisian soils, on one hand due to an occurrence of salt-affected soils in depressions and in the main “sebkhas” and “chotts” (dry alkali flats, usually near the sea, and interior salt lake areas, respectively), and on the other hand due to secondary salinity derived from low-quality irrigation water that is rich in dissolved salts.

Alfalfa (*Medicago sativa*) is a perennial forage with high yield and good nutritional quality, interesting for cropping practices in many agricultural areas, including some in North Africa (Basigalup et al. 2014). Its diploid annual relative *Medicago truncatula* is a major model legume and is used for molecular studies of physiological responses to stresses such as salinity and Fe deficiency (Rodríguez-Celma et al. 2013; Zahaf et al. 2012). This species presents a large diversity and geographic distribution in the Mediterranean basin and in particular in diverse Tunisian soils (Ellwood et al. 2006; Lazrek et al. 2009). *M. truncatula* shows a broad adaptation including tolerance to severe growth conditions, with some ecotypes characterized as displaying a high tolerance to salinity and calcareous soil conditions, and hence *M. truncatula* gemplasm can be screened for molecular-ecological adaptation (Friesen et al. 2010; Friesen et al. 2014). *M. truncatula* natural variation lines and genome sequences have been successfully used for association genetics to pinpoint novel genetic loci and genes for variation of responses (<http://www.noble.org/medicago/ecotypes.html>). However, a successful approach for exploiting natural variation relies on the successful identification of lines with interesting properties, followed by combined comparative genomics and functional genomics analysis of the lines that have contrasting abilities, e.g., to show tolerance or

susceptibility towards salt or Cd stress (Friesen et al. 2010; Rahoui et al. 2016; Zahaf et al. 2012). Such approaches can ultimately help to elucidate candidate genes and functional pathways that have been selected during ecological adaptation.

Salt tolerance relies to a large extent on the sequestration and secretion of cellular ions and the counteraction of osmotic effects and reduced transpiration (Hanin et al. 2016). Calcareous soils affect Fe uptake in dicotyledonous species, which mobilize Fe in the soil *via* proton extrusion and reduction of Fe(III) to Fe(II) (Abadia et al. 2011). The differences in the signaling responses and tolerance mechanisms between Fe deficiency and calcareous soil conditions are still not fully understood (Hsieh and Waters 2016). In Poaceae the up-regulation of Fe acquisition correlated with tolerance to saline-alkaline stress (Li et al. 2016), suggesting that Fe deficiency is a major problem on such soils. Recently, it has become evident that secondary compounds secreted by dicotyledonous plant roots upon Fe deficiency could play important roles in the mobilization of Fe upon alkaline and calcareous growth conditions. For example, Arabidopsis mutants can develop leaf chlorosis if the production and secretion of phenolic coumarin compounds in roots is perturbed (Fourcroy et al. 2014; Schmid et al. 2014). *Medicago truncatula* and sugar beet roots produce and secrete flavins, instead of phenolics, in response to Fe deficiency (Andaluz et al. 2009; Rodríguez-Celma et al. 2013; Rodríguez-Celma et al. 2011a; Rodríguez-Celma et al. 2011b; Susin et al. 1993), and it has been demonstrated that extracellular flavins allow Fe-deficient sugar beet roots to dissolve soil Fe(III)-oxides at high pH *via* reductive mechanisms (Sisó-Terraza et al. 2016b).

In this present work we investigated the interactive effects of salinity and calcareous/alkaline soil conditions on germination, plant growth, leaf pigment content, root morphology parameters and root flavin content and secretion in selected lines of *M. truncatula*, to identify and characterize lines sensitive and tolerant to these stresses. We made use of the natural diversity from Tunisia by studying the responses of 11 accessions derived from the South Australian Research and Development Institute (SARDI) collection to identify among them tolerant and susceptible lines. We suspect that these lines will be related to each other due to their close origin of collection in Tunisia. Our aim was to identify lines with contrasting stress response behavior to use them as tool for future molecular dissection.

## Materials and Methods

### Plant material

We used the wild type reference *M. truncatula* Jemalong A17 line, kindly sent by Jean-Marie Prosperi, INRA Montpellier. Eleven Tunisian *M. truncatula* lines were selected from the SARDI collection, kindly provided by Steve Hughes, South Australian Research and Development Institute (SARDI). This selection was based on the origin of the collected lines, using criteria such as soil texture and pH. The locations for collection of accessions covered a large area from the north to the south of Tunisia (Supplementary Fig. 1).

### Plant growth

*M. truncatula* plants were grown under controlled conditions in a scientific incubator (Percival Scientific AR-36 L2, Perry, IA, U.S.A.), using day/night cycles of 16/8 h, 24 °C/18 °C, and a relative humidity of 70%. Seeds were mechanically scarified by placing them on a fine grit sand paper sheet and rubbing gently with another piece of sand paper, until visible signs of abrasion appeared. Seeds were sterilized in 10% Na hypochlorite for 8 min and then abundantly rinsed with distilled water.

For soil experiments, seeds were imbibed in sterile water for 2 days at 4 °C and then planted in soil. For salinity treatments, different concentrations of NaCl ranging from 75 to 500 mM were used for soil watering, as indicated in the text. For calcareous and alkaline conditions (shortly termed as alkalinity in the text) the soil was supplemented with different mixtures of CaCO<sub>3</sub> and NaHCO<sub>3</sub>. These mixtures are abbreviated throughout the text as “n/m BIC”, with n and m being the amounts of CaCO<sub>3</sub> and NaHCO<sub>3</sub>, respectively (in g kg<sup>-1</sup> soil). BIC treatments ranged from 5/3 to 50/15 BIC, as indicated in the text. Combined soil salinity and alkalinity experiments consisted of combinations of salt and BIC treatments, as indicated in the text.

For the hydroponic system, sterilized seeds were germinated for 4 days at 20 °C in Petri dishes on constantly moistened filter paper. Four day-old seedlings were transferred to a half strength aerated nutrient solution for 4 days. Then, seedlings of similar size were selected and cultured in groups of six plants in one-L pots filled with full strength aerated nutrient solution. The composition of the full strength nutrient solution was: 1.5 mM Ca(NO<sub>3</sub>)<sub>2</sub>,

1.25 mM KNO<sub>3</sub>, 0.75 mM MgSO<sub>4</sub>, 0.5 mM KH<sub>2</sub>PO<sub>4</sub> and 10 μM H<sub>3</sub>BO<sub>3</sub>, 50 μM Fe(III)Na-EDTA, 1 μM MnSO<sub>4</sub>, 0.5 μM ZnSO<sub>4</sub>, 0.05 μM (NH<sub>4</sub>)<sub>6</sub>Mo<sub>7</sub>O<sub>24</sub> and 0.4 μM CuSO<sub>4</sub>. Five different treatments were applied during 8 days using nutrient solutions modified as follows: control (50 μM Fe(III)Na-EDTA; C), carbonate-induced Fe deficiency (50 μM Fe(III)Na-EDTA, 1 g L<sup>-1</sup> CaCO<sub>3</sub> and 10 mM NaHCO<sub>3</sub>; BIC), Fe deficiency (0 μM Fe(III)Na-EDTA; -Fe), salinity (50 μM Fe(III)Na-EDTA and 100 mM NaCl; NaCl) and combined stress (50 μM FeNa-EDTA, 1 g L<sup>-1</sup> CaCO<sub>3</sub>, 10 mM NaHCO<sub>3</sub> and 100 mM NaCl; BIC/NaCl). The pH was adjusted to 6.0 for the treatments C, -Fe and NaCl and to 7.0 for treatments BIC and BIC/NaCl. The nutrient solution was renewed every 5 days. Plants were analyzed according to Supplementary Fig. 1 and as indicated in the text.

### Determination of the germination rate and dry weight

To assess the germination rate, we counted the number of plants with emerged cotyledons (Supplementary Fig. 1). To obtain the dry weight (DW), plant shoot and root material was dried in an oven at 70 °C for 48 h and weighed.

### Photosynthetic leaf pigment measurements

Leaf pigments were extracted from fresh leaves (leaf number 2, Supplementary Fig. 1) in 80% acetone and assayed spectrophotometrically according to (Arnon 1949) using the TECAN infinite 200 PRO multimode reader at 645 nm, 663 nm and 470 nm wavelengths. Readings were then used to calculate total *Chl* and carotenoid contents in mg g<sup>-1</sup> leaf fresh weight.

### Root morphology

Root systems were excised and thoroughly cleaned from soil particles if plants were grown in soil. Then, roots were laid out on a scanner, and root architectural parameters were recorded using the scanned images with the help of the WinRHIZO software (Regent Instruments Inc., Québec, Canada).

### Extraction, analysis and localization of flavins in roots

Flavins were extracted from 1 to 1.5 cm root tips dissected from the main root as described in (Rodríguez-

Celma et al. 2011b). Root extracts were dried, re-suspended in mobile phase (85% methanol and 0.1% formic acid) and analyzed for flavins using high-performance liquid chromatography with photodiode array detection coupled in-line to time-of-flight mass spectrometry [HPLC-UV/VIS-MS(TOF)], as described (Sisó-Terraza et al. 2016a). The HPLC system (Alliance 2795, Waters, Mildford, MA, U.S.A) included an analytical HPLC column (Symmetry R C<sub>18</sub>, 15 cm × 2.1 mm i.d., 5 µm spherical particle size, Waters) protected by a guard column (Symmetry R C<sub>18</sub>, 10 mm × 2.1 mm i.d., 3.5 µm spherical particle size, Waters). A gradient mobile phase built with 0.1% (v/v) formic acid in water and 0.1% (v/v) formic acid in methanol was used. A PDA 2996 (Hsieh and Waters) and an MS(TOF) equipped with a electrospray ionization (ESI) source (microTOF, Bruker Daltonics Bremen, Germany) were used for flavin detection. Flavin quantification was carried out by external calibration using the peak areas at *m/z* of the corresponding [M + H]<sup>+</sup> ions and a *Rbfl* calibration curve.

Flavin localization in roots was studied using fluorescence microscopy of *ca.* 100 µm root cross sections taken 1–1.5 cm above the tip of the main root, with excitation and emission wavelengths of 422 and 528 nm, respectively, on an Axio Imager 2 microscope (Zeiss, Jena, Germany).

## Results

Establishment of growth conditions using the *M. truncatula* reference line Jemalong A17

First, we established a soil growth system for *M. truncatula* plants with saline and alkaline growth conditions, in order to evaluate plant morphological and physiological traits. Initially, we tested saline and alkaline conditions separately. For the saline condition, we grew seedlings of the reference line Jemalong A17 and irrigated the soil with different saline solutions, ranging from 75 to 500 mM NaCl, during a period of 15 days (Fig. 1). Treatment with 100 to 200 mM NaCl decreased the germination rates significantly by 10–30%, compared with the control and the 75 mM NaCl treatment (Fig. 1a). At 300 mM NaCl, a further significant drop (60%) in the germination rate was observed (Fig. 1a). At higher salinity rates, 400 and 500 mM NaCl, seed germination was completely inhibited during the tested time (Fig. 1a). Up

to 150 mM NaCl, the root and shoot DWs as well as the lengths of the main root were similar in salt-treated and control plants (Fig. 1b, c). At 200 mM NaCl, a significant drop in biomass and main root length was observed, and effects were intensified significantly at 300 mM NaCl.

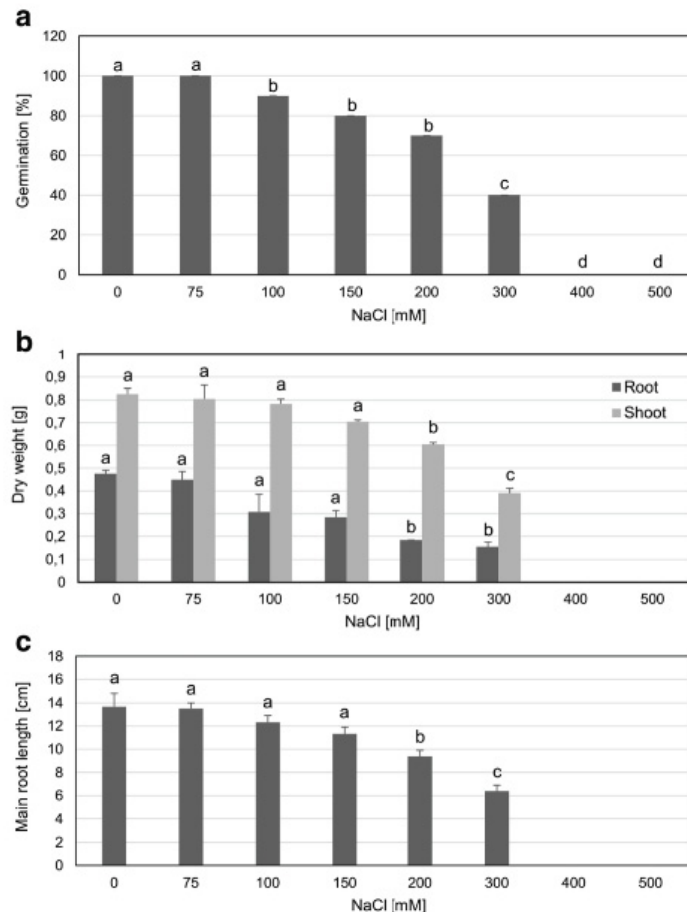
Next, we tested alkaline-induced changes of plant growth by mixing the soil with different BIC systems prepared with different amounts of CaCO<sub>3</sub> and NaHCO<sub>3</sub> (labeled as BIC n/m, with n and m being the amounts of CaCO<sub>3</sub> and NaHCO<sub>3</sub>, respectively, in g kg<sup>-1</sup> soil). Compared to the untreated control, the germination rate was reduced by 10, 30 and 80% upon supply of 10/6, 20/9 and 30/12 BIC, respectively, whereas at 50/15 BIC no germination was observed (Fig. 2a). A marked root DW reduction (30–50%) took place at 20/9 and 30/12 BIC, whereas the main root was significantly reduced in size (*ca.* 40%) at 30/12 BIC (Fig. 2c). The shoot DW was significantly reduced by 20–50% at 10/6, 20/9 and 30/12 BIC (Fig. 2b). These preliminary results were used to narrow down appropriate combinations of saline and alkaline environmental conditions in further experiments.

We then tested ten combinations of NaCl and BIC (alkalinity) treatments in the soil growth system, choosing combinations of those single stress treatments that did not affect or affected only moderately plant growth (see Fig. 3). Germination rates were significantly decreased at 75 mM NaCl when supplemented with 10/6 and 20/9 BIC (by 10 and 20%), and at 100 and 150 mM when supplemented with 5/3 (by 10% each), 10/6 (by 10% each) and 20/9 BIC (by 20 and 40%), with 20/9 BIC causing the highest drop (by 40%) in germination at 150 mM NaCl (Fig. 3e). Similarly, shoot DWs dropped clearly at 75–150 mM NaCl when supplemented with 20/9 BIC (by 25, 70 and 70%) (Fig. 3b). Root DWs were also most affected under these conditions (Fig. 3b). Main root lengths were shorter at 100 and 150 mM NaCl in the presence of 20/9 BIC (by 35 and 60%) (Fig. 3c). Thus, we observed in several combined stress conditions a decline in the growth compared to single stresses. For screening experiments under combined stress, we decided to apply 10/6 BIC in combination with 150 mM NaCl, which was the highest BIC treatment tolerated by Jemalong A17.

Effects of individual and combined stress in hydroponic system on wild-type Jemalong A17

A combined stress condition was also applied to Jemalong A17 using a hydroponic system. We observed that the effect of combined stress (1 g L<sup>-1</sup> CaCO<sub>3</sub>,

**Fig. 1** Effect of salt stress in *M. truncatula* Jemalong A17. **(A)** Germination rate; **(B)** biomass production; **(C)** main root length in *M. truncatula* wild type (Jemalong A17) grown during 15 days in soil with different salt concentrations. Data are means  $\pm$  SD;  $n = 4$ ; means with the same letter are not significantly different at  $P \leq 0.05$  according to Analysis of variance (= ANOVA) and Fisher's Least Significant Difference (= LSD) test



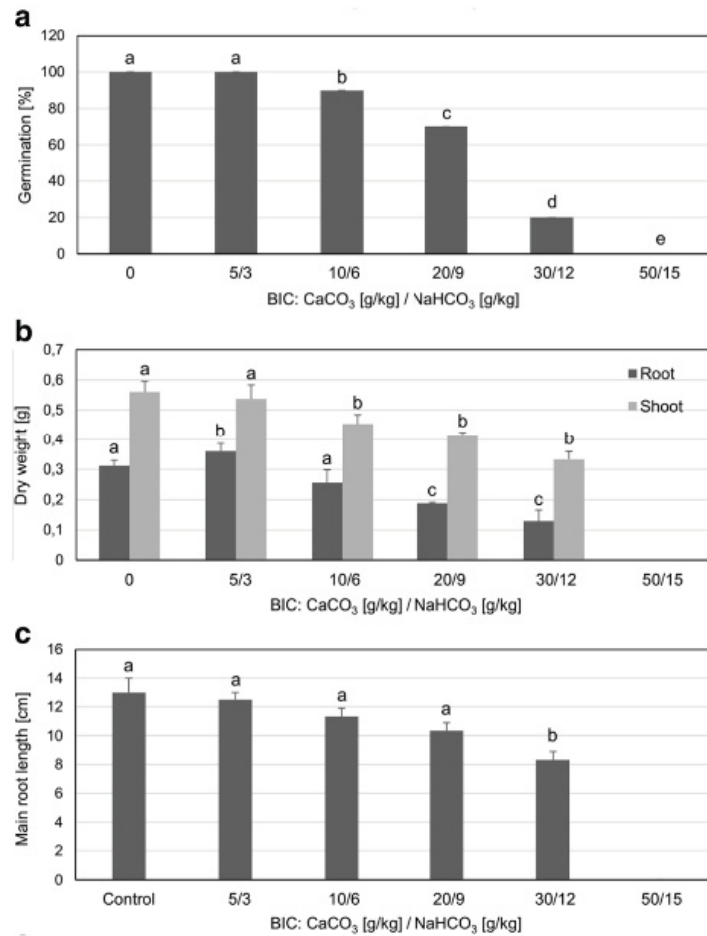
10 mM NaHCO<sub>3</sub>, 100 mM NaCl) was as harmful as BIC alone on shoot DW, main root length and carotenoid content, but more harmful than effects of single stresses on root DW, number of secondary roots and *Chl* content (Fig. 4). An effect of the single NaCl treatment was only noted for the number of secondary roots (Fig. 4d). These data confirmed that the combination of salt and alkalinity stress had stronger and more pronounced effects on *M. truncatula* plants than the individual stresses.

Screening of 11 Tunisian *M. truncatula* lines of the SARDI collection under combined stress

We examined 11 different *M. truncatula* genotypes (SARDI collection, lines 1–11) along with the reference line JA17 using the above selected combination of salt and alkalinity stresses in soil conditions (10/6 BIC in

combination with 150 mM NaCl). We found that the germination rates were decreased by 10% or more under combined stress compared to the untreated controls up to day 10 in four out of the 11 lines, namely lines 1, 8, 9 and 10, and JA17 (Fig. 5a, hatched bars). The ratios of germination upon combined stress versus control differed slightly between the lines (Fig. 5a). Combined stress resulted in a significant decrease of root DWs in lines 2, 3, 4, 5, 7, 8, 9 and JA17 (Fig. 5b, hatched bars). The ratios of combined stress versus control were lowest for lines 2 and 4, indicating more than 80% reduction, and lines 7, 8, 9, indicating 30–50% reduction of root dry weights. Root DWs of lines 1, 6, 10 and 11 appeared fairly unaffected by the stress treatment (Fig. 5b, filled bars). Combined stress caused a significant drop of shoot DW in lines 1, 7, 9, 10 and 11 (Fig. 5c, hatched bars), but not for the other tested lines (Fig. 5c, filled bars). The ratio of combined stress versus control regarding shoot DW was lowest for line 9,

**Fig. 2** Effect of bicarbonate (BIC) stress in *M. truncatula* Jemalong A17. **(A)** Germination rate; **(B)** biomass production; **(C)** main root length in *M. truncatula* wild type (Jemalong A17) grown during 15 days in soil with different BIC concentrations. Data are means  $\pm$  SD;  $n = 4$ ; means with the same letter are not significantly different at  $P \leq 0.05$  according to ANOVA and Fisher's LSD test



indicating a 60% reduction (Fig. 5c). The total *Chl* content was significantly diminished upon the combined stress versus the control in line 4 (by more than 20%), but however increased in the lines 8, 10 and 11 (by 40%) (Fig. 5d, hatched bars). The carotenoid content was lowered upon the combined stress in lines 4 and 6 (by more than 60%) and again enhanced in lines 10 and 11 (by 40%) (Fig. 5d, hatched bars).

Total root length and root surface were significantly increased in line 4 (hatched bars), and the root surface decreased in line 3 (hatched bar), while total root length and root surface remained unchanged in all other lines (filled bars) upon combined stress versus the respective control (Fig. 6a, b). The root diameter was significantly changed only in line 4 (decreased by 30%) in the stress versus the control condition (Fig. 6c, hatched bar). While the ratios of combined stress versus control did

not vary significantly between the lines for the parameters total root length and root surface (Fig. 6a, b), some differences were noted for root diameter measurements for some lines. For example, lines 10 and 11 had a higher ratio compared to lines 4 and 9, indicating that despite of the non-significant changes of root parameter data within lines 10, 11 and 9, differences were better apparent when comparing between the lines.

Taken together, our results show that the 11 investigated *M. truncatula* lines from the SARDI collection show variations in the responses to combined salinity and alkalinity stress versus the control, that are apparent at the level of germination, biomass production, photosynthetic pigment contents and root morphology. For better comparison of the lines, we plotted the combined stress versus control ratios in a single table and calculated a mean response ratio from the four parameters, namely

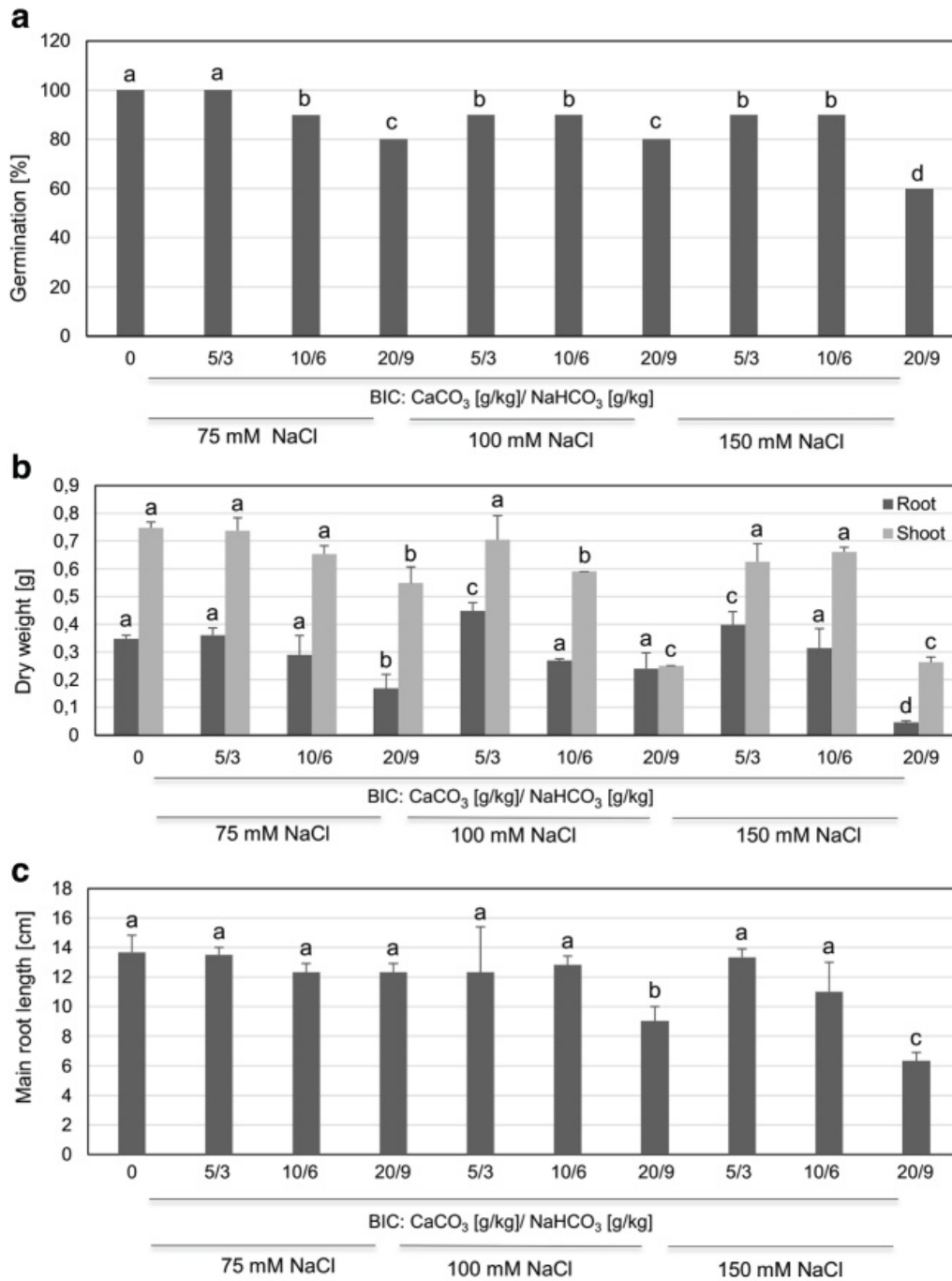


**Fig. 3** Effect of combined salt and bicarbonate (BIC) stress in *M. truncatula* Jemalong A17. **(A)** Germination rate; **(B)** biomass production; **(C)** main root length of *M. truncatula* wild type (Jemalong A17) grown during 15 days in soil with different salt

and BIC concentrations. Data are means  $\pm$  SD;  $n = 4$ ; means with the same letter are not significantly different at  $P \leq 0.05$  according to ANOVA and Fisher's LSD test

germination, biomass (average of root and shoot DWs), pigment content (average of total *Chl* and carotenoid

contents), root morphology (average of total root length, diameter and surface) (Fig. 7). Three lines showed a high

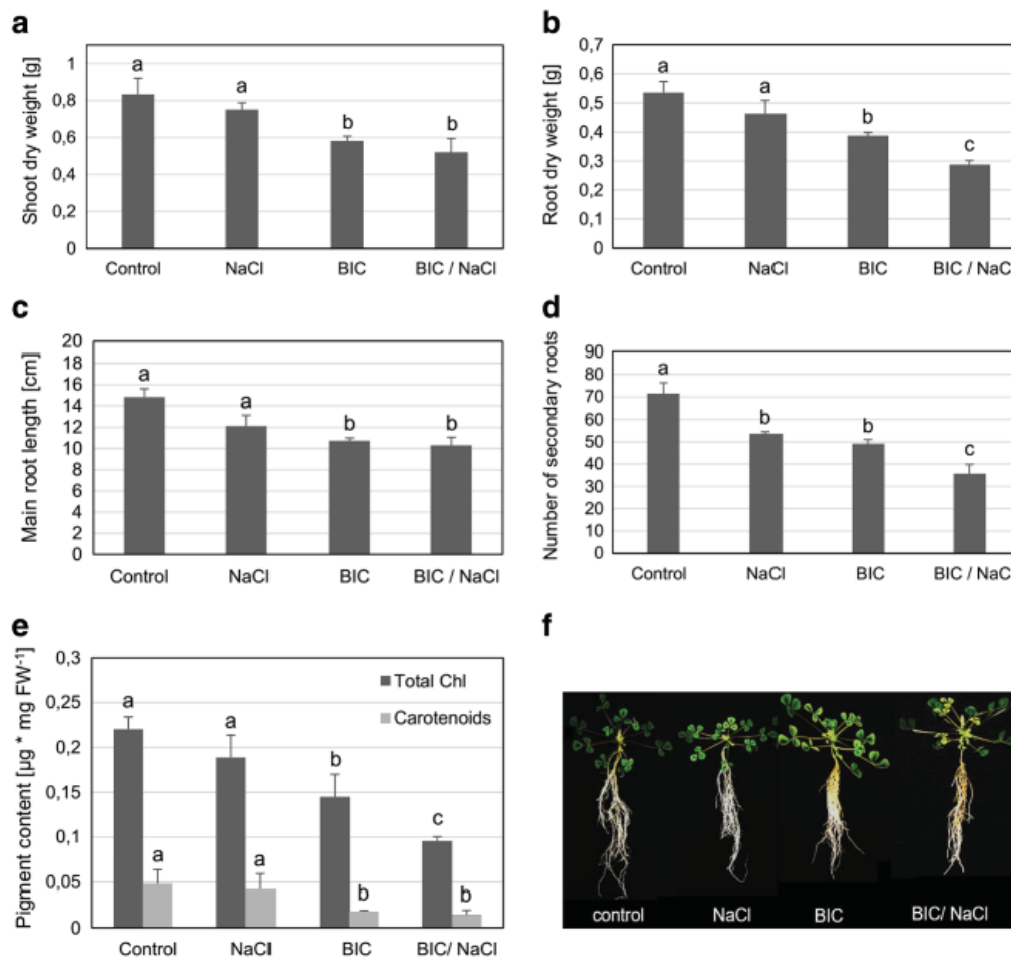


**Fig. 4** Effects of individual and combined stress in *M. truncatula Jemalong A17* upon hydroponic growth. **(A)** Shoot DW; **(B)** root DW; **(C)** main root length; **(D)** number of secondary roots; **(E)** leaf pigment content; **(F)** plant images of *M. truncatula* WT (Jemalong A17) grown during 15 days in a hydroponic system under control (regular) conditions, salt (+ 100 mM NaCl), BIC (+ 1 g/L

$\text{CaCO}_3$  + 10 mM  $\text{NaHCO}_3$ ), and BIC/NaCl combined stress (+ 1 g/L  $\text{CaCO}_3$  + 10 mM  $\text{NaHCO}_3$  + 100 mM NaCl). Data are means  $\pm$  SD;  $n = 3$ ; means with the same letter are not significantly different with  $P \leq 0.05$  according to ANOVA and Fisher's LSD test

mean ratio level of more than 95% and were considered tolerant to the combined stress, namely lines 8, 10 and 11. Six lines gave a ratio below 86% and were considered sensitive to the combined stress, namely lines 1, 2, 4, 6, 7 and 9. Lines 3 and 5 with values inbetween were designated neutral.

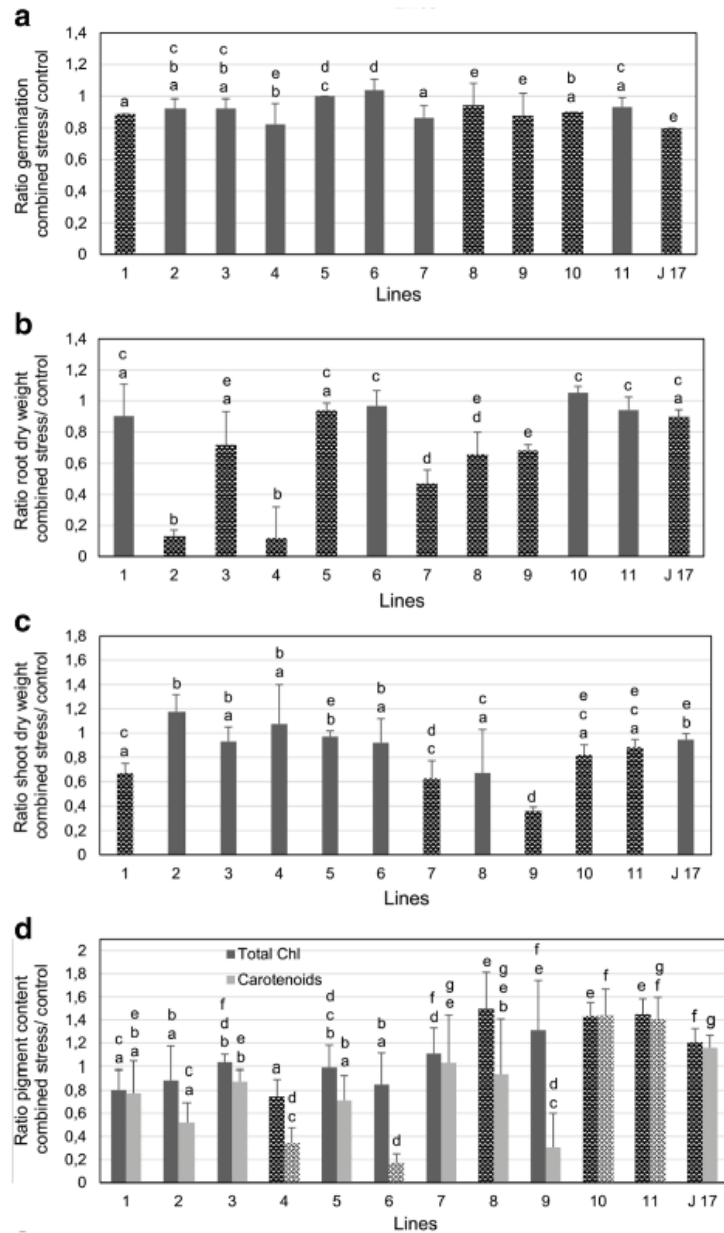
Analysis of selected tolerant and sensitive *M. truncatula* lines to the combined stress in a hydroponic system

We selected four lines (7, 9, 10 and 11) to validate and re-examine the responses to the combined stress conditions, this time using hydroponic growth. The aim was

to conduct additional studies to deduce potential mechanisms of tolerance.

In hydroponic growth, the total *Chl* contents of the sensitive lines 7 and 9 were reduced by 40–55% upon combined stress versus control, while that of the tolerant line 10 was decreased by only 30% (Fig. 8a, hatched bars). For tolerant line 11, no significant drop in *Chl* content was noted (Fig. 8a, filled bar). The sensitive lines showed a significant root DW reduction of ca. 65% compared to 30–35% reduction for the tolerant ones (Fig. 8b, hatched bars). Shoot DW, on the other hand, was significantly decreased in all lines by 20–30% upon the combined stress versus the control (represented by hatched bars), but no differences

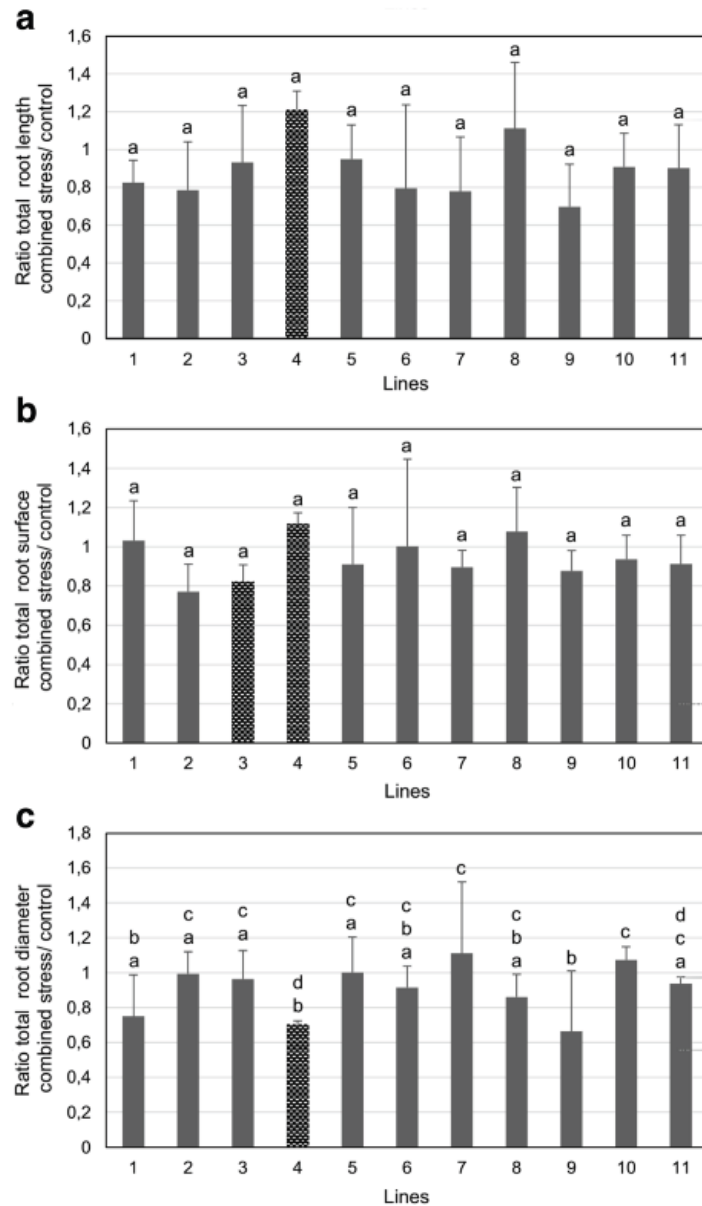
**Fig. 5** Natural variation of Tunisian *M. truncatula* lines in response to combined alkaline and saline stress, effect on plant growth. Ratios of combined stress versus control of (A) germination rate; (B) root DW; (C) shoot DW; (D) pigment contents of 11 Tunisian *M. truncatula* lines (SARDI collection, lines 1–11) and Jemalong A17 (J17) grown during 15 days in soil with 10 g/kg CaCO<sub>3</sub>, 6 g/kg NaHCO<sub>3</sub> and 150 mM NaCl. Values are the means of the ratios of individual stress values versus mean control values ± SD, that were calculated using the Taylor expansion method (Livak 1997); *n* = 4; means with the same letter are not significantly different at *P* ≤ 0.05 according to ANOVA and Fisher's LSD test. Hatched bars indicate that the difference between treatment and respective control condition was significant, while in the case of filled bars it was not significant, as tested in pairwise comparisons by t-test with *n* = 4, *P* ≤ 0.05



were apparent between the lines (Fig. 8b). The main root lengths were also found decreased upon the stress in all lines by about 40–45% (hatched bars) with no significant differences between the lines (Fig. 8c). However, with respect to the number of secondary roots a stronger decrease of 60 and 70% was noted for sensitive lines 7 and 9 compared to the tolerant lines 10 and 11 with a reduction of 25 and 30% (Fig. 8c).

Finally, we investigated whether *Rbfl* accumulation in the root tips could be a relevant trait for tolerance to the stress treatments as described previously for Fe deficiency (Rodríguez-Celma et al. 2011b). Two major flavins were found in the root extracts, *Rbfl* and 7-hydroxy-*Rbfl*, confirming previous results (Rodríguez-Celma et al. 2011b). Lines 7 and 11 had low *Rbfl* contents in root tips, whereas they were comparatively

**Fig. 6** Natural variation of Tunisian *M. truncatula* lines in response to combined alkaline and saline stress, effect on root growth. Ratios of combined stress versus control of (A) total root length; (B) total root surface; (C) total root diameter of 11 Tunisian *M. truncatula* lines (SARDI collection, lines 1–11) grown during 15 days in soil with 10 g/kg CaCO<sub>3</sub>, 6 g/kg NaHCO<sub>3</sub> and 150 mM NaCl. Values are the means of the ratios of individual stress values versus mean control values  $\pm$  SD, that were calculated using the Taylor expansion method (Livak 1997);  $n = 4$ ; means with the same letter are not significantly different at  $P \leq 0.05$  according to ANOVA and Fisher's LSD test. Hatched bars indicate that the difference between treatment and respective control condition was significant, while in the case of filled bars it was not significant, as tested in pairwise comparisons by t-test with  $n = 4$ ,  $P \leq 0.05$



higher in lines 9 and 10 (Fig. 9a). However, a difference between sensitive and tolerant lines was found for 7-hydroxy-*Rbfl*, which was detected (in amounts much lower than those of *Rbfl*) only upon the double stress treatment and only in the sensitive lines 7 and 9 (Fig. 9b). Another finding was that the distribution of flavins in root sections close to the main root tips visualized using fluorescence microscopy differed between sensitive and tolerant lines. While the sensitive lines 7 and 9

accumulated fluorescent compounds in the stele and adjacent inner root regions upon double stress, the tolerant lines 10 and 11 showed intense staining in the epidermis and to a weaker extent in the stele (Fig. 9c). A relatively homogeneous distribution of fluorescence was present upon the control treatments, with the staining being stronger in line 10 (Fig. 9c), thus matching the quantitative measurements shown above (Fig. 9a). Furthermore, the 7-hydroxy-*Rbfl* concentrations in the

**Fig. 7** Summary assessment of Tunisian *M. truncatula* lines for responses to combined stress. The ratios for the different physiological and growth parameters of combined stress versus control (see Figs. 5, 6) were represented as percent values in a table. The mean percent ratio was calculated from four parameters, namely germination, biomass (average of root and shoot DWs), pigment content (average of total *chl* and carotenoid contents), root morphology (average of total root length, diameter and surface). The colour code indicates whether the lines behaved as tolerant, sensitive or neutral

Line	Germination		Biomass		Pigment		Root morphology			Mean
	Germination	RDW	SDW	Total Chl	Carotenoids	TRL	RD	TRSA		
1	89%	90%	67%	80%	77%	83%	75%	103%	83%	
2	92%	13%	117%	89%	52%	79%	99%	77%	78%	
3	92%	72%	93%	103%	88%	93%	97%	82%	90%	
4	82%	12%	107%	74%	34%	121%	70%	112%	74%	
5	100%	94%	97%	99%	71%	95%	100%	91%	94%	
6	104%	97%	92%	85%	17%	79%	92%	100%	85%	
7	86%	47%	63%	111%	103%	78%	111%	90%	85%	
8	94%	66%	67%	149%	94%	111%	86%	108%	96%	
9	88%	68%	35%	131%	31%	70%	66%	88%	74%	
10	90%	105%	82%	143%	144%	91%	107%	94%	106%	
11	93%	94%	88%	145%	140%	90%	94%	91%	105%	

RDW: Root dry weight  
 SDW: Shoot dry weight  
 TRL: Total root length  
 TRSA: Total root surface area  
 RD: Root diameter

Green: Tolerant, T >95 %  
 Blue: Neutral, N  
 Red: Sensitive, S <86 %

nutrient solution were larger in the tolerant lines 10 and 11 than in the sensitive ones 7 and 9, whereas the amounts of *Rbfl* present in three of the lines were small (7, 10 and 11; Fig. 10). The difference between tolerant and sensitive lines was best described by the percentage of 7-hydroxy-*Rbfl* of the total flavins in nutrient solution, which was 91–100% in the tolerant lines and 0–30% in the sensitive ones.

In summary, the physiological and morphological analysis of hydroponically grown plants confirmed that lines 7 and 9 reacted in a more sensitive way to the combined BIC/NaCl treatments than the tolerant lines 10 and 11. Root morphology as well as flavin composition and the cellular distribution and secretion of flavins represent potential mechanisms that could contribute to the adaptation to the combined stress, whereas *Chl* contents and plant biomass are likely direct consequences of the genotype tolerance and sensitivity.

**Discussion**

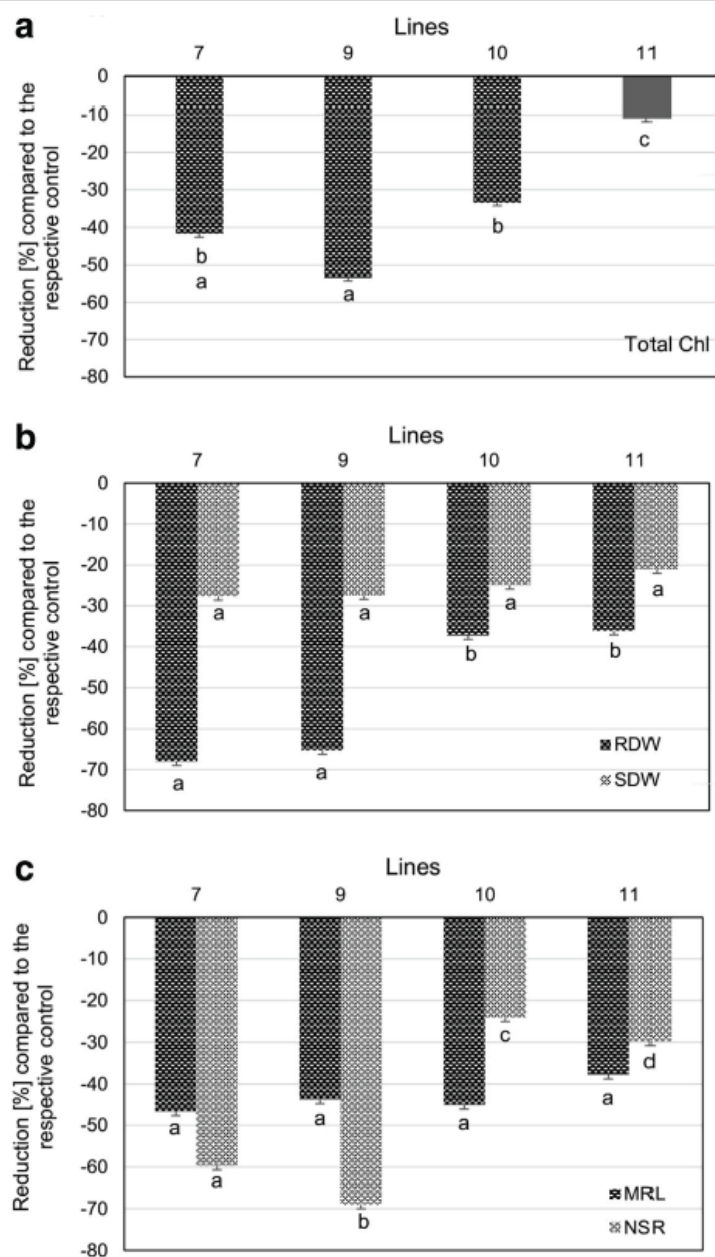
In this study, we show that salinity and alkalinity affected different growth parameters of *M. truncatula* plants, and that both factors combined led in an additive manner to a failure of germination and in a synergistic manner to an increase of stress symptoms in terms of decreased biomass production. Using Tunisian genotypes of the SARDI *M. truncatula* collection, we found natural variation in tolerance to the combined saline and

alkaline stress condition. This natural diversity allowed us to identify tolerant and susceptible lines. Differences in flavin distribution patterns, flavin concentrations in the growth medium and root morphology support that these traits could be key mechanisms contributing to stress tolerance.

Combined salinity and alkalinity conditions lead to additive and synergistic stress effects

Stress symptoms were assessed using different growth parameters, ranging from germination to biomass production, photosynthetic pigment content and root architecture. Germination is a very critical period in the plant’s life cycle and seeds are under the control of intrinsic (hormonal) and extrinsic (temperature, light and water) factors (Fenner and Thompson 2005). Germination is affected by many biotic and abiotic factors, and both salinity and alkalinity are abiotic factors that restrict germination of alfalfa seeds (Gao et al. 2011; Guan et al. 2009). Under the effect of salt stress of 100 mM or more NaCl, the low water potential of the soil likely prevented proper imbibition and seed germination. Salt toxicity may in addition have been detrimental to cells. Likewise, we found a decrease of the germination rate with increasing BIC concentrations, starting at 10/9 BIC and being most severe starting at 50/18 BIC. Certainly, the detrimental effects on germination were not due to the actual concentrations of Na ions but rather

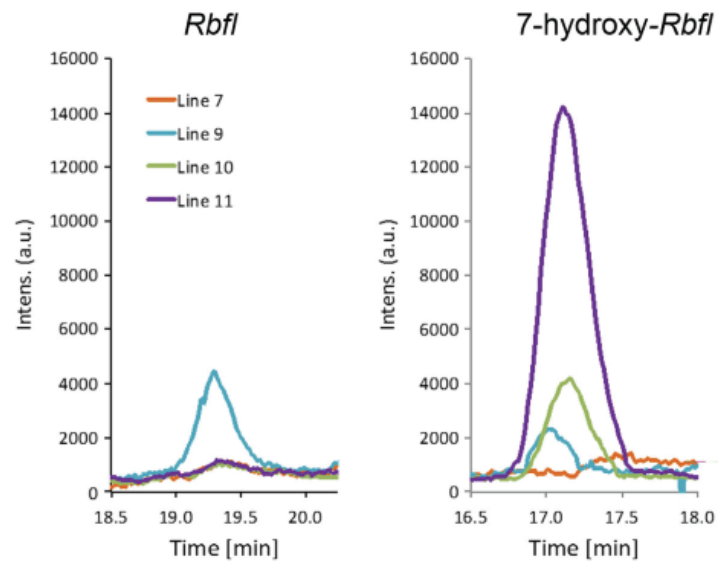
**Fig. 8** Effect of combined bicarbonate and salt stress (BIC/NaCl) in selected sensitive and tolerant *M. truncatula* lines. Relative reduction under combined stress versus control of (A) total chlorophyll contents; (B) root and shoot DWs; (C) main root length (MRL) and number of secondary roots (NSR). Lines 7 and 9 were selected as sensitive, whereas lines 10 and 11 as tolerant to the stress. *M. truncatula* plants were grown during 15 d in a hydroponic system under control and BIC/NaCl combined stress (+ 1 g/L CaCO<sub>3</sub> + 10 mM NaHCO<sub>3</sub> + 100 mM NaCl) conditions. Values are the means of the ratios of individual stress values versus mean control values ± SD, that were calculated using the Taylor expansion method (Livak 1997); *n* = 3; means with the same letter are not significantly different at *P* ≤ 0.05 according to ANOVA and Fisher's LSD test. Hatched bars indicate that the difference between treatment and respective control condition was significant, while in the case of filled bars it was not significant, as tested in pairwise comparisons by *t*-test with *n* = 3, *P* ≤ 0.05



caused by the elevated soil pH. High pH leads to reduced solubility and absorption of micronutrients, and this effect is also relevant in the apoplast of cells. Thus, the perturbation of remobilization and circulation of nutrients is the likely cause for the drastic reduction of germination upon high pH. Biomass production depends on photosynthesis and a proper utilization of macro- and micronutrients. Salt negatively

affects ion usage, e.g., K and Ca (Cramer et al. 1991), whereas alkaline conditions cause a reduction in Fe and P utilization (Lucena 2000). When investigating the combined stress, we found that an effect of 5/3, 10/6 or 20/9 BIC on germination was similar at 75 and 100 mM NaCl (Fig. 3a) and in the absence of salt (Fig. 2a). Hence, a clear additive or synergistic effect of the double stress was not present. However, at the higher salt concentration

**Fig. 10** HPLC-MS (TOF) chromatograms of flavins isolated from nutrient solutions after growth of sensitive and tolerant *M. truncatula* lines. *Rbfl* and 7-Hydroxy-*Rbfl* chromatograms were extracted at  $m/z$  377.15 and 379.12, respectively, with a precision of 0.05  $m/z$  units, showing peaks corresponding to these flavins. Plants were grown as described in Fig. 8



Root morphology and flavin cellular distribution are potential mechanisms for tolerance to combined stress in the natural diversity of *M. truncatula*

Our work revealed two potential mechanisms that may contribute to the tolerance.

The first mechanism is related to root architecture. Single and double stress treatments always had a negative effect on biomass and root dry weight. The even smaller reduction of the root DW in the tolerant vs. sensitive lines upon the combined stress was likely caused by the smaller decrease in the number of lateral roots. Despite of the stress, tolerant lines thus seemed better suited to sustain root growth. Therefore, the previously reported arrest of root growth to alleviate stress periods (Bailey-Serres and Voesenek 2010) does not seem to be the relevant adaptive mechanism in our studied case. Future studies can be conducted to measure the impact of root architectural changes on stress tolerance. For example, it would be interesting to find out whether the roots of tolerant plants express those genes at higher level that code for proteins, enzymes and transporters involved in the vacuolar storage and exclusion of salt. Alternatively, the root of tolerant plants might show signs for induced nutrient mobilization to deal with potential deficiencies upon the calcareous growth condition. Interestingly, we observed upon establishment of the growth conditions that the 5/3 BIC treatment was a positive stress and stimulated slightly but significantly root dry weight, while higher BIC

treatments were a negative stress and decreased root biomass. Previously, it was described that the plant hormone abscisic acid (ABA) resulted in a similar root growth dose response curve in *M. truncatula*. Low ABA concentrations promoted and high ABA concentrations inhibited root growth (Ariel et al. 2010). ABA is involved in salt stress responses and perhaps it mediates also calcareous stress responses.

A second key mechanism relies on the allocation of flavins in root epidermal cells and flavin secretion to the growth medium, and specifically the secretion of the *Rbfl* derivative 7-hydroxy-*Rbfl*. The total concentrations of flavins in the root extracts did not allow differentiating between tolerant and sensitive lines. However, in the two tolerant lines examined, flavin fluorescence was preferentially located in the epidermal cells, the root contents of 7-hydroxy-*Rbfl* were undetectable, and 7-hydroxy-*Rbfl* was the major flavin compound in the nutrient solution. In contrast, in the two sensitive lines examined flavin fluorescence was preferentially allocated to inner parts of the root, 7-hydroxy-*Rbfl* was detected in the root, and 7-hydroxy-*Rbfl* was either undetected or a minor flavin component in the nutrient solution. These results are very interesting and match the previous observations that 7-hydroxy-*Rbfl* can be a major flavin in the extracts especially under low Fe conditions (Rodriguez-Celma et al. 2011b). Our findings strongly support that the allocation of *Rbfl* in epidermal cells and the secretion (extracellular allocation) of oxygenated *Rbfl* derivatives are crucial for tolerance to alkalinity

stress in *M. truncatula* and that there is genetic diversity in this trait.

The relevance of the accumulation of flavins in the epidermal cells under Fe deficiency conditions is in line with the hypothesis that flavins in root cells constitute a potent Fe reduction system in combination with the plasma membrane ferric chelate reductase (López-Millán et al. 2000). In root tips of Fe-deficient sugar beet, accumulated (oxidized) flavins can act as an electron shuttle between reduced pyridine nucleotides in the cell (produced by the high mitochondrial activity fueled by  $\text{HCO}_3^-$  fixation via phosphoenolpyruvate carboxylase) and the plasma membrane ferric chelate reductase (López-Millán et al. 2000). Indeed, Fe deficiency leads to increases in phosphoenolpyruvate carboxylase, root flavins and ferric chelate reductase activity in *M. truncatula* (Andaluz et al. 2009). Flavin production and secretion at high pH is ecologically meaningful if plants are grown under alkaline and calcareous soil where Fe deficiency occurs. Besides the two effects on flavins and root architecture it is well conceivable that additional mechanisms of tolerance to the double stress come into play, like e.g. soil acidification as a means to mobilize nutrients as well as salt tolerance reactions based on exclusion and detoxification of salts.

Extracellular flavins enable the establishment of a long-distance electron transfer chain between the reducing power in the root and soil Fe(III)-oxides (even at high pH), resulting in the formation of soluble Fe species for the plasma membrane Fe uptake system (Sisó-Terraza et al. 2016a). The Fe(III)-oxide reduction rates were similar for *Rbfl* and *Rbfl*-sulfates but were strongly dependent on the flavin concentration (Sisó-Terraza et al. 2016b). Therefore, the secretion of flavin species with a high solubility (e.g., hydroxylated ones) can constitute an ecological advantage to mine Fe from calcareous soil. For instance, the solubility of *Rbfl*-sulfates (the major flavin component secreted by sugar beet roots) is one to two orders of magnitude higher than that of *Rbfl* (Susin et al. 1993). In this context, coumarins secreted by *A. thaliana* roots, effective in dissolving soil Fe oxides at high pH values, also include a number of hydroxylated species that become predominant at high pH (Siso-Terraza et al. 2016a).

In summary, the combined stress affected most of the tested *M. truncatula* lines. Tolerant and sensitive lines were collected from various parts of Tunisia, and their geographic distribution might be correlated with their degree of evolutionary relatedness to some extent. Further studies at the genomics level may provide answers

to this. The selected double stress-tolerant and sensitive lines can be used as contrasting pairs for comparative RNA-Seq experiments to search for adaptive changes in gene regulation and gene sequences. Also, the relevance for tolerance to stress of the flavin allocation in the epidermal root cells and the secretion of 7-hydroxy-*Rbfl* by roots should be validated in further studies with *M. truncatula* and the molecular basis for this mechanism explored in detail. These tolerant genotypes may be cultivated on salt-affected soils prone to alkalinity-induced Fe deficiency. In future experiments the interplay of Na and Ca and resulting effects on soil structure could be further explored using natural soils.

**Acknowledgements** This work was supported partly by a DAAD Stibed stipend to H. B. A. provided through the Heinrich Heine University, and Spanish MINECO projects AGL2013-42175-R and AGL2016-75226-R (co-financed with FEDER) to J. A. and A. A.-F.

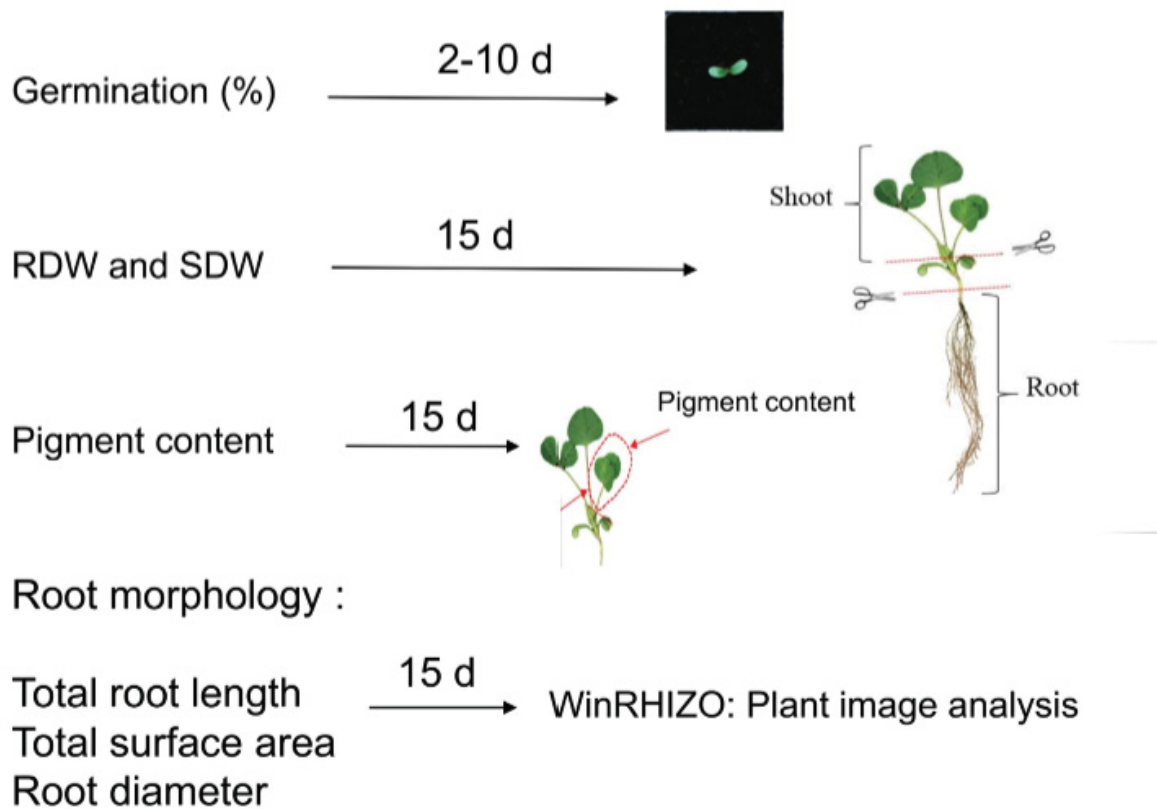
## References

- Abadia J, Vazquez S, Rellan-Alvarez R, El-Jendoubi H, Abadia A, Alvarez-Fernandez A, Lopez-Millan AF (2011) Towards a knowledge-based correction of iron chlorosis. *Plant Physiol Biochem* 49:471–482. <https://doi.org/10.1016/j.plaphy.2011.01.026>
- Andaluz S, Rodríguez-Celma J, Abadía A, Abadía J, López-Millán A-F (2009) Time course induction of several key enzymes in *Medicago truncatula* roots in response to Fe deficiency. *Plant Physiol Biochem* 47:1082–1088
- Ariel F, Diet A, Verdenaud M, Gruber V, Frugier F, Chan R, Crespi M (2010) Environmental regulation of lateral root emergence in *Medicago truncatula* requires the HD-Zip I transcription factor HB1. *Plant Cell* 22:2171–2183. <https://doi.org/10.1105/tpc.110.074823>
- Arnon DI (1949) Copper enzymes in isolated chloroplasts. Polyphenoloxidase in *Beta vulgaris*. *Plant Physiol* 24:1
- Bailey-Serres J, Voesenek LA (2010) Life in the balance: a signaling network controlling survival of flooding. *Curr Opin Plant Biol* 13:489–494. <https://doi.org/10.1016/j.pbi.2010.08.002>
- Basigalup D, Irwin J, Mi F, Abdelguefri-Laouar M (2014) Perspectives of alfalfa in Australia, China, Africa and Latin America. *The journal of the International Legume Society: Legume Perspectives* 9–10
- Briat J-F, Dubos C, Gaymard F (2015) Iron nutrition, biomass production, and plant product quality. *Trends Plant Sci* 20: 33–40
- Cramer GR, Epstein E, Läuchli A (1991) Effects of sodium, potassium and calcium on salt-stressed barley. *Physiol Plant* 81:197–202
- Ellwood S, D'souza N, Kamphuis L, Burgess T, Nair R, Oliver R (2006) SSR analysis of the *Medicago truncatula* SARDI core collection reveals substantial diversity and unusual genotype

- dispersal throughout the Mediterranean basin. *Theor Appl Genet* 112:977–983
- Fenner M, Thompson K (2005) *The ecology of seeds*. Cambridge University Press
- Fourcroy P, Siso-Terraza P, Sudre D, Saviron M, Reyt G, Gaymard F, Abadia A, Abadia J, Alvarez-Fernandez A, Briat JF (2014) Involvement of the ABCG37 transporter in secretion of scopoletin and derivatives by *Arabidopsis* roots in response to iron deficiency. *New Phytol* 201:155–167. <https://doi.org/10.1111/nph.12471>
- Friesen ML, Cordeiro MA, Penmetsa RV, Badri M, Huguet T, Aouani ME, Cook DR, Nuzhdin SV (2010) Population genomic analysis of Tunisian *Medicago truncatula* reveals candidates for local adaptation. *Plant J* 63:623–635
- Friesen ML, von Wettberg EJ, Badri M, Moriuchi KS, Barhoumi F, Chang PL, Cuellar-Ortiz S, Cordeiro MA, Vu WT, Arraouadi S (2014) The ecological genomic basis of salinity adaptation in Tunisian *Medicago truncatula*. *BMC Genomics* 15:1
- Gao ZW, Zhu H, Gao JC, Yang CW, Mu CS, Wang DL (2011) Germination responses of Alfalfa (*Medicago sativa* L.) seeds to various salt-alkaline mixed stress. *Afr J Agric Res* 6:3793–3803
- Guan B, Zhou D, Zhang H, Tian Y, Japhet W, Wang P (2009) Germination responses of *Medicago ruthenica* seeds to salinity, alkalinity, and temperature. *J Arid Environ* 73:135–138. <https://doi.org/10.1016/j.jaridenv.2008.08.009>
- Hanin M, Ebel C, Ngom M, Laplaze L, Masmoudi K (2016) New Insights on Plant Salt Tolerance Mechanisms and Their Potential Use for Breeding. *Front Plant Sci* 7:1787. <https://doi.org/10.3389/fpls.2016.01787>
- Hsieh EJ, Waters BM (2016) Alkaline stress and iron deficiency regulate iron uptake and riboflavin synthesis gene expression differently in root and leaf tissue: implications for iron deficiency chlorosis. *J Exp Bot* 67:5671–5685. <https://doi.org/10.1093/jxb/erw328>
- Lazrek F, Roussel V, Ronfort J, Cardinet G, Chardon F, Aouani M, Huguet T (2009) The use of neutral and non-neutral SSRs to analyse the genetic structure of a Tunisian collection of *Medicago truncatula* lines and to reveal associations with eco-environmental variables. *Genetica* 135:391–402
- Li Q, Yang A, Zhang WH (2016) Efficient acquisition of iron confers greater tolerance to saline-alkaline stress in rice (*Oryza sativa* L.). *J Exp Bot* 67:6431–6444. <https://doi.org/10.1093/jxb/erw407>
- Livak K (1997) ABI prism 7700 sequence detection system user bulletin# 2 relative quantification of gene expression. ABI company publication
- López-Millán AF, Morales F, Andaluz S, Gogorcena Y, Abadía A, De Las RJ, Abadía J (2000) Responses of sugar beet roots to iron deficiency. Changes in carbon assimilation and oxygen use. *Plant Physiol* 124:885–898
- Lucena JJ (2000) Effects of bicarbonate, nitrate and other environmental factors on iron deficiency chlorosis. A review. *J Plant Nutr* 23:1591–1606
- Naranjo-Arcos MA, Bauer P (2016) Nutritional Deficiency. Chapter 4: Iron Nutrition, Oxidative Stress, and Pathogen Defense. INTECH Open Access Publisher
- Rabhi M, Barhoumi Z, Ksouri R, Abdely C, Gharsalli M (2007) Interactive effects of salinity and iron deficiency in *Medicago ciliaris*. *C R Biol* 330:779–788
- Rahoui S, Martinez Y, Sakouhi L, Ben C, Rickauer M, El Ferjani E, Gentzbittel L, Chaoui A (2016) Cadmium-induced changes in antioxidative systems and differentiation in roots of contrasted *Medicago truncatula* lines. *Protoplasma*: 1–17
- Rengasamy P (2016) Soil Salinization. OXFORD RESEARCH ENCYCLOPEDIA, ENVIRONMENTAL SCIENCE. <https://doi.org/10.1093/acrefore/9780199389414.013.65>
- Rodriguez-Celma J, Lattanzio G, Grusak MA, Abadía A, Abadía J, Lopez-Millan AF (2011a) Root responses of *Medicago truncatula* plants grown in two different iron deficiency conditions: changes in root protein profile and riboflavin biosynthesis. *J Proteome Res* 10:2590–2601. <https://doi.org/10.1021/pr2000623>
- Rodriguez-Celma J, Lin WD, Fu GM, Abadía J, Lopez-Millan AF, Schmidt W (2013) Mutually exclusive alterations in secondary metabolism are critical for the uptake of insoluble iron compounds by *Arabidopsis* and *Medicago truncatula*. *Plant Physiol* 162:1473–1485. <https://doi.org/10.1104/pp.113.220426>
- Rodriguez-Celma J, Vazquez-Reina S, Orduna J, Abadía A, Abadía J, Alvarez-Fernandez A, Lopez-Millan AF (2011b) Characterization of flavins in roots of Fe-deficient strategy I plants, with a focus on *Medicago truncatula*. *Plant cell physiol* 52:2173–2189. <https://doi.org/10.1093/pcp/pcr149>
- Schmid NB, Giehl RF, Doll S, Mock HP, Strehmel N, Scheel D, Kong X, Hider RC, von Wiren N (2014) Feruloyl-CoA 6'-Hydroxylase1-dependent coumarins mediate iron acquisition from alkaline substrates in *Arabidopsis*. *Plant Physiol* 164:160–172. <https://doi.org/10.1104/pp.113.228544>
- Sisó-Terraza P, Luis-Villarroya A, Fourcroy P, Briat JF, Abadía A, Gaymard F, Abadía J, Álvarez-Fernández A (2016a) Accumulation and Secretion of Coumarinolignans and other Coumarins in *Arabidopsis thaliana* Roots in Response to Iron Deficiency at High pH. *Front Plant Sci* 7:1711. <https://doi.org/10.3389/fpls.2016.01711>
- Sisó-Terraza P, Rios JJ, Abadía J, Abadía A, Álvarez-Fernández A (2016b) Flavins secreted by roots of iron-deficient *Beta vulgaris* enable mining of ferric oxide via reductive mechanisms. *New Phytol* 209:733–745. <https://doi.org/10.1111/nph.13633>
- Skujinš J (1984) *Microbial ecology of desert soils*. Springer, *Advances in microbial ecology*
- Susín S, Abián J, Sánchez-Baeza F, Peleato ML, Abadía A, Gelpí E, Abadía J (1993) Riboflavin 3'- and 5'-sulfate, two novel flavins accumulating in the roots of iron-deficient sugar beet (*Beta vulgaris*). *J Biol Chem* 268:20958–20965
- Yousfi S, Mahmoudi H, Abdely C, Gharsalli M (2007) Effect of salt on physiological responses of barley to iron deficiency. *Plant Physiol Biochem* 45:309–314
- Zahaf O, Blanchet S, De Zélicourt A, Alunni B, Plet J, Laffont C, De Lorenzo L, Imbeaud S, Ichanté J-L, Diet A (2012) Comparative transcriptomic analysis of salt adaptation in roots of contrasting *Medicago truncatula* genotypes. *Mol Plant* 5:1068–1081



**Suppl. Fig. 1: Geographical distribution map of the lines and collection of plant samples.** The upper map shows the geographical distribution of the 11 *M. truncatula* lines (SARDI) collection. Red circles indicate sensitive lines (S) and green circles indicate tolerant lines (T) as determined by the combined stress experiments conducted in this study. The sampling scheme for the plant materials assessed is shown below.



**Author contribution to Manuscript 3:**

Natural variation reveals contrasting abilities to cope with alkaline and saline soil among different *Medicago truncatula* genotypes (**published**). (Abdallah et al. 2017).

Heithem Ben Abdallah

Performed and analyzed all experiments, except Rbfl measurements, contributed to the writing of the manuscript, prepared figures, reviewed and commented on the manuscript.

Hans-Jörg Mai

Helped in analyzing experiments, statistical analysis and commented on the manuscript.

Ana Alvarez Fernandez and Javier Abadia

Performed the Rbfl measurements using HPLC-MS (Figure 9 and 10).

Petra Bauer

Designed the outline of the manuscript, supervised the study, provided funding, wrote and corrected the manuscript.

Abdallah HB, Mai H-J, Álvarez-Fernández A, Abadía J, Bauer P (2017) Natural variation reveals contrasting abilities to cope with alkaline and saline soil among different *Medicago truncatula* genotypes. *Plant and Soil* 418: 45-60.

# **Manuscript 4**

**RNA-sequencing analysis of contrasting rice genotypes  
exposed to high iron**

## Manuscript 4: RNA-sequencing analysis of contrasting rice genotypes exposed to high iron

Heithem Ben Abdallah<sup>1</sup>, Saradia Kar<sup>1,2</sup>, Hans Jörg Mai<sup>1</sup>, Andrea Bräutigam<sup>3</sup>, Samantha Kurz<sup>4</sup>, Sanjib Kumar Panda<sup>2</sup>, Petra Bauer<sup>1,5</sup>

<sup>1</sup> Institute of Botany, Heinrich Heine University Düsseldorf, Universitätsstrasse 1, D-40225, Düsseldorf, Germany

<sup>2</sup> Department of Life Science and Bioinformatics, Assam University, Silchar - 788011, Assam, India

<sup>3</sup> IPK Gatersleben, Network Analysis and Modeling, Corrensstrasse 3, 06466 Seeland, Germany

<sup>4</sup> Institute of Plant Biochemistry, Heinrich Heine University, Universitätsstrasse 1, D-40225, Düsseldorf, Germany

<sup>5</sup> CEPLAS Cluster of Excellence on Plant Sciences Heinrich Heine University, Universitätsstraße 1, D-40225 Düsseldorf

### Abstract:

Iron (Fe) is an essential element that is involved in various important redox processes in plants. Its deficiency as well as toxicity are serious agricultural problems for the production of rice (*Oryza sativa*), one of the most widely consumed staple foods for most part of the world's population. Fe toxicity is a major nutritional disorder for rice grown under flooded conditions in acidic soils, where Fe is preponderant in the ferrous form, which is more bioavailable than the ferric form. Excessive cellular Fe promotes the Fenton reaction leading to oxidative damage, leaf bronzing and ultimately plant failure. Genetic diversity provides a suitable resource to identify tolerance mechanisms evolved for rice adaptation to Fe toxicity. Previously a susceptible and a tolerant cultivar of Indica rice have been selected. We exposed the susceptible and tolerant cultivars, namely Hacha and Lachit, for a short term to high Fe in a controlled hydroponic system. Physiological and morphological assessment of root and shoot growth parameters, the leaf bronzing score showed that plants from the susceptible cultivar Hacha exhibited more severe symptoms of Fe toxicity than Lachit. In contrast to Hacha, Lachit plants were able to recover from the short-term stress. To shed light on the molecular tolerance mechanisms we conducted a comparative transcriptomics RNAseq experiment of roots and L2 leaves. We grouped the differentially expressed genes into clusters reflecting either genotype, Fe regime or genotype Fe regime effects and compared the molecular signatures of the tolerant versus the susceptible

cultivars with previously reported mechanisms. From the physiological and molecular data we conclude that Lachit responds differently to Fe toxicity than the sensitive cultivar Hacha and also different from other Indica rice cultivars reported to be tolerant to high Fe.

**Keywords:** RNA-Sequencing, bronzing score, Fe toxicity, *Oryza sativa*, antioxidants, molecular responses.

### 1. Introduction

Iron (Fe) along with zinc, manganese and copper (Cu) belongs to biologically relevant transition metals that occur in cells as ions in different oxidation states. These metals are essential and catalyze a number of biochemical redox reactions as part of cofactors. Transition metals are micronutrients for plants and taken up via the root system from the soil. Organic soils are rich in nutrients, optimal for most agriculturally important plants, and the slightly acidic conditions favor adequate concentrations of bioavailable ferrous Fe. Calcareous and alkaline soils hamper acquisition of Fe, which is mostly present in ferric form bound to minerals. Such poor soils require adaptation by specialist plants. However, for rice agriculture a different problem with Fe nutrition occurs related to excessive uptake of Fe in acidic paddy fields, as in North-East India. In acidic flooded conditions, concentrations of bioavailable ferrous Fe exceed those optimal for plant growth. Plants do not prevent excessive uptake of Fe under these growth conditions (Quinet et al. 2012). Consequently, high levels of cellular Fe cause oxidative stress and damage of cellular compounds. Free Fe causes the Fenton reaction, a non-enzymatic conversion of hydrogen peroxide into hydroxyl radicals catalyzed by ferrous Fe. Hydroxyl radicals are considered more reactive ROS species cause oxidative stress resulting in fairly unspecific damage of cellular components and cellular death. In leaves, purple anthocyanin pigmentation and brownish spots appear, known as leaf bronzing, developing from leaf tip to base (Tanaka et al. 1966), while in roots, root system architecture changes and root growth is inhibited under elevated Fe (Becker and Asch 2005; Naranjo-Arcos and Bauer 2016).

Rice is a model organisms to study the natural adaptation to high levels of Fe in paddy fields. Usually, rice takes up Fe in the ferric form bound to phytosiderophores. These chelators belong to the mugineic acids and are produced and secreted into the rhizosphere by Poaceae (Takagi et al. 1984), known as Fe uptake Strategy II (Marschner and Römheld 1994). Strategy II is a pH-

independent Fe acquisition strategy, which makes Poaceae relatively Fe-efficient also under elevated pH and calcareous soil conditions. However, especially on paddy fields, rice can also take up efficiently ferrous Fe, which is known as Fe uptake Strategy I, utilized by most plant species (Marschner et al. 1986). Rice natural variation is exploited to identify high Fe tolerant rice genotypes and reveal two main tolerance mechanisms using microarrays (see summary in Table 1) and quantitative trait loci (QTL) mapping of candidate tolerance genes and comparative transcriptomics (Wu et al. 2014). One main mechanism addresses cellular Fe levels directly and is the effective combination of exclusion and elimination of Fe by repressing Fe acquisition in the root, preventing its translocation to shoots, sequestering it in the cell wall and vacuole and/or chelating Fe, all with the purpose to lower free cytoplasmic Fe levels. Similar mechanisms have also been widely described in the context of salt tolerance and heavy metal phytoremediation (Liang et al. 2016). Ion exclusion and elimination tolerance mechanisms of tolerant versus susceptible plants may rely on altered transporter properties, e.g. changed strength of expression or new cell-specific expression patterns or intracellular protein localization, altered control of transporter stabilities and activities. Chelation requires biosynthesis of chelators and tolerance could arise e.g. from increased expression of the biosynthetic chains, different regulation of enzymes or from changing the transport of the chelators in the plants. Another main tolerance mechanism addresses ROS toxicity directly and targets the decrease of ROS in cells. ROS is effectively eliminated in tolerant versus susceptible plants by increased expression and activities of ROS scavenging enzymes and by altered expression of enzymes generating antioxidants, that non-enzymatically alter the cellular ROS pool (Bode et al. 1995; Czarnocka and Karpiński 2018; Li et al. 2010).

A recent GWAS analysis of Indica rice detected potential high Fe QTLs linked with oxidative stress signaling genes (Zhang et al. 2017). Another GWAS-QTL study using MAGIC populations, on the other hand, discussed that identified high Fe QTLs are partly linked with genes affecting root Fe uptake (Meng et al. 2017). Comparative transcriptomics exploits the natural variation to ascribe the physiological adaptations to concrete molecular patterns. The extent of transcriptional response patterns reveals particular genotype-specific Fe tolerance response clusters. A recent study by (Wu et al. 2017) investigated the Fe stress responses of tolerant and susceptible Indica rice using microarrays, and the identified genotype-specific main tolerance mechanism to high Fe was the decrease of ROS by reduced levels of antioxidants and reduced expression of enzymes

producing antioxidants, such as glutathione in shoots. Hence, we conclude from these studies that different mechanisms account for the tolerance of different rice lines to high Fe, making it necessary to collect more data on the tolerance in individual lines.

Here, we applied a comparative transcriptomics approach using RNAseq to a novel pair of susceptible and tolerant Indica rice lines. The identified clusters of genes reflecting specific genotype and Fe regime response patterns indicate that several tolerance mechanisms act in the tolerant line. We compared our data with previous reports on Fe tolerance mechanisms.

**Table 1:** Literature review of recent research publications on iron toxicity in rice cultivars.

Previous reports	Lines	Plant part analyzed	Stress duration	Iron level
Wu et al 2016	Intolerant : IR29 Tolerant : FL483	Shoot + Roots	4 days	Control = 10 $\mu\text{M}$ Fe $\text{Cl}_3$ Stress = 14 Mm FeSO <sub>4</sub>
Finatto et al 2015	cv. Nipponbare	Shoot	4 days	Control = 10 $\mu\text{M}$ Fe-EDTA Stress = 7 mM Fe <sup>2+</sup> + 10 $\mu\text{M}$ Fe-EDTA
Quinet et al 2012	cv. I Kong Pao (IKP)	Shoot + Roots	3 days 3 weeks	Control = 0 mM FeSO <sub>4</sub> Stress = 0.5 mM FeSO <sub>4</sub>
Bashir et al 2014	cv. Nipponbare	Shoot + Roots	1 week	Control = 100 $\mu\text{M}$ Fe-EDTA Stress = 500 $\mu\text{M}$ Fe-EDTA
Zheng et al 2009	cv. Nipponbare	Shoot + Roots	10 days	+ Fe = 0.036 mM FeCl <sub>3</sub> - Fe = 0 mM FeCl <sub>3</sub>
Wakasa 2014	cv. Nipponbare	Shoot + Roots	7 days	Another stress

Some of the recent research work on rice cultivars has been listed in Table 1. It includes the previous reports using microarray studies under iron stress at different concentrations. Generally, the overall transcriptomics reports in short-term response to iron excess of the wild type “Nipponbare” seedlings, includes activation of genes involved in iron homeostasis and iron transport, oxidative stress, transcription factors and ROS detoxification genes in the leaves. When comparing the transcriptomic changes of rice seedlings exposed to short and long term iron overload stress were compared, these results showed that short term stress showed more up and downregulated gene expression regarding both the number and function than long-term stress (Quinet et al. 2012). One of the recent papers using contrasting Indica rice genotypes mainly

focused in the shoot tolerance mechanisms (Wu et al. 2017). Therefore, in our present work we are checking both the root and shoot tolerance mechanisms and selected only short term Fe stress.

## **2. Materials and Methods**

### **2.1. Plant material**

Previously, two rice (*Oryza sativa* L. ssp. indica) genotypes were identified based on their contrasting response patterns to Fe toxicity (Kar and Panda, Assam University, India, unpublished data) and used in this work, namely high Fe-intolerant Hacha (CRM 53 X IR 64) and high Fe-tolerant Lachit (from a cross between CRM 13-3241 and Kalinga 2).

### **2.2. Hydroponic plant growth**

Experiments were conducted in a controlled growth chamber, with a 16 hours light/ 8 hours dark cycle, a light intensity of  $150 \mu\text{mol m}^{-2} \text{s}^{-1}$ , a day/night temperature of  $26 \text{ }^\circ\text{C}$ . The rice growth procedure is depicted in Fig. 2. Rice seeds were first disinfected using 1% sodium hypochlorite for 15 min. Subsequently, soaked seeds were vernalized for one day at  $4^\circ\text{C}$  and transferred for 3 days in the dark to  $30^\circ\text{C}$  for germination. Homogenously grown seedlings were transplanted into 11 pots filled with half-strength modified Hoagland solution for further hydroponic growth until day 5. Then, half-strength nutrient solution was replaced with a full-strength solution containing 1 mM calcium nitrate, 2.5 mM potassium nitrate, 1 mM potassium dihydrogen phosphate, 1 mM magnesium sulfate,  $50 \mu\text{M}$  boric acid ( $\text{H}_3\text{BO}_3$ ),  $50 \mu\text{M}$  potassium chloride,  $10 \mu\text{M}$  manganese sulfate,  $2 \mu\text{M}$  zinc sulfate,  $1.5 \mu\text{M}$  copper sulfate, and  $0.075 \mu\text{M}$  ammonium molybdate and  $50 \mu\text{M}$  Fe Na EDTA at pH 6.2, which also represented the control treatment condition. The nutrient solutions were renewed every second day. At day 11, a 2-day Fe stress treatment with full-strength Hoagland medium plus 15 mM Fe sulfate at pH 5.2 was applied in addition to a control treatment without added Fe sulfate at pH 6.2. For revival experiments, the plants were re-exposed to control medium after the stress condition and again the medium was renewed every second day. For the RNAseq experiment 15 plants per line and treatment and per biological sample were used. In total, three biological replicates were prepared. The revival experiment was conducted with 9 plants per line and treatment. For physiological and morphological experiments 12 plants per line and treatment were grown.

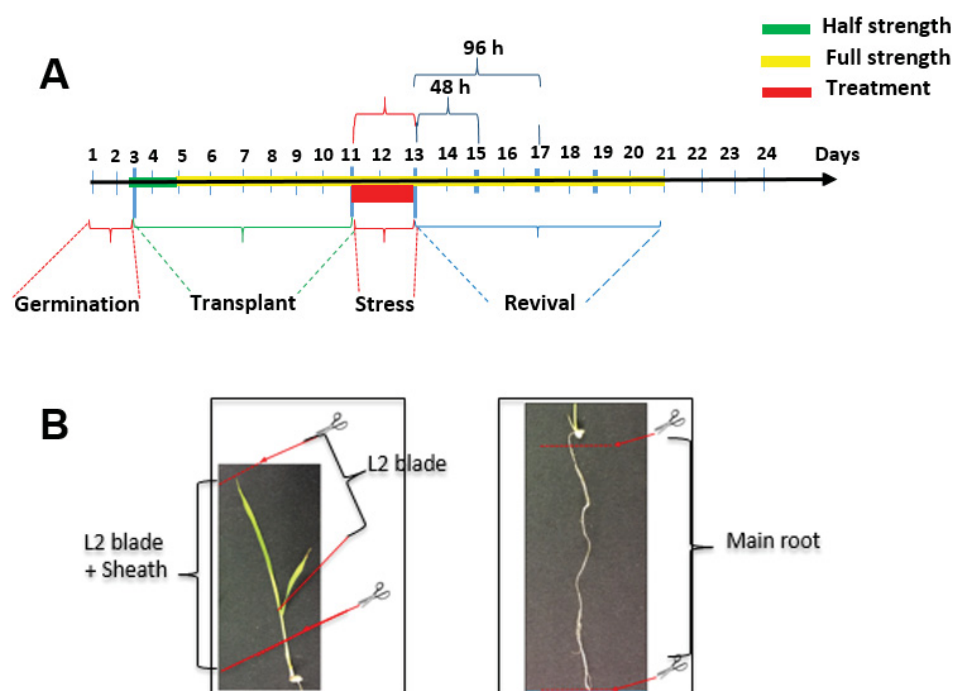


**Figure 2:** Experimental setup of the Fe-stress treatment and revival experiment. (A) Growth scheme; (B) Harvesting of L2 blade, L2 blade with sheath and roots for experiments; L2 leaf blade sections and root samples were excised as indicated in the figure.

### 2.3. Bronzing score determination

Bronzing of leaf blades indicates the severity of Fe toxicity (Becker and Asch 2005). In this assay, we used 3 independent biological replicates. The longer leaf (L2) were detached, placed in a test tube and kept under normal growth chamber condition and then observed. Leaf blades were scored by subjective visual assessment of the bronzing using the ImageJ software and expressed as % leaf area affected (Peng and Yamauchi 1993).

### 2.4. DAB (diaminobenzidine) staining for hydrogen peroxide

DAB is oxidized by hydrogen peroxide, the result is a staining that generates a dark brown precipitation. L2 leaf blades were excised and placed in 5 ml working solution (1mg/ml 3,3'-diaminobenzidine tetrahydrochloride in 50 mM MES, pH6.5). The samples were infiltrated in vacuum for 5 minutes followed by incubation of 1 hour in the shaker. DAB staining solution was removed and washed with distilled water. The sample was placed into 80% ethanol solution and boiled at 80 °C for 30 min. Then leaves were washed three times with distilled water. Finally, the samples were observed using a stereoscope.

**2.5. Determination of hydrogen peroxide contents**

Hydrogen peroxide contents were determined using the Amplex Red kit (ThermoFisher) according to manufacturer instructions and (Brumbarova et al. 2016). Briefly, 50 mg plant sample were grinded in 200  $\mu$ l potassium phosphate buffer (20 mM, pH 6.5). After centrifugation, 50  $\mu$ l supernatant were mixed with 100  $\mu$ l Amplex Red reagent and 0.2 units  $\text{ml}^{-1}$  horseradish peroxidase (HRP) in a 96-well plate along with appropriate controls and incubated for 30 min at room temperature in the dark. The absorbance of resorufin at 560 nm was determined with a plate reader and the content of hydrogen peroxide was calculated based on a hydrogen peroxide mass standard curve. The values are expressed in  $\text{pmol H}_2\text{O}_2 \text{ mg}^{-1}$  fresh weight.

**2.6. Ascorbate assay**

Ascorbate contents were determined using a fluorescence-based ascorbate assay kit (<https://www.caymanchem.com/product/700420>) according to manufacturer's instructions. Briefly, 40 mg of plant material was immersed in 1 ml of 6% thiobarbituric acid reactive substances (TBARS), then the samples were vortexed and centrifuged at 13000g for 5 minutes at 4 °C. The supernatant was collected and followed by manufacturer's instructions for the determination. The ascorbate content was expressed as  $\text{pmol ascorbate mg}^{-1}$  fresh weight.

**2.7. RNA isolation, RNA sequencing library preparation and sequencing**

Three independent biological replicates were harvested per experimental sample condition and line. RNA was isolated from 100 mg plant material using the RNA plant mini kit (Qiagen, Cat No. /ID: 74904). The quality and quantity of total RNA was analyzed using the Bioanalyzer 2100 (Agilent Technologies). RNA samples with intact bands on agarose gels, a 260/280 ratio should ranging from to 1.8-2.2 and an RNA integrity number  $>7.0$  were used (no degradation of RNA). The library was prepared with a preparation Kit (Illumina Technologies, Nextera DNA Library Preparation Kit) following the manufacturer's instructions. Double-stranded cDNA was purified for end repair, adaptor ligation, and DNA fragment enrichment. The libraries were sequenced as 101 bp paired-end reads using Illumina HiSeq according to the manufacturer's instructions at the BMFZ (Biologisch-Medizinisches Forschungszentrum, Heinrich Heine University).

## **2.8. Analysis of RNAseq data**

All sequence reads were mapped to the *Oryza\_sativa*.IRGSP-1.0.31.cdna.all and *Oryza\_indica*.ASM465v1.31.cdna.all.fa reference transcriptome sequences downloaded from Ensembl Plants (plants.ensembl.org). Since the mapping to the *Oryza\_sativa* reference transcriptome had about 10% higher mapping efficiency than that of *Oryza\_indica*, all downstream analyses were conducted using the *O. sativa* annotations. Read mapping and quantification of the transcripts were performed using kallisto (Bray et al. 2016). The identified transcripts and their respective counts were further analyzed using the statistical software R (Team 2013). Transcripts per million (Tpm) counts for all samples were used for principal component analyses (R: prcomp) and for hierarchical clustering (R: dist/cor, hclust). Estimated counts were used to perform statistical analysis after normalization for between-samples comparison (R: edgeR). Gene expression histograms were created using R (R: ggplot). Venn diagrams were created using the online tool that is available under <http://bioinformatics.psb.ugent.be/webtools/Venn/>.

## **2.9. Statistical Analysis**

Except for RNA-Seq data, all other statistical analyses were carried out using Origin Pro 9.0. Comparison of means were performed with ANOVA and Tukey HSD as a post-hoc test.

## **3. Results**

### **3.1. Morphological changes in contrasting rice lines in response to Fe stress and a subsequent revival phase**

At first, we verified the tolerant and sensitive growth characters of rice plants grown in a hydroponic system and exposed to a two-day high Fe stress (15 mM Fe<sup>2+</sup>), and we tested their ability to recover from the stress in a revival experiment. The length increase of blade L2, of L2 blade and sheath and the length increase of the primary roots were measured (figure 3). In the two lines the Fe stress caused a reduction in L2 leaf blade and root growth. Generally, we noted that Hacha grew less than Lachit under control conditions. However, under the stress the difference between Lachit and Hacha growth reduction between control and high Fe stress was different and the tolerant Lachit line grew more than Hacha. This became even more evident in the subsequent revival phase. Lachit continued to grow even for six days during the revival period, but needed

## **Manuscript 4**

some waiting time in the first 48 hours before it resumed growth. Hacha, on the other side, stopped growing after 48 hours and could not resume growth any more. Hence, Lachit behaved as more tolerant line than Hacha. Hacha plants dried after the high Fe stress treatment, but not Lachit.

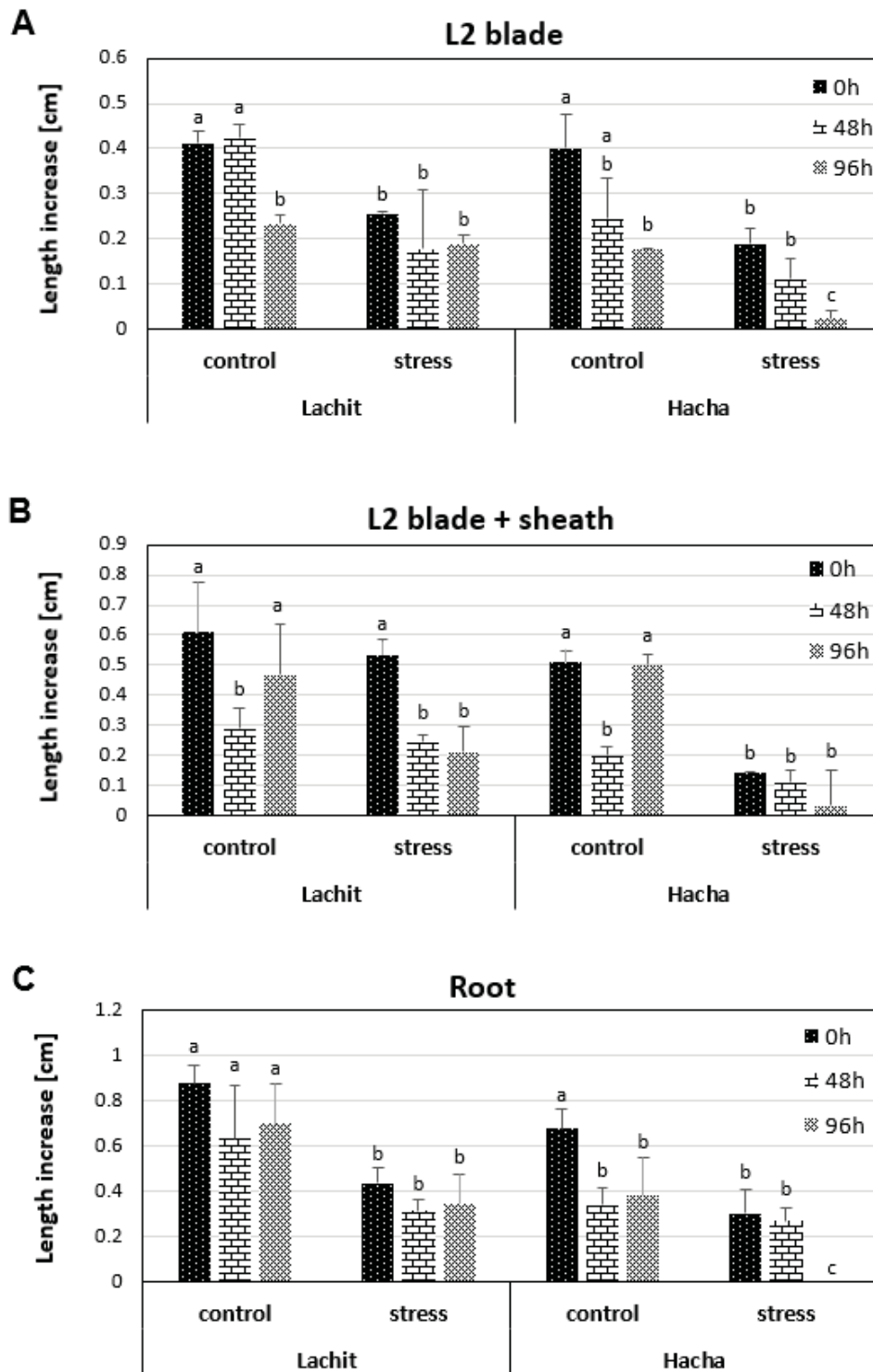
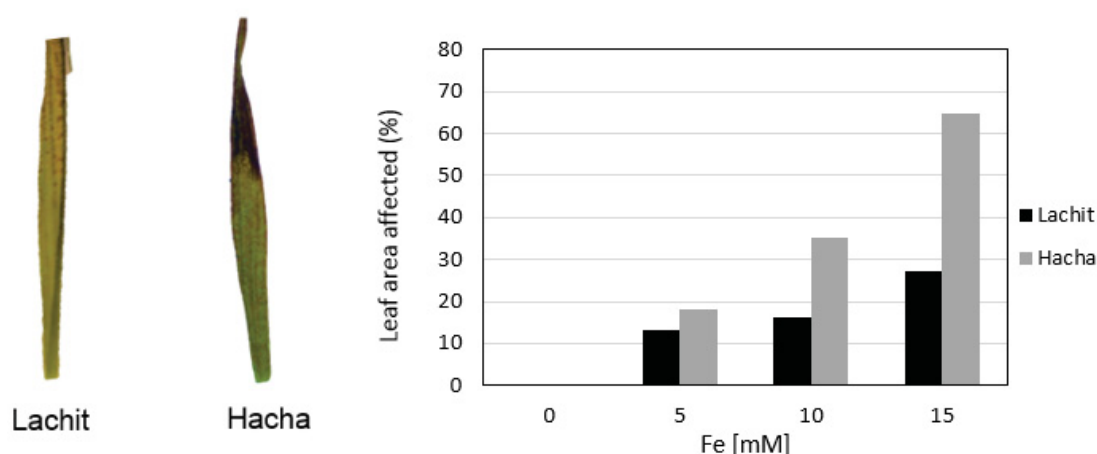


Figure 3: Length increase of (A) L2 blade, (B) entire L2 leaves with blade and sheath, (C) main root length. Treatment (0h), 48 hours and 96 hours after the treatment in a revival phase (48h and 96h). Bars

represent standard deviation of the mean (n =9). Means with the same letter are not significantly different at  $P \leq 0.05$  according to ANOVA and Tukey's HSD test.

### 3.2. Physiological changes in Lachit and Hacha plants exposed to high Fe stress

Bronzing presents a nutritional disorder that can have a direct impact on the yield and growth of rice plants. Its symptoms are detected in the leaves by the appearance of brownish spots after increased Fe uptake. The contrasting rice lines produced a varying degree of bronzing symptoms after being exposed to 15 mM iron stress for 48 hours in the hydroponic system. The browning of Hacha leaves covered a larger leaf surface including the leaf veins than in Lachit. Lachit showed only a few brown spots at the leaf surface. The bronzing of the L2 blade was subsequently quantified. (Figure 4). Bronzing is a sign of cell death that might have been caused through the Fe-mediated accumulation of hydrogen peroxide ROS species.



**Figure 4: Bronzing symptoms of L2 blade in contrasting rice lines in responses to high iron stress:** Hacha and Lachit rice seedlings were grown for 13 days in a hydroponic system. After 48 hours of Fe stress, bronzing of leaves occurred in the contrasting rice genotypes Lachit and Hacha.

To check hydrogen peroxide distribution in the leaves of the contrasting rice genotypes, we performed DAB staining. Both lines showed a significantly higher level of DAB staining under the Fe stress compared to the control. The tolerant genotype Lachit showed lower staining of DAB in the leaves as compared to Hacha. The qualitative DAB staining was confirmed by quantification for the leaf samples. In roots, stress treatment caused higher hydrogen peroxide contents in Hacha, but not to a significant level in Lachit. Hence the DAB staining and hydrogen peroxide contents

confirm that high Fe had more deleterious effects resulting in Fenton reaction-like phenotypes compared to Lachit.

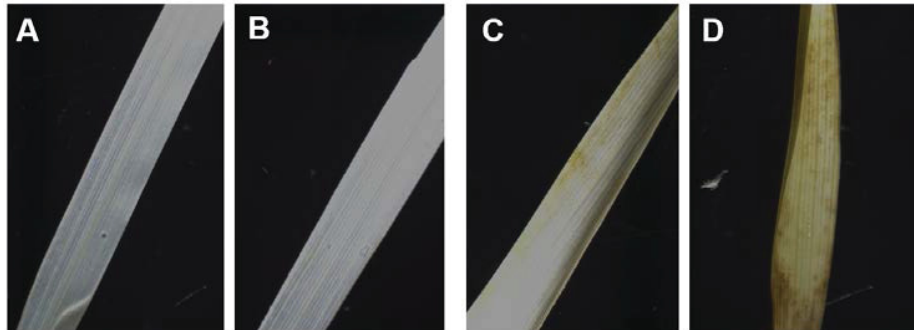


**Figure 5. DAB staining of the L2 blade among contrasting rice lines under overload iron stress:** Hacha and Lachit rice seedlings were grown for 13 days in a hydroponic system. H<sub>2</sub>O<sub>2</sub> detection in the leaves of contrasting rice genotypes. Leaves of control plants at 48 hours after DAB staining for (A) Lachit and (B) Hacha. Leaves of stressed plants (15 mM Fe) at 48 hours after DAB staining for (C) Lachit and (D) Hacha.

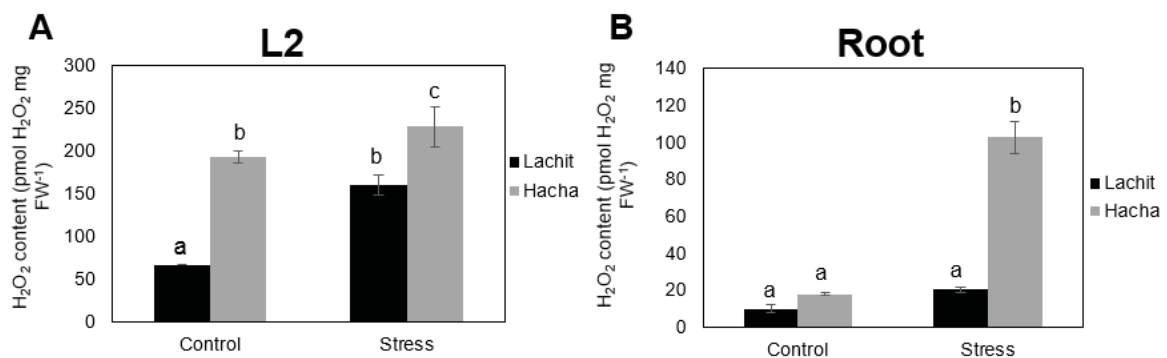


**Figure 6. Effects of iron toxicity on H<sub>2</sub>O<sub>2</sub> levels in L2 blade (A) and roots (B) of the two rice cultivars: Lachit and Hacha.** Hacha and Lachit rice seedlings were grown for 13 days in a hydroponic system. H<sub>2</sub>O<sub>2</sub> was determined after 2 days of treatment. n = 3; Means with the same letter are not significantly different at P ≤ 0.05 according to ANOVA and Tukey's HSD test.

#### 4.2.2. Ascorbate accumulation

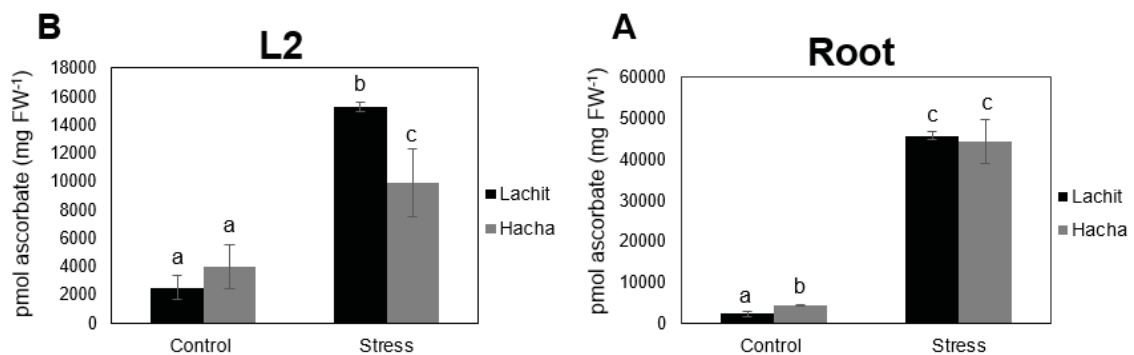


**Figure 7. Influence of iron toxicity on ascorbate levels L2 blade (A) and roots (B) of contrasting rice genotypes:** Hacha and Lachit rice seedlings were grown for 13 days in a hydroponic system. Ascorbate was determined after 2 days of treatment.  $n = 3$ ; Means with the same letter are not significantly different at  $P \leq 0.05$  according to ANOVA and Tukey's HSD test.

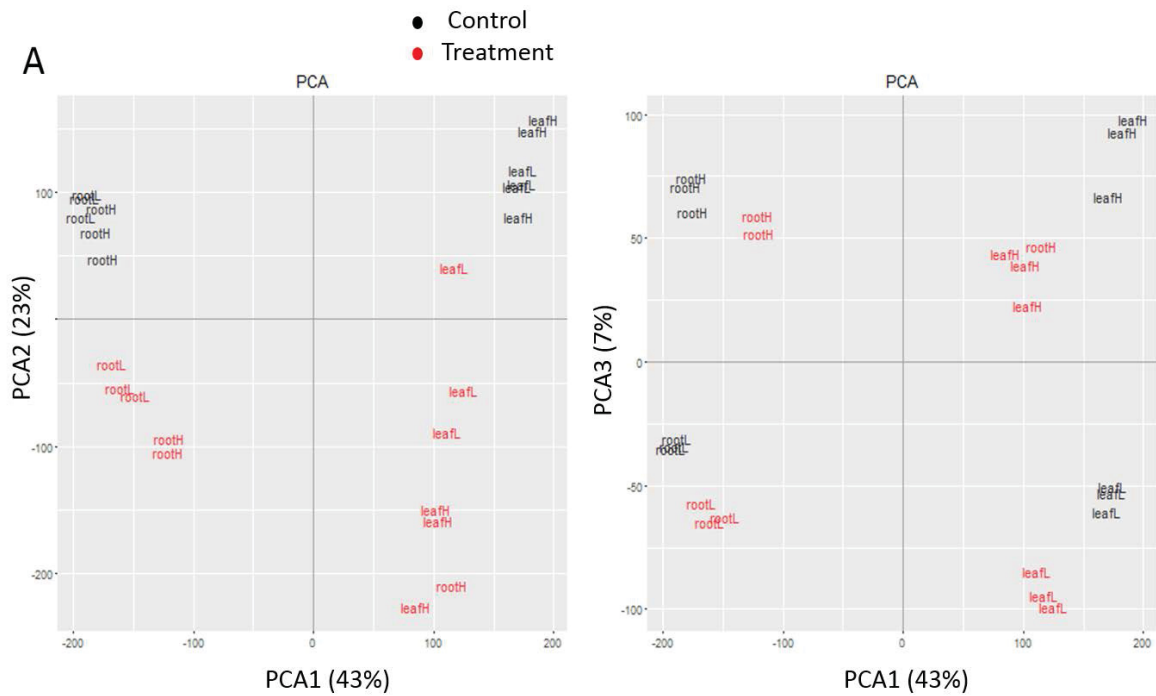
Ascorbate (vitamin C in humans) is a major antioxidant and prevents formation of free radicals in the cell, minimizing the damage caused by ROS. Ascorbate was produced in much higher quantities under stress versus the control in both lines. However, in stressed shoots Hacha had a lower ascorbate content than Lachit, while in roots there was no difference under stress and a mild increase in the control condition.

Taken together, besides the morphological growth phenotypes, Lachit also showed better physiological tolerance to high Fe. The elevated ascorbate levels might have contributed to preventing too excessive oxidative stress, otherwise leading to leaf bronzing and growth disturbance.

### 3.3. Global comparative transcriptome analysis between contrasting lines using RNA-seq

Having confirmed the tolerant and sensitive characters in our growth system, we aimed at studying the global responses of plants to high Fe and we expected to identify several additional molecular tolerance mechanisms. Towards this end we conducted a comparative RNA-seq analysis with three biological replicate samples of roots and L2 leaf sections, harvested from two day-treated controls and high Fe (15 mM  $\text{Fe}^{2+}$ )-stressed plants of the sensitive Hacha and tolerant Lachit genotypes. Each sample was harvested from eight plants to keep the variability in gene expression caused by genetic background low. The generated data table contained estimated counts as well as normalized absolute gene expression values for rice genes across the 24 samples. At first, we judged the quality of our RNA-seq data performing principal component analysis (PCA) and hierarchical clustering. These analyses visualized distances, correlations, and hence the relatedness between the data of the different samples (Figure 8). PCA separates the tissue types (root versus leaves) with 43% of the variation in the first dimension, the treatments (high Fe stress versus control) with 23% in the second dimension and resolves genotype-specific differences (Lachit versus Hachit) with 7% of the variation in the third dimension (Figure 8A). A similar observation is noted for hierarchical clustering. The first dichotomy (counted from left) separates the two tissue types, the second dichotomy forks the two treatments whereas the third dichotomy forks the two cultivars (Figure 8B). The most important conclusions that can be drawn are as follows: The stress

treatment had a more severe impact on the transcriptomes than had the genotypes, which facilitates finding specific differences of the lines in terms of high Fe responses. For both leaf and root samples, the iron effect is different between the genotypes and the Lachit high Fe stress samples are closer to the controls than are the Hacha samples, which implies that the stress affected Hacha more severely than Lachit. The biological replicates clustered generally very well together confirming the very high reproducibility and thus quality of the samples (with exception of the root Hacha excess iron sample number 3 (rootHachaPlusFe3), which was mis-assigned and therefore excluded from further analyses).



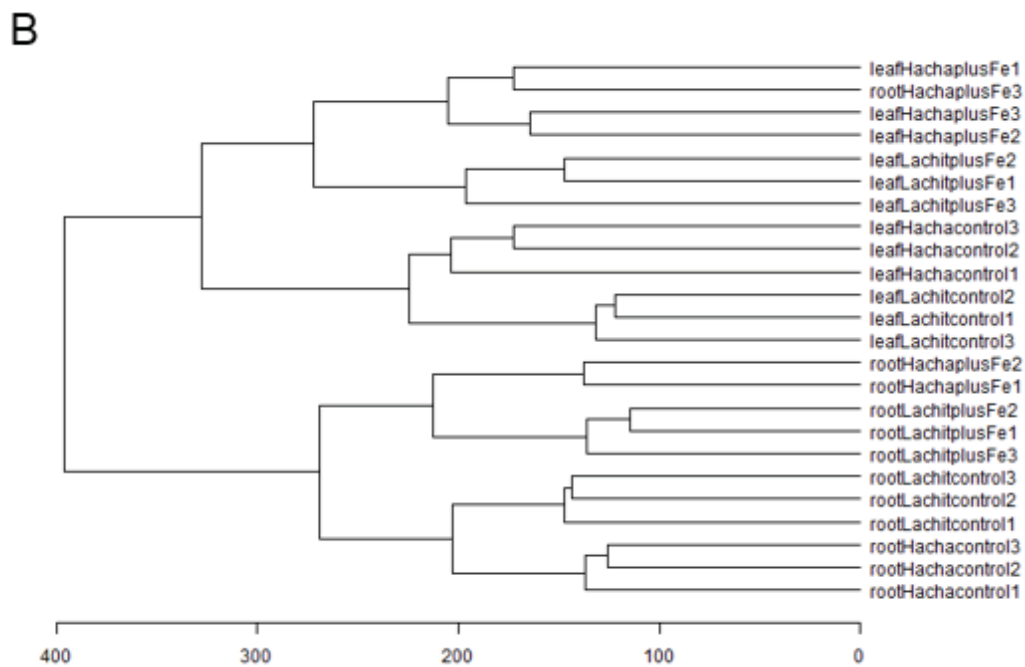


**Figure 8:** Principal component analysis (A) and hierarchical clustering (B) of roots and leaves among contrasting rice genotypes under control and Fe-stress conditions ( $P < 0.05$  and fold change  $> 2$ ). Each point represent a profile of biological replicate. The score represent a % of a total variation.

In the next step, we calculated fold change values of gene expression of Lachit versus Hacha and of high Fe stress versus control treatments, separately for root and leaf samples, in order to statistically evaluate the impact of high Fe stress depending on the line effects. A first approach simply evaluates the Fe effect separated by tissue and species and asks which responses are common to both species and with are different.

Using linear modeling we found that the effect of Fe treatment was genotype-dependent which was expected because the phenotypes of Lachit and Hacha in response to Fe were different. In other words, there is a genotype effect, a Fe effect and a genotype/Fe interaction effect.

Classical pairwise comparisons showed more changes in the root compared to the leaves and approximately equal number of up- and down-regulations (Figure 9). Leaves showed fewer changes than roots and Lachit showed fewer changes than Hacha (Figure 9). In the root, the majority of changes was shared between the genotypes (Figure 9, left two panels), both with regard

to up- and to down-regulations. In leaves, fewer changes were shared than were unique to a genotype (Figure 9, right two panels). To test for a common “Fe overload” response, overlaps between all samples were calculated for up and down. In both cases, very few responses were shared compared to the responses that occur in both Hacha and Lachit roots and leaves.

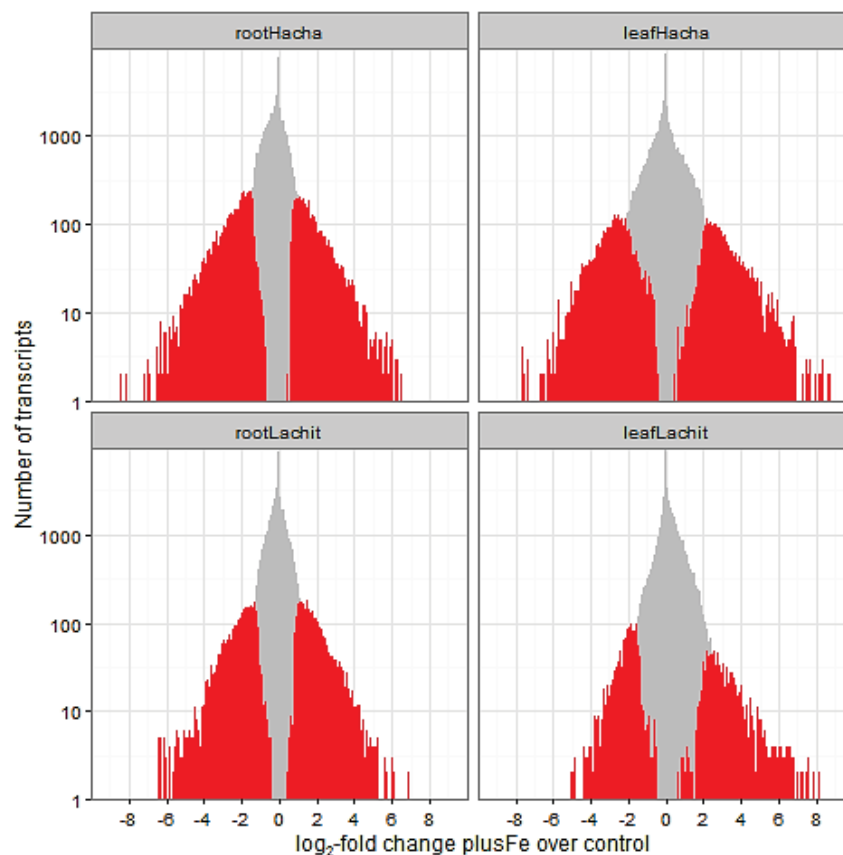


**Figure 9:** Classical pair-wise comparisons between the transcriptome of roots and shoots from control and Fe-stressed plants in two contrasting rice genotypes ( $P < 0.05$  and fold change  $> 2$ ).

### 3.3.1. Detailed comparative transcriptome analysis to identify differentially regulated genes in roots

The transcriptomic data showed that 5403 genes were up-regulated in the roots of both genotypes upon the high Fe stress versus the control and/or in Lachit versus Hacha in either treatment, whereas 5951 genes were down-regulated in the same comparisons. To identify candidate genes that may allow understanding the tolerance mechanism, we constructed Venn diagrams. Out of the 5403 up-regulated genes (Fig. 10), there were 1787 genes that responded to the stress similarly

and were expressed at similar levels in Lachit and Hacha. This Venn diagram partition included some metal homeostasis genes like the METAL TOLERANCE PROTEIN 8 (MTP8) which plays a major role in redistribution of iron during development stage and maintains manganese and iron homeostasis in the seeds (Eroglu et al. 2017), and the phenolic efflux zero 1 protein, PEZ1, which secretes phenolic to solubilize apoplasmic Fe (Ishimaru et al. 2011). These genes are regulated by high Fe stress in a genotype-independent manner, therefore unlikely to play a major role in the specific tolerance mechanisms. Our attention was drawn to clusters that indicated genes involved in a genotype-dependent high Fe stress response. Such clusters comprised the 127 and 44 genes that were up-regulated in Lachit but not in Hacha in the high Fe stress versus the control and expressed at a higher level in Lachit versus Hacha in the stress. There were also 30 genes induced in both genotypes by the stress versus the control, but still the expression levels were higher in Lachit versus Hacha in the stress condition. This list of genes encoded CDT2 and CDT3 with a role in cadmium tolerance (Xia et al. 2013), and ferritin FER1, that complexes and stores Fe in plastids. Other interesting intersections contain 10 and 479 genes encoding for example, the divalent metal transporter ZIP1 since this group of genes is also expressed at higher level in Lachit versus Hacha under the stress condition.

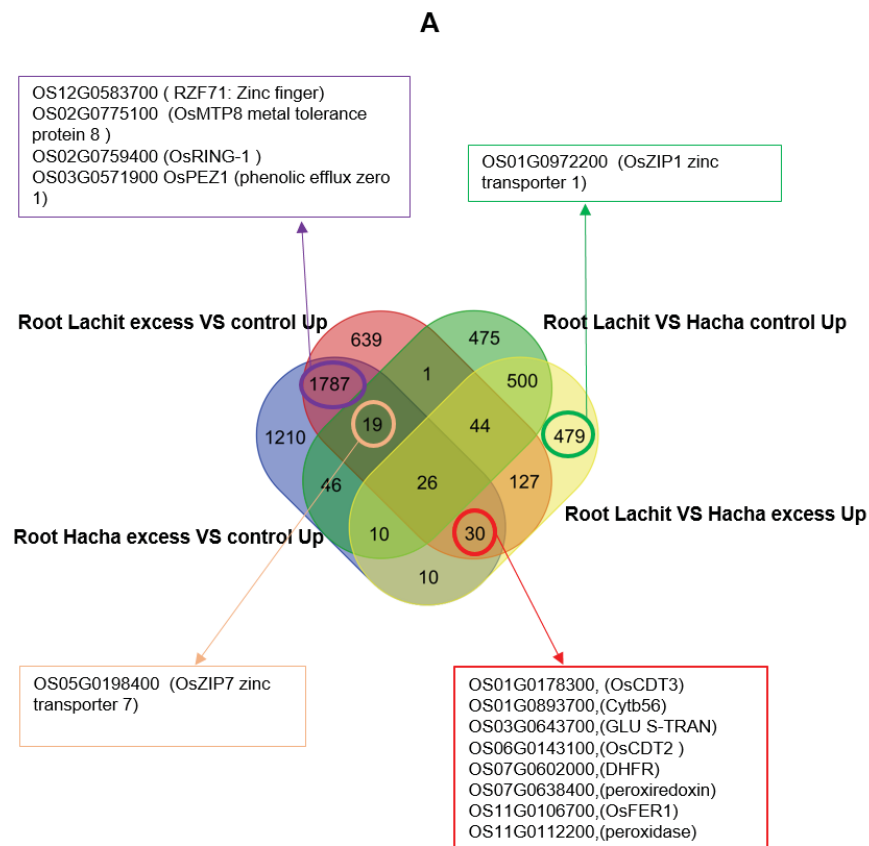


**Figure 10:** Venn diagram of the up-regulated genes after two days of Fe stress in roots of the two contrasting rice genotypes Hacha (sensitive) and Lachit (tolerant). The numbers present the number of differentially regulated genes of the respective sections in the Venn diagram. Example genes of interest are indicated.

Conversely, among the down-regulated genes in roots some sets showed genotype and treatment effects. The cluster of 2015 genes again contains numerous genotype-independent high Fe stress markers. Following the above logic the clusters of 693, 31, 8, 12 and 4 genes were particularly interesting since they were expressed at lower level in Lachit compared to Hacha, which could be relevant for the tolerance mechanism, again containing some genes with a potential role in metal homeostasis (Fig. 11).

B

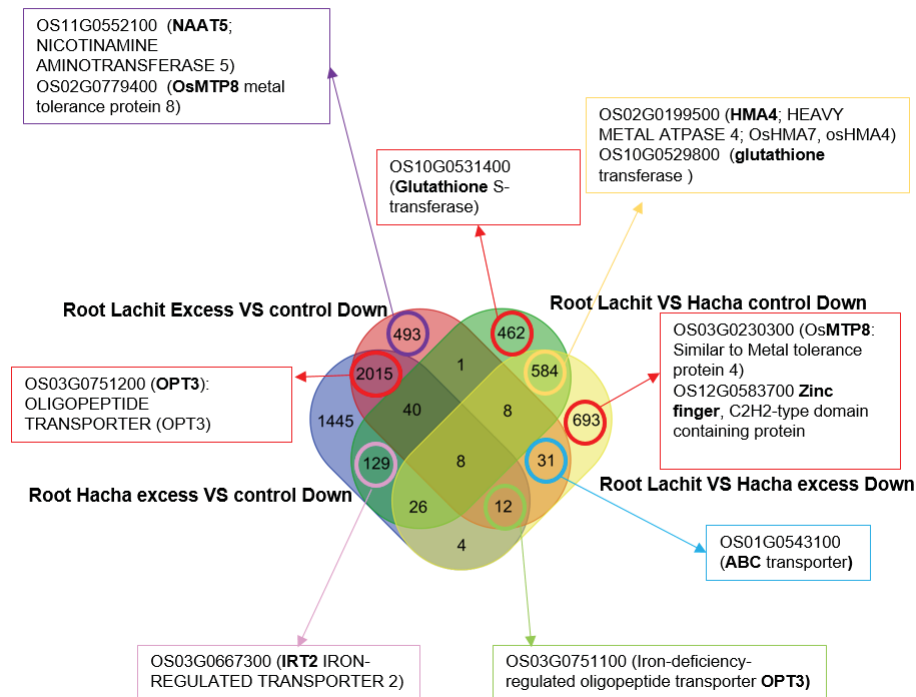


**Figure 11:** Venn diagram of the down-regulated genes after two days of Fe stress in roots of the two contrasting rice genotypes Hacha (sensitive) and Lachit (tolerant). The numbers present the number of differentially regulated genes of the respective sections in the Venn diagram. Example genes of interest are indicated.

### 3.3.2. Detailed comparative transcriptome analysis to identify differentially regulated genes in leaves

In the leaves, 3696 genes were significantly up-regulated and 3684 genes down-regulated upon high Fe stress, hence about a third less than in the roots. 322 and 750 genes represent high Fe stress markers independent of genotypes (Fig. 12, 13). Like for root-expressed genes, we are interested in the genes that are different between the tolerant and the sensitive line under Fe excess (in equivalence to the previous paragraph clusters with 104, 7, 4, 2 and 3 up-regulated genes in Fig. 12 and 345, 7, 3, 1 and 2 down-genes in Fig. 13). In the 345 gene cluster several genes encoded glutathione S transferase, possibly related to the tolerance. Glutathione S transferases catalyze the conjunction of xenobiotics.



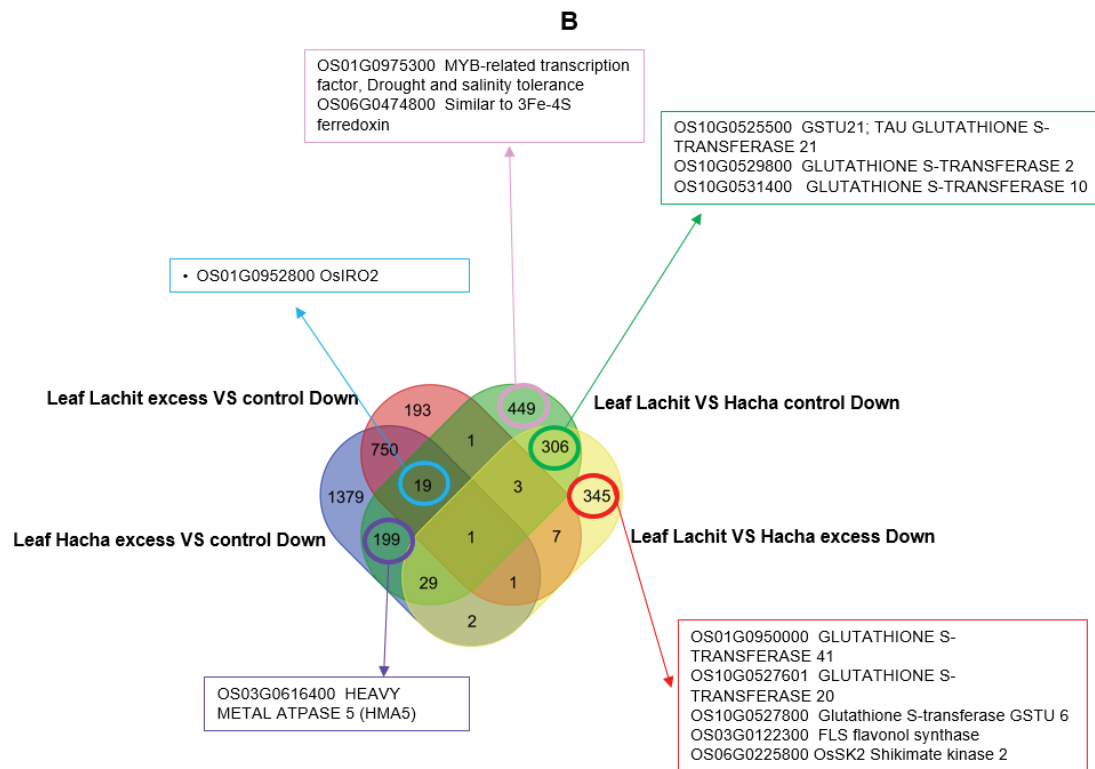


**Figure 13:** Venn diagram of the down-regulated genes after two days of Fe stress in roots of the two contrasting rice genotypes Hacha (sensitive) and Lachit (tolerant). The numbers present the number of differentially regulated genes of the respective sections in the Venn diagram. Example genes of interest are indicated.

#### 4. Discussion

Rice, an important food crop, is sensitive to high iron stress (Asch et al. 2005). However, tolerance to iron stress in rice could be genotype-specific (Stein et al. 2014). Despite the extensive studies analyzing the responses of rice to salt stress (De Leon et al. 2017; Mishra et al. 2013; Takagi et al. 2015), only some few recent studies specifically investigated the mechanism by which contrasting rice plants respond and tolerate to moderate iron stress (Devi et al. 2016; Wu et al. 2017). Two rice genotypes differing in their tolerance to high iron stress, Hacha and Lachit, were used in this investigation to explore physiological and molecular mechanisms underlying the tolerance to excessive iron stress. Our results showed an intense leaf coloration, which is in accordance with the study of (Frei et al. 2016). They observed these visual symptoms of Fe excess in tissues which is a clear damage of the leaf tissues accompanied with the development of brown spots along the veins. In our study, compared to the Lachit cultivar, more brown spots were observed in the leaves

of the Hacha cultivar which suggests that this latter was more affected and seems to be more sensitive to Fe stress. In addition, our result showed a significant reduction in the root and shoot lengths at different time points. (Engel et al. 2012) showed that the tolerance to an overload in Fe was associated with fewer visual symptoms in the leaves and a low Fe content related to an exclusion mechanism where the majority of Fe is retained in the roots and some Fe transported to the aerial parts of the plant. Due to the involvement of Fe in the Fenton reaction more reactive oxygen species (ROS) are produced, very toxic, causing damage to plant cells under high Fe stress compared to the control (Tewari et al. 2013). In agreement, our results showed an evident higher increase in the hydrogen peroxide levels and DAB staining in the Hacha than Lachit leaves and roots under high Fe stress. This finding confirms that Hacha is more sensitive to excess Fe than Lachit. Similar results were obtained by (Wu et al. 2017) using contrasting rice genotypes. As a result, plant tends to increase their synthesis of enzymatic antioxidants (catalase, glutathione reductase and superoxide dismutase) and non-enzymatic compounds (ascorbic acid, glutathione and phenolic) (Gill and Tuteja 2010) to detoxify the plants from the effects of reactive oxygen species (Briat and Lebrun 1999; Sytar et al. 2013). In our study, ascorbate levels were increased in the two studied cultivars under stress condition. In the case of Lachit, the plant shoot parts the ascorbate contents were higher compared to those in Hacha. This implies that the Lachit genotype is more efficient in detoxification than Hacha.

An RNA sequencing approach was conducted to determine the differential gene expression between the two analyzed cultivars. Our data, showed that many of the genes were significantly up- or down-regulated in both leaves and roots in both cultivars under Fe stress. From our morphological physiological results, we already assumed that the tolerance to iron stress is related to two mechanisms. The first mechanism is related to the root since roots present the first defense line to excess Fe. The second mechanism is the shoot-based mechanism based in Fe detoxification or portioning where we can compare our results with the recent work from (Wu et al. 2017). Annotation analysis of specifically up-regulated genes in Lachit roots showed that some of these genes are related to heavy metal stress and could be involved in the tolerance. FER1 binds Fe and hence detoxifies it in roots. CDTs could detoxify Fe similarly to Cd, the exact function of these proteins is not known yet (Xia et al. 2013). Phenylalanine is the precursor for phenolics-based secondary metabolites and is part of the plant defense system (Dixon 2001). These genes were up-regulated in both lines but more in the tolerant line (Lachit) than the sensitive one (Hacha). GST

(Glutathione-S-transferase) was also up-regulated in the leaves, that catalyzes the conjugation of xenobiotic metabolism since it is included in the protection of tissue from oxidative damage (Sandermann 1992).

In the perspectives of this work, biochemical analysis should be conducted with the differentially expressed genes indicating the specific tolerance mechanism of Lachit. The function of genes can be confirmed in transgenic overexpression or knockdown approaches. Another possibility would be to cross Hacha and Lachit and prove the importance of respective genes in the genetically derived lines.

## 5. References:

- Asch F, Becker M, Kpongor DS (2005) A quick and efficient screen for resistance to iron toxicity in lowland rice. *Journal of Plant Nutrition and Soil Science* 168: 764-773.
- Becker M, Asch F (2005) Iron toxicity in rice—conditions and management concepts. *Journal of Plant Nutrition and Soil Science* 168: 558-573.
- Bode K, Döring O, Lühje S, Neue H-U, Böttger M (1995) The role of active oxygen in iron tolerance of rice (*Oryza sativa* L.). *Protoplasma* 184: 249-255.
- Bray NL, Pimentel H, Melsted P, Pachter L (2016) Near-optimal probabilistic RNA-seq quantification. *Nature biotechnology* 34: 525.
- Briat J-F, Lebrun M (1999) Plant responses to metal toxicity. *Comptes Rendus de l'Académie des Sciences-Series III-Sciences de la Vie* 322: 43-54.
- Brumbarova T, Le C, Bauer P (2016) Hydrogen Peroxide Measurement in Arabidopsis Root Tissue Using Amplex Red. *Plant Physiology*.
- Czarnocka W, Karpiński S (2018) Friend or foe? Reactive oxygen species production, scavenging and signaling in plant response to environmental stresses. *Free Radical Biology and Medicine*.
- De Leon TB, Linscombe S, Subudhi PK (2017) Identification and validation of QTLs for seedling salinity tolerance in introgression lines of a salt tolerant rice landrace 'Pokkali'. *PloS one* 12: e0175361.
- Devi AG, Yadav GS, Devi HL, Ngachan S (2016) Effect of Acute Iron Toxicity on Key Antioxidative Enzymes in Contrasting Rice (*Oryza sativa* L.) Cultivars of North-East India. *International Journal of Bio-Resource & Stress Management* 7.
- Dixon RA (2001) Natural products and plant disease resistance. *Nature* 411: 843.
- Engel K, Asch F, Becker M (2012) Classification of rice genotypes based on their mechanisms of adaptation to iron toxicity. *Journal of Plant Nutrition and Soil Science* 175: 871-881.
- Eroglu S, Giehl RF, Meier B, Takahashi M, Terada Y, Ignatyev K, Andresen E, Küpper H, Peiter E, von Wirén N (2017) Metal Tolerance Protein 8 mediates manganese homeostasis and iron reallocation during seed development and germination. *Plant physiology* 174: 1633-1647.
- Frei M, Tetteh RN, Razafindrazaka AL, Fuh MA, Wu L-B, Becker M (2016) Responses of rice to chronic and acute iron toxicity: genotypic differences and biofortification aspects. *Plant and soil* 408: 149-161.
- Gill SS, Tuteja N (2010) Reactive oxygen species and antioxidant machinery in abiotic stress tolerance in crop plants. *Plant physiology and biochemistry* 48: 909-930.
- Ishimaru Y, Kakei Y, Shimo H, Bashir K, Sato Y, Sato Y, Uozumi N, Nakanishi H, Nishizawa NK (2011) A rice phenolic efflux transporter is essential for solubilizing precipitated apoplasmic iron in the plant stele. *Journal of Biological Chemistry* 286: 24649-24655.
- Li R, Shi F, Fukuda K, Yang Y (2010) Effects of salt and alkali stresses on germination, growth, photosynthesis and ion accumulation in alfalfa (*Medicago sativa* L.). *Soil Science & Plant Nutrition* 56: 725-733.
- Liang L, Liu W, Sun Y, Huo X, Li S, Zhou Q (2016) Phytoremediation of heavy metal contaminated saline soils using halophytes: current progress and future perspectives. *Environmental Reviews* 25: 269-281.
- Marschner H, Römheld V (1994) Strategies of plants for acquisition of iron. *Plant and soil* 165: 261-274.
- Marschner H, Römheld V, Kissel M (1986) Different strategies in higher plants in mobilization and uptake of iron. *Journal of plant nutrition* 9: 695-713.
- Meng L, Zhao X, Ponce K, Qian Q, Ye G (2017) Association Mapping of Ferrous, Zinc, and Aluminum Tolerance at the Seedling Stage in Indica Rice using MAGIC Populations. *Frontiers in plant science* 8: 1822.

- Mishra P, Bhoomika K, Dubey R (2013) Differential responses of antioxidative defense system to prolonged salinity stress in salt-tolerant and salt-sensitive Indica rice (*Oryza sativa* L.) seedlings. *Protoplasma* 250: 3-19.
- Naranjo-Arcos MA, Bauer P (2016) Nutritional Deficiency. Chapter 4: Iron Nutrition, Oxidative Stress, and Pathogen Defense. *Nutritional Deficiency Chapter 4: Iron Nutrition, Oxidative Stress, and Pathogen Defense*.
- Peng X, Yamauchi M (1993) Ethylene production in rice bronzing leaves induced by ferrous iron. *Plant and Soil* 149: 227-234.
- Quinet M, Vromman D, Clippe A, Bertin P, Lequeux H, Dufey I, Lutts S, Lefevre I (2012) Combined transcriptomic and physiological approaches reveal strong differences between short-and long-term response of rice (*Oryza sativa*) to iron toxicity. *Plant, cell & environment* 35: 1837-1859.
- Sandermann H (1992) Plant metabolism of xenobiotics. *Trends in biochemical sciences* 17: 82-84.
- Stein RJ, Lopes SIG, Fett JP (2014) Iron toxicity in field-cultivated rice: Contrasting tolerance mechanisms in distinct cultivars. *Theoretical and Experimental Plant Physiology* 26: 135-146.
- Sytar O, Kumar A, Latowski D, Kuczynska P, Strzałka K, Prasad M (2013) Heavy metal-induced oxidative damage, defense reactions, and detoxification mechanisms in plants. *Acta physiologiae plantarum* 35: 985-999.
- Takagi H, Tamiru M, Abe A, Yoshida K, Uemura A, Yaegashi H, Obara T, Oikawa K, Utsushi H, Kanzaki E (2015) MutMap accelerates breeding of a salt-tolerant rice cultivar. *Nature biotechnology* 33: 445-449.
- Takagi Si, Nomoto K, Takemoto T (1984) Physiological aspect of mugineic acid, a possible phytosiderophore of graminaceous plants. *Journal of Plant Nutrition* 7: 469-477.
- Tanaka A, Loe R, Navasero S (1966) Some mechanisms involved in the development of iron toxicity symptoms in the rice plant. *Soil Science and Plant Nutrition* 12: 32-38.
- Team RC (2013) R: A language and environment for statistical computing.
- Tewari RK, Hadacek F, Sassmann S, Lang I (2013) Iron deprivation-induced reactive oxygen species generation leads to non-autolytic PCD in *Brassica napus* leaves. *Environmental and experimental botany* 91: 74-83.
- Wu L-B, Shhadi MY, Gregorio G, Matthus E, Becker M, Frei M (2014) Genetic and physiological analysis of tolerance to acute iron toxicity in rice. *Rice* 7: 8.
- Wu LB, Ueda Y, Lai SK, Frei M (2017) Shoot tolerance mechanisms to iron toxicity in rice (*Oryza sativa* L.). *Plant, cell & environment* 40: 570-584.
- Xia J, Yamaji N, Ma JF (2013) A plasma membrane-localized small peptide is involved in rice aluminum tolerance. *The Plant Journal* 76: 345-355.
- Zhang J, Chen K, Pang Y, Naveed SA, Zhao X, Wang X, Wang Y, Dingkuhn M, Pasuquin J, Li Z (2017) QTL mapping and candidate gene analysis of ferrous iron and zinc toxicity tolerance at seedling stage in rice by genome-wide association study. *BMC genomics* 18: 828.

**Author contribution to Manuscript 4:** Comparative studies on tolerance of two contrasting rice genotypes differing in their tolerance to moderate iron toxicity **(in preparation)**.

Heithem Ben Abdallah

Performed and analyzed experiments (Figure 3, 6 and 7 together with SK, plant experiment for RNA-seq, RNA-seq data analysis (Figure 10-13). Wrote, reviewed and commented on the manuscript.

Hans-Jörg Mai

Analyzed the RNA-seq data and commented on the manuscript.

Andrea Bräutigam

Analyzed the RNA-seq data (Figure 8 and 9).

Samantha Kurz

Performed the library preparation.

Saradia Kar

Performed and analyzed experiments (Figure 3, 6 and 7 together with HBA).

Sanjib Kumar Panda

Provided plant material and designed experiments.

Petra Bauer

Designed experiments, supervised the study, provided funding, wrote, corrected and commented the manuscript.

## Discussion and Conclusions

### 6. Final discussion and conclusions from the dissertation:

*Hedysarum carnosum* is a Tunisian endemic species belonging to Fabaceae family. It grows under salt and calcareous soil conditions and presents a large natural phenotypic and genetic variation (Neji et al. 2013). Due the high economic value of this species in Tunisia as a good wild fodder and an important source of proteins as well as its marked adaptation to salinity and the aridity of many Tunisian regions arid climate (Gandour et al. 2014; Neji et al. 2013), recent studies have been recently carried out to unravel the potential of the Tunisian populations of this species to cope with biotic and abiotic stresses (Gandour et al. 2014; Hidri et al. 2016; Jlassi et al. 2013). As a complement to the previous work, the present study was devoted to analyze the responses of selected *H. carnosum* ecotypes in response to iron deficiency. Despite the increasing number of studies in this species, its genome reference is still unavailable. Thus, for our molecular analysis, we used the genomic resources of the closely related species *M. truncatula*, which is also an endemic Tunisian legume characterized by its high genetic variation (Friesen et al. 2014; Vu et al. 2015), adaption to wide ranges of environmental constraints and interestingly, the availability of the complete sequence of its small genome (<http://www.MedicagoGenome.org>). In our study, the physiological and molecular analyses showed that the three *Hedysarum carnosum* ecotypes, Karkar, Thelja and Douiret were differently sensitive to iron deficiency linked to their natural soil characteristics. Thelja and Douiret were found to be more tolerant to -Fe in terms of biomass and leaf iron deficiency symptoms than Karkar which was the most susceptible. Contrary to the root dry weight, the shoot dry weight was not significantly different among the three lines. In the other hand, the main root length showed a significant difference among the ecotypes. The three isolates induced Fe acquisition responses at -Fe by the development of a leaf chlorosis, acidification of the plant medium and induced the expression of *HcIRT1*. Under iron deficiency conditions, the slight decline of the photon yield in PSII it could be explained by the changes in the electron transport chain. Furthermore, (Dallali et al. 2012) noticed that *H. carnosum*, was able to grow better in higher salinity levels during the adult stage than *H. coronarium*. So studying stress in the adult stage with *Hedysarum carnosum* may lead to better understanding of the mechanism of iron deficiency in this leguminous species. -Fe condition lead to a decrease in the metal content in various plant species such as *A. thaliana* (Long et al. 2010), *M. truncatula* (Li et al. 2014) and *Oryza sativa* cultivars (Silveira et al. 2007). Under -Fe conditions, Zn and Cu contents were affected by -Fe in Karkar and Douiret but not in Thelja. Thelja may display a different mechanism

## Discussion and Conclusions

in the roots and can use efficiently the metabolism contrary to Karkar and Douiret. Thus Thelja and Douiret may grow in areas where Fe needs to be efficiently used and internally distributed inside the plant as their environment is characterized by low bioavailable iron. The different efficiencies of metal uptake observed between the ecotypes can be used like a trait for analyzing the tolerance to iron deficiency in leguminous plants (Lin et al. 2007; Singh and Agrawal 2010). Under stress conditions, ROS is harmful to the plants because of its potential toxicity and elevated energetic demand (Choudhury et al. 2017). Likewise, (Rahoui et al. 2014) showed that oxidative defense used efficiency by contrasting *M. truncatula* genotypes could be another mechanism to the tolerance to stress. These lines can be used to improve the agriculture of North Africa. The results of our physiological and gene expression analyses suggest that the individual lines have distinct adaptation capacities to react to iron deficiency. They might involve mechanisms of iron homeostasis and internal distribution.

*Medicago truncatula* is a model of leguminous plant the genome of which has been sequenced. Databases and tools are available for screening and deep molecular work. Due to its being native to Tunisia, it was important to study natural variations of *Medicago truncatula* from different geographical sites. The seeds were obtained from the SARDI collection in Australia. From more than 900 lines obtained we selected just eleven based in criteria mentioned before. In the field, crops and different plants are routinely subjected to a blend of various abiotic stresses. In Tunisia, a large area of land is affected by salinity and alkalinity and *Medicago truncatula* appeared to a native plant species there. For this reason, we screened 11 Tunisian *M. truncatula* lines in order to check their responses to combined stress. We could choose between the examined lines, two tolerant and two sensitive in response to simultaneous alkaline and salt stress. Among these lines we observed that they showed a different level of flavin production both in roots and in the nutrient solution. This resulted in identifying two types of lines: one is tolerant and the other susceptible. The previously mentioned differences justify the idea that these traits could be key mechanisms contributing to stress tolerance. Differences in flavin distribution patterns, flavin concentrations in the growth medium and root morphology support that these traits could be key mechanisms contributing to stress tolerance.

The first mechanism is related to root structure. Single and double stress treatments always had a negative effect on biomass and root dry weight. The even smaller reduction of the root DW in the

## Discussion and Conclusions

tolerant vs. sensitive lines upon the combined stress was likely caused by the smaller decrease in the number of lateral roots. Despite of the stress, tolerant lines, thus seemed better suited to sustain root growth. Therefore, the previously reported arrest of root growth to alleviate stress periods (Bailey-Serres and Voesenek 2010) does not seem to be the relevant adaptive mechanism in our studied case. Future studies can be conducted to measure the impact of root architectural changes on stress tolerance. Similarly, a localization of Flavin has been reported in many species such as, *Beta vulgaris* (López-Millán et al. 2000; Sisó-Terraza et al. 2016), and cucumber (Pavlovic et al. 2013) where roots release flavins under iron deficiency conditions. A second key mechanism relies on the allocation of flavins in root epidermal cells and flavin secretion to the growth medium, and specifically the secretion of the Rbfl derivative 7-hydroxy-Rbfl. The total concentrations of flavins in the root extracts did not allow differentiating between tolerant and sensitive lines. However, in the two tolerant lines examined, flavin fluorescence was preferentially located in the epidermal cells, the root contents of 7-hydroxy-Rbfl were undetectable, and 7-hydroxy-Rbfl was the major flavin compound in the nutrient solution. In contrast, in the two sensitive lines examined flavin fluorescence was preferentially allocated to inner parts of the root, 7-hydroxy-Rbfl was detected in the root, and 7-hydroxy-Rbfl was either undetected or a minor flavin component of the nutrient solution. These results are very interesting and match the previous observations that 7-hydroxy-Rbfl can be a major flavin in the extracts, especially under low Fe conditions (Rodríguez-Celma et al. 2011). This study justified that the secretion of Rbfl is different among the genotypes, and that, interestingly, the presence of 7-hydroxy-Rbfl was higher inside the roots of tolerant lines. Our findings support the fact that tolerance to alkalinity stress in *M. truncatula* needs the allocation of Rbfl in epidermal cells and the secretion (extracellular allocation) of oxygenated Rbfl derivatives. Moreover, this trait bears genetic diversity. The relevance for tolerance to stress of the flavin allocation in the epidermal root cells and the secretion of 7-hydroxy-Rbfl by roots should be validated using RNA sequencing technique in further studies with *M. truncatula* in aim to explore the molecular basis for this mechanism in detail. These tolerant genotypes may be cultivated on salt-affected soils prone to alkalinity-induced Fe deficiency. In this chapter, we showed that *M. truncatula* secrete riboflavin in response to combined stress. Quite possibly this production is involved in the tolerance mechanism under salt and alkaline stress. Other relevant mechanisms for salt and alkaline stress includes, changes in root architecture and localization and

## Discussion and Conclusions

secretion of Flavin in root epidermal cells in *M. truncatula*. Finally, the secretion of 7-hydroxy-*Rbfl* by roots should be validated in further explored using *M. truncatula*.

Fe is a fundamental component in plants that is involved in numerous physiological processes, however, that can also be dangerous when taken up in high amount (Becker and Asch 2005). Excess in iron would lead to inhibiting the development and decreasing the yield. For instance, rice is a very sensitive crop to high level of iron (Asch et al. 2005). This overload of iron stress could be tolerated through the use of a genotype particular (Stein et al. 2014). In spite of the broad investigations to analyze the responses of rice to salt stress (De Leon et al. 2017; Mishra et al. 2013; Takagi et al. 2015), but a couple of the latest studies have focused mainly on discovering the mechanism through which researchers would differentiate the responses of rice plants to moderate iron stress (Devi et al. 2016; Wu et al. 2017). Contrasting rice genotypes, Hacha and Lachit which differing in their response to overload iron stress were used to explore physiological and molecular mechanisms underlying the tolerance to high iron stress. Under overload iron stress in rice, physiological and transcriptomic study in short and long term showed a genotype variation (Bashir et al. 2014; Finatto et al. 2015; Quinet et al. 2012). Our results showed an intense leaf chlorosis was in accordance with the study of (Frei et al. 2016), where visual symptoms of iron excess in tissues were observed, with clear damage of the leaf tissues accompanied by the development of brown spots along the veins. In our study, compared to Lachit genotype, more brown spots were observed in the leaves of Hacha genotype which suggests that this latter was more affected and seems to be more sensitive to iron stress. In addition, our result showed a significant reduction of the root and shoot length at different time points. Clearly, such reduction was found to be very different between the two genotypes which is in agreement with the results reported by (Viana et al. 2017). The root retention mechanism was reported first by (Becker and Asch 2005). Moreover, (Engel et al. 2012) showed that the tolerance to overload iron was associated with few visual symptoms in leaves and low iron content related to exclusion mechanism where the most part of iron was retained in the root and only a few part was transported to the aerial part. On the other hand, excess iron can lead to a reduction of oxygen molecules which occurs due to the involvement of iron in the Fenton reaction. As a result, higher amounts of reactive oxygen species (ROS) are produced. Hydrogen peroxide is one such ROS which increases during iron stress conditions (Tewari et al. 2013). In agreement, our results showed an evident increase

## Discussion and Conclusions

in the level of hydrogen peroxide in Hacha leaves and roots under 15mM of Fe<sup>2+</sup> stress. This finding confirms that Hacha is more sensitive to excess iron than Lachit. By using the DAB indicator, Lachit leaves were found to be less stained than showed those of Hacha genotype which confirms that peroxide content generated in Hacha was more than that of Lachit. Similar results were obtained by (Wu et al. 2017) using contrasting rice genotypes. Abiotic stress generally leads to the imbalance of cellular redox potential. As a result, plant tends to increase their synthesis of antioxidants (glutathione and ascorbate) by the help of antioxidant enzymes to detoxify the plants from the effects of reaction oxygen species (Briat and Lebrun 1999; Sytar et al. 2013). In our study, the antioxidant content was found to be increased in the two studied genotypes under stress condition. In case of Lachit, the plant shoot part showed significant increase of ascorbate content. This implies that Lachit genotype generates detoxification than Hacha. However, it should be noted that much higher antioxidant level was detected in Lachit compared to Hacha genotype.

For a deep understanding of the morphological physiological results, an RNA seq approach was conducted in order to check the differential gene expression between the two analyzed genotypes. Our data, showed a large number of genes significantly up or down-regulated in both leaves and roots in both genotypes under the overload of iron. From our morphological physiological results, we assume that the tolerance to iron stress is related to two mechanisms. The first mechanism is related to the root, since roots presented the first defence line to excess iron. The precipitation of Fe<sup>2+</sup> leads to the formation of a physical barrier named root plaque (Wu et al. 2012). The second mechanism is the shoot based mechanism where we can compare with the recent work from (Wu et al. 2017) among two rice cultivars. Our results showed that, more genes were found to be upregulated in roots than in shoot in the condition of Fe excess. Annotation analysis, showed that these genes included many transporter genes belonging to different families such as Zip transporters, metal tolerance protein, phenolic efflux zero1 protein which transports phenolic to solubilize apoplasmic Fe (Ishimaru et al. 2011). In shoots, only 3696 upregulated genes were observed in Fe excess. Interestingly, some genes related to phenylalanine was up-regulated, this compound act as a secondary metabolite and included in the plant defence system. This compound is present in both lines but more genes in the tolerant line (Lachit) than the sensitive one (Hacha). GST (Glutathione-S-transferase) was also present, that catalyze the conjunction of xenobiotic

## Discussion and Conclusions

metabolism (Sandermann 1992) since it is included in the protection of tissue from oxidative damage.

### Conclusions

Leguminous plants are often used in agriculture because of their ability to fix nitrogen, high protein level and to increase the soil fertility. For decades leguminous plants have been transferred from the Mediterranean basin into multitude farming systems. After testing *Hedysarum* ecotypes, we conclude that they have not responded in the same manner under iron deficiency condition due to their ability to solubilize iron. Therefore, *Hedysarum* ecotypes can be a promising project used in the ministry of agriculture and innovation in Tunisia in order to further understand the internal iron homeostasis regulation events. One of the recent powerful strategies for deep molecular analyses is the RNA seq approach.

This approach could be used to investigate deep transcriptomic analyzes and gene expression studies even in non-model species without the need to reference genome sequence. Thus, to achieve our future aims, this approach will be used to analyze the differential gene expression of the previously studied lines under different level of iron deficiency. Furthermore, we have shown that contrasting *Medicago* lines differ in their responses to combined stress. The root architecture, flavin root localization in epidermal cells and flavin secretion are relevant tolerance mechanisms. Our data showed that Line 10 and 11 respond to simultaneous alkaline and salt stress in highly contrasting ways compared to the line 7 and 9. The line 10 and 11 line can be used in a structured farming system and growing in the field where salinity and iron deficiency occurs. These lines can be checked by comparing the root specific transcript profiling among the tolerant and sensitive lines to identify genes that are involved in plant salinity-alkalinity tolerance.

These lines can be checked by comparing the root specific transcript profiling among the tolerant and sensitive lines to identify genes that are involved in plant salinity-alkalinity tolerance. There are several candidate genes with expected differential regulation for single and combined stress in *Medicago truncatula*. Firstly, we could check the known genes encoding enzymes involved in the riboflavin biosynthesis pathways, some of them are upregulated under iron deficiency in *Medicago truncatula* (Medtr2g009270, Medtr4g119220, and Medtr7g080120) (Rodríguez-Celma et al. 2013). Second, iron deficiency stress, genes could be up regulated that are represented by iron

## Discussion and Conclusions

regulated genes in *Medicago truncatula*, IRT1 (MTR4g083570) and FRO2 (MTR7g038180) (Li et al. 2014). There is also salt stress which can be checked by the expression of Salt Overly Sensitive (SOS) genes with the expression of SOS1 (XP003595114), SOS2 and SOS3 (Medtr3g091440) genes (Liu et al. 2015). There is the possibility of some candidate genes encodes MYB transcription factors such as MtMYBS1 (Medtr1g073170) which is induced in the tolerance to salinity and many other abiotic stresses (Dong et al. 2017).

Due to the importance of rice as staple food in Asia, our study is one of the few that check contrasting rice genotypes under iron excess. Our morphological and molecular results showed a difference in the response to high iron among the contrasting rice genotypes. Further studies are in progress to validate our RNA sequencing data in goal to accomplish the mechanism behind the response of the tolerant and the sensitive genotypes. We are in the process of checking and validating candidate genes that can be used for genetic improvement to produce stress-tolerant rice genotypes. Further research is needed to tie the different mechanism in the roots and shoots of contrasting *Hedysarum*, *Medicago* and rice genotypes.

### 7. References:

- Asch F, Becker M, Kpongor DS (2005) A quick and efficient screen for resistance to iron toxicity in lowland rice. *Journal of Plant Nutrition and Soil Science* 168: 764-773.
- Bailey-Serres J, Voeselek LA (2010) Life in the balance: a signaling network controlling survival of flooding. *Current opinion in plant biology* 13: 489-494.
- Bashir K, Hanada K, Shimizu M, Seki M, Nakanishi H, Nishizawa NK (2014) Transcriptomic analysis of rice in response to iron deficiency and excess. *Rice* 7: 18.
- Becker M, Asch F (2005) Iron toxicity in rice—conditions and management concepts. *Journal of Plant Nutrition and Soil Science* 168: 558-573.
- Briat J-F, Lebrun M (1999) Plant responses to metal toxicity. *Comptes Rendus de l'Académie des Sciences-Series III-Sciences de la Vie* 322: 43-54.
- Choudhury FK, Rivero RM, Blumwald E, Mittler R (2017) Reactive oxygen species, abiotic stress and stress combination. *The Plant Journal* 90: 856-867.
- Dallali H, Maalej EM, Boughanmi NG, Haouala R (2012) Salicylic acid priming in *hedysarum carnosum* and *hedysarum coronarium* reinforces NaCl tolerance at germination and the seedling growth stage. *Australian Journal of Crop Science* 6: 407.
- De Leon TB, Linscombe S, Subudhi PK (2017) Identification and validation of QTLs for seedling salinity tolerance in introgression lines of a salt tolerant rice landrace 'Pokkali'. *PloS one* 12: e0175361.
- Devi AG, Yadav GS, Devi HL, Ngachan S (2016) Effect of Acute Iron Toxicity on Key Antioxidative Enzymes in Contrasting Rice (*Oryza sativa* L.) Cultivars of North-East India. *International Journal of Bio-Resource & Stress Management* 7.
- Dong W, Song Y, Zhao Z, wei Qiu N, Liu X, Guo W (2017) The *Medicago truncatula* R2R3-MYB transcription factor gene MtMYBS1 enhances salinity tolerance when constitutively expressed in *Arabidopsis thaliana*. *Biochemical and biophysical research communications* 490: 225-230.
- Engel K, Asch F, Becker M (2012) Classification of rice genotypes based on their mechanisms of adaptation to iron toxicity. *Journal of Plant Nutrition and Soil Science* 175: 871-881.
- Finatto T, de Oliveira AC, Chaparro C, Da Maia LC, Farias DR, Woyann LG, Mistura CC, Soares-Bresolin AP, Llauro C, Panaud O (2015) Abiotic stress and genome dynamics: specific genes and transposable elements response to iron excess in rice. *Rice* 8: 13.
- Frei M, Tetteh RN, Razafindrazaka AL, Fuh MA, Wu L-B, Becker M (2016) Responses of rice to chronic and acute iron toxicity: genotypic differences and biofortification aspects. *Plant and soil* 408: 149-161.
- Friesen ML, von Wettberg EJ, Badri M, Moriuchi KS, Barhoumi F, Chang PL, Cuellar-Ortiz S, Cordeiro MA, Vu WT, Arraouadi S (2014) The ecological genomic basis of salinity adaptation in Tunisian *Medicago truncatula*. *BMC genomics* 15: 1160.
- Gandour M, Neji M, Hessini K, Smida M, Abdelly C, Taamalli W (2014) Assessing the Salt Tolerance of Genotypes by Agronomic Indicators. *Agronomy Journal* 106: 185-190.
- Hidri R, Barea J, Mahmoud OM-B, Abdelly C, Azcón R (2016) Impact of microbial inoculation on biomass accumulation by *Sulla carnosa* provenances, and in regulating nutrition, physiological and antioxidant activities of this species under non-saline and saline conditions. *Journal of plant physiology* 201: 28-41.
- Ishimaru Y, Kakei Y, Shimo H, Bashir K, Sato Y, Sato Y, Uozumi N, Nakanishi H, Nishizawa NK (2011) A rice phenolic efflux transporter is essential for solubilizing precipitated apoplasmic iron in the plant stele. *Journal of Biological Chemistry* 286: 24649-24655.
- Jlassi A, Zorrig W, Khouni AE, Lakhdar A, Smaoui A, Abdelly C, Rabhi M (2013) Phytodesalination of a moderately-salt-affected soil by *Sulla carnosa*. *International journal of phytoremediation* 15: 398-404.

## References

- Li G, Wang B, Tian Q, Wang T, Zhang W-H (2014) *Medicago truncatula* ecotypes A17 and R108 differed in their response to iron deficiency. *Journal of plant physiology* 171: 639-647.
- Lin A-J, Zhang X-H, Wong M-H, Ye Z-H, Lou L-Q, Wang Y-S, Zhu Y-G (2007) Increase of multi-metal tolerance of three leguminous plants by arbuscular mycorrhizal fungi colonization. *Environmental geochemistry and health* 29: 473-481.
- Liu M, Wang T-Z, Zhang W-H (2015) Sodium extrusion associated with enhanced expression of *SOS1* underlies different salt tolerance between *Medicago falcata* and *Medicago truncatula* seedlings. *Environmental and Experimental Botany* 110: 46-55.
- Long TA, Tsukagoshi H, Busch W, Lahner B, Salt DE, Benfey PN (2010) The bHLH transcription factor *POPEYE* regulates response to iron deficiency in *Arabidopsis* roots. *The Plant Cell* 22: 2219-2236.
- López-Millán AF, Morales F, Andaluz S, Gogorcena Y, Abadía A, De Las Rivas J, Abadía J (2000) Responses of sugar beet roots to iron deficiency. Changes in carbon assimilation and oxygen use. *Plant Physiology* 124: 885-898.
- Mishra P, Bhoomika K, Dubey R (2013) Differential responses of antioxidative defense system to prolonged salinity stress in salt-tolerant and salt-sensitive *Indica* rice (*Oryza sativa* L.) seedlings. *Protoplasma* 250: 3-19.
- Neji M, Taamalli W, Smida M, Abdelly C, Gandour M (2013) Phenotypic and Molecular Genetic Variation in Tunisian Natural Populations of. *Agronomy Journal* 105: 1094-1100.
- Pavlovic J, Samardzic J, Maksimović V, Timotijevic G, Stevic N, Laursen KH, Hansen TH, Husted S, Schjoerring JK, Liang Y (2013) Silicon alleviates iron deficiency in cucumber by promoting mobilization of iron in the root apoplast. *New Phytologist* 198: 1096-1107.
- Quinet M, Vromman D, Clippe A, Bertin P, Lequeux H, Dufey I, Lutts S, Lefevre I (2012) Combined transcriptomic and physiological approaches reveal strong differences between short-and long-term response of rice (*Oryza sativa*) to iron toxicity. *Plant, cell & environment* 35: 1837-1859.
- Rahoui S, Ben C, Chaoui A, Martinez Y, Yamchi A, Rickauer M, Gentzbittel L, El Ferjani E (2014) Oxidative injury and antioxidant genes regulation in cadmium-exposed radicles of six contrasted *Medicago truncatula* genotypes. *Environmental Science and Pollution Research* 21: 8070-8083.
- Rodríguez-Celma J, Lin W-D, Fu G-M, Abadía J, López-Millán A-F, Schmidt W (2013) Mutually exclusive alterations in secondary metabolism are critical for the uptake of insoluble iron compounds by *Arabidopsis* and *Medicago truncatula*. *Plant Physiology* 162: 1473-1485.
- Rodríguez-Celma J, Vázquez-Reina S, Orduna J, Abadía A, Abadía J, Álvarez-Fernández A, López-Millán A-F (2011) Characterization of flavins in roots of Fe-deficient strategy I plants, with a focus on *Medicago truncatula*. *Plant and Cell Physiology* 52: 2173-2189.
- Sandermann H (1992) Plant metabolism of xenobiotics. *Trends in biochemical sciences* 17: 82-84.
- Silveira VCd, Oliveira APd, Sperotto RA, Espindola LS, Amaral L, Dias JF, Cunha JBd, Fett JP (2007) Influence of iron on mineral status of two rice (*Oryza sativa* L.) cultivars. *Brazilian Journal of Plant Physiology* 19: 127-139.
- Singh R, Agrawal M (2010) Effect of different sewage sludge applications on growth and yield of *Vigna radiata* L. field crop: Metal uptake by plant. *Ecological Engineering* 36: 969-972.
- Sisó-Terraza P, Rios JJ, Abadía J, Abadía A, Álvarez-Fernández A (2016) Flavins secreted by roots of iron-deficient *Beta vulgaris* enable mining of ferric oxide via reductive mechanisms. *New Phytologist* 209: 733-745.
- Stein RJ, Lopes SIG, Fett JP (2014) Iron toxicity in field-cultivated rice: Contrasting tolerance mechanisms in distinct cultivars. *Theoretical and Experimental Plant Physiology* 26: 135-146.
- Sytar O, Kumar A, Latowski D, Kuczynska P, Strzałka K, Prasad M (2013) Heavy metal-induced oxidative damage, defense reactions, and detoxification mechanisms in plants. *Acta physiologiae plantarum* 35: 985-999.

## References

- Takagi H, Tamiru M, Abe A, Yoshida K, Uemura A, Yaegashi H, Obara T, Oikawa K, Utsushi H, Kanzaki E (2015) MutMap accelerates breeding of a salt-tolerant rice cultivar. *Nature biotechnology* 33: 445-449.
- Tewari RK, Hadacek F, Sassmann S, Lang I (2013) Iron deprivation-induced reactive oxygen species generation leads to non-autolytic PCD in *Brassica napus* leaves. *Environmental and experimental botany* 91: 74-83.
- Viana V, Marini N, Finatto T, Ezquer I, Busanello C, Dos Santos R, Pegoraro C, Colombo L, de Oliveira AC (2017) Iron excess in rice: from phenotypic changes to functional genomics of WRKY transcription factors. *Genetics and Molecular Research* 16.
- Vu WT, Chang PL, Moriuchi KS, Friesen ML (2015) Genetic variation of transgenerational plasticity of offspring germination in response to salinity stress and the seed transcriptome of *Medicago truncatula*. *BMC evolutionary biology* 15: 59.
- Wu C, Ye Z, Li H, Wu S, Deng D, Zhu Y, Wong M (2012) Do radial oxygen loss and external aeration affect iron plaque formation and arsenic accumulation and speciation in rice? *Journal of experimental botany* 63: 2961-2970.
- Wu LB, Ueda Y, Lai SK, Frei M (2017) Shoot tolerance mechanisms to iron toxicity in rice (*Oryza sativa* L.). *Plant, cell & environment* 40: 570-584.